

LA-3725

C.4

LOS ALAMOS SCIENTIFIC LABORATORY
of the
University of California
LOS ALAMOS • NEW MEXICO

Theory of a Radio-Frequency "Spin Filter"
for a Metastable Hydrogen, Deuterium, or
Tritium Atomic Beam



FOR REFERENCE

NOT TO BE TAKEN FROM THIS ROOM

CAT. NO. 1935

LIBRARY BUREAU

UNITED STATES
ATOMIC ENERGY COMMISSION
CONTRACT W-7405-ENG. 36

LEGAL NOTICE

This report was prepared as an account of Government sponsored work. Neither the United States, nor the Commission, nor any person acting on behalf of the Commission:

A. Makes any warranty or representation, expressed or implied, with respect to the accuracy, completeness, or usefulness of the information contained in this report, or that the use of any information, apparatus, method, or process disclosed in this report may not infringe privately owned rights; or

B. Assumes any liabilities with respect to the use of, or for damages resulting from the use of any information, apparatus, method, or process disclosed in this report.

As used in the above, "person acting on behalf of the Commission" includes any employee or contractor of the Commission, or employee of such contractor, to the extent that such employee or contractor of the Commission, or employee of such contractor prepares, disseminates, or provides access to, any information pursuant to his employment or contract with the Commission, or his employment with such contractor.

This report expresses the opinions of the author or authors and does not necessarily reflect the opinions or views of the Los Alamos Scientific Laboratory.

Printed in the United States of America. Available from
Clearinghouse for Federal Scientific and Technical Information
National Bureau of Standards, U. S. Department of Commerce
Springfield, Virginia 22151

Price: Printed Copy \$3.00; Microfiche \$0.65

LA-3725
UC-34, PHYSICS
TID-4500

LOS ALAMOS SCIENTIFIC LABORATORY
of the
University of California
LOS ALAMOS • NEW MEXICO

Report written: July 1967

Report distributed: October 26, 1967

Theory of a Radio-Frequency "Spin Filter"
for a Metastable Hydrogen, Deuterium, or
Tritium Atomic Beam

LOS ALAMOS NATL. LAB. LIBS.

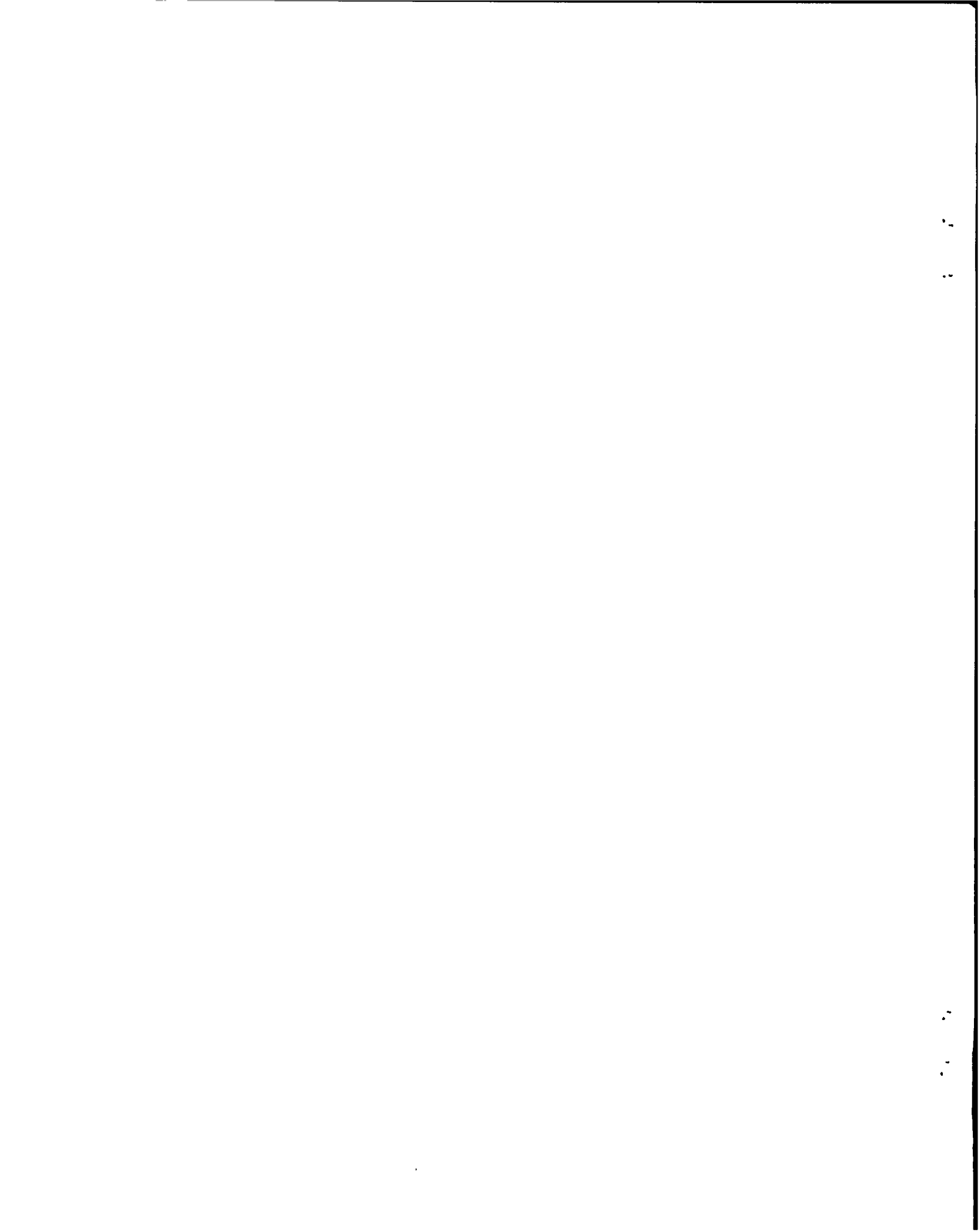
3 9338 00314 9118

by

Gerald G. Ohlsen

Joseph L. McKibben





CONTENTS

Abstract.	5
1. Introduction.	5
2. Energy Levels of the Hydrogen Atom.	6
3. Selection Rules	8
4. Discussion of the General Spin State Selection Problem	15
5. Quantum Mechanical Formulation of the Four-Level Problem	16
6. Matrix Elements	18
7. Analytic Solution of the Three-Level Problem.	22
8. The Four-Level Problem.	33
9. Adiabatic Variation of the Electric Fields.	40
Acknowledgments	42
References.	42
Appendix A: A Computer Program for Evaluating the Analytic Solution of the Three-Level Equations.	43
Appendix B: A Computer Program for Numerical Inte- gration of the Four-Level Equations.	49

TABLES

I. Parameters Characterizing the Hyperfine Structure of the $n = 2$ States of Hydrogen, Deuterium, and Tritium Atoms.	8
II. Hydrogen Atom 2S States	9
III. Hydrogen Atom 2P States	10
IV. Deuterium Atom 2S States.	11
V. Deuterium Atom 2P States.	12
VI. Tritium Atom 2S States.	13
VII. Tritium Atom 2P States.	14
VIII. $n = 2$ Hydrogen Atom Wave Functions in a Magnetic Field	19
IX. Factors Required for the Computation of the Hydrogen Atom Wave Functions in an Arbitrary Magnetic Field	20
X. $n = 2$ Electric Dipole Matrix Elements	21
XI. Transmission of Unselected Substates	27



THEORY OF A RADIO-FREQUENCY "SPIN FILTER" FOR A
METASTABLE HYDROGEN, DEUTERIUM, OR TRITIUM ATOMIC BEAM

by
Gerald G. Ohlsen and Joseph L. McKibben

ABSTRACT

Techniques for selection of metastable hydrogen, deuterium, or tritium atoms with a particular nuclear spin polarization are discussed. The emphasis is on the "three-level interaction" technique, which promises to be the most versatile and satisfactory of those available.

1. INTRODUCTION

In connection with the development of the Los Alamos Scientific Laboratory "metastable hydrogen" polarized ion source, calculations about possible nuclear spin selection techniques have been made. The discussion of these calculations, which have been partially reported,^{1,2} comprises the main part of this report. However, for orientation purposes, the basic operating scheme for the LASL polarized ion source is reviewed. The discussion in this section is in terms of protons, although the scheme works as well for deuterons or for tritons.

A beam of protons is extracted from a duoplasmatron and then decelerated to a velocity ($\sim 3 \times 10^7$ cm/sec) corresponding to 500 eV. Additional electrons are injected to space-charge neutralize the beam, which is then passed through a curtain of cesium vapor. Collisions in the cesium convert a large number of protons into H^{2S} atoms,³ together with ground-state atoms, and positive and negative ions. The beam then enters a longitudinal magnetic field of about 500 to 600 G. A transverse "clearing" electric field separates the charged particles from the neutral atoms (H^{2S} and H^{1S}). The neutral atoms then pass through a radio-frequency transition region where the H^{2S} atoms possessing any but the desired nuclear spin magnetic quantum number are

quenched to the ground state while a large fraction of the atoms with the selected m_I remain in the H^{2S} state. This mixture of $\sim 100\%$ polarized H^{2S} and essentially unpolarized* H^{1S} atoms is then passed through an argon exchange cell, where, at this particular velocity, the reaction $H^{2S} + A \rightarrow H^- + A^+$ occurs with a probability very much larger than does the corresponding ground-state reaction.⁴

One interesting point is that the LASL nuclear spin selection method selects rather than rejects a particular nuclear spin state. Thus, a deuteron beam corresponding to a pure $m_I = 1, 0,$ or -1 state may be obtained with a single radio-frequency selection device. The selection device, which employs perpendicular radio-frequency and static electric fields, behaves as a filter which allows only those metastable atoms with a specific nuclear spin quantum number (m_I) to pass through without being quenched to the ground state. This device is hereinafter referred to as a "spin filter."

The theoretical upper limit for transmission of the desired nuclear spin state through the spin filter is $1/2$. Thus, for deuterons, at least $5/6$ of the

*The portion of the H^{1S} produced background current which arises from decay of H^{2S} atoms in the rf region is in fact partially polarized in the opposite sense.

incident metastable beam will be quenched, while for protons or tritons at least 3/4 of the incident metastable beam will be quenched. In addition, the incident atomic beam will have a large (perhaps 80 or 90%) ground-state component.

The degree of selection achieved in the argon exchange reaction depends on the ratio of the $H^{2S} + A \rightarrow H^- + A^+$ reaction cross section (denoted by σ^{2S}) to the $H^{1S} + A \rightarrow H^- + A^+$ reaction cross section (denoted by σ^{1S}). This ratio is not accurately known at present. The quantity which can be readily measured is the quenching ration Q; that is, the ratio of the negative ion yield obtained through a cesium exchange reaction followed by an argon exchange reaction without and with the application of intervening fields sufficient to quench the entire metastable component of the beam. This ratio can be expressed in terms of the fraction of the atomic beam in the metastable state, f, as follows:

$$Q = (1 - f) + f(\sigma^{2S}/\sigma^{1S}).$$

The quenching ratio is related to the resulting nuclear spin state purity (p) by

$$p = 1 - 4/Q\eta$$

for protons and tritons, and by

$$p = 1 - 6/Q\eta$$

for deuterons, where η is the efficiency of the spin filter. That is, $\eta = 1$ if the theoretical upper limit of 1/2 for transmission is reached. The relationship between p and the beam polarization parameters is given below.

Spin 1/2 Particles		
m_I		P
1/2		p
-1/2		-p

Spin 1 Particles		
m_I	P_z	P_{zz}
1	p	p
0	0	-2p
-1	-p	p

In the above $P = N(1/2) - N(-1/2)$, $P_z = N(1) - N(-1)$, and $P_{zz} = N(1) + N(-1) - 2N(0)$, where $N(m_I)$ is the fraction of the beam particles with quantum

number m_I .

A measured value of $Q = 90$ was reported in Reference 4. This corresponds, for $\eta = 0.8$ (about the value expected), to a spin state purity corresponding to 91.7% for deuterons and 94.5% for protons and tritons. However, preliminary data obtained at LASL suggest that this value may be high by a factor of ~ 2 . For intense beams, the achievable Q seems to be further reduced to about 30. If these preliminary indications are correct, a spin state purity of about 83% for protons and tritons, and 75% for deuterons, would be expected.

2. ENERGY LEVELS OF THE HYDROGEN ATOM

We begin by reviewing briefly some facts about the $n = 2$ energy levels of the hydrogen atom. Figure 1 shows the $n = 2$ energy levels in a weak external magnetic field. At zero magnetic field, the energy difference between the $n = 2$ and $n = 1$ states is $13.6(\frac{1}{1^2} - \frac{1}{2^2})eV = 10.15 eV$. The $2S_{1/2} - 2P_{1/2}$ level spacing (the Lamb shift) corresponds to about 1059 MHz while the $2P_{3/2} - 2P_{1/2}$ level separation corresponds to about 10,968 MHz. In a weak magnetic field, the $2P_{3/2}$ states are split into four magnetic substates and the $2P_{1/2}$ and $2S_{1/2}$ levels each split into two magnetic substates. The $2P_{3/2}$ substates are usually referred to as a (for $m_J = 3/2$), b (for

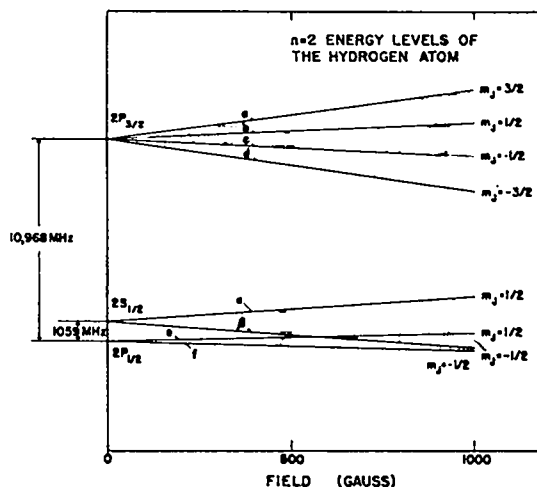


Fig. 1. The $n = 2$ levels of the hydrogen atom in a weak magnetic field; nuclear hyperfine structure is neglected.

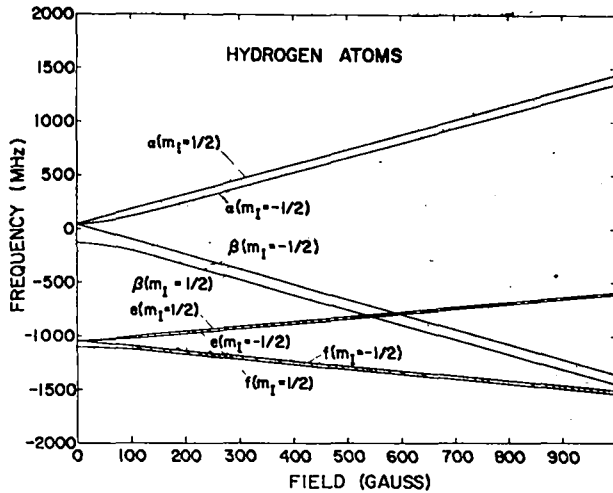


Fig. 2. The $2S_{1/2}$ and $2P_{1/2}$ levels of the hydrogen atom vs magnetic field with nuclear hyperfine structure included. The diagram for tritium atoms is nearly identical.

$m_J = 1/2$), c (for $m_J = -1/2$), and d (for $m_J = -3/2$). Similarly, the $2P_{1/2}$ states are referred to as e (for $m_J = 1/2$) and f (for $m_J = -1/2$); the $2S_{1/2}$ states are referred to as α (for $m_J = 1/2$) and β (for $m_J = -1/2$).

As shown in Figs. 2 and 3 for the $2S_{1/2}$ and $2P_{1/2}$ levels, which are the ones of primary interest here, the nuclear hyperfine interaction further modifies the energies. In sufficiently large magnetic fields, each magnetic substate, for hydrogen or tritium atoms, is split into two nuclear magnetic substates.

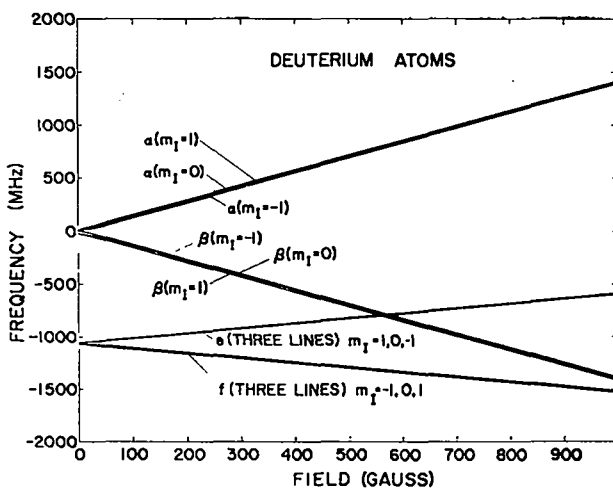


Fig. 3. The $2S_{1/2}$ and $2P_{1/2}$ levels of the deuterium atom vs magnetic field with nuclear hyperfine structure included. The order of the e and f levels is the same as the order of the α and β levels, respectively.

That is, there is a substate corresponding to each of the allowed nuclear magnetic quantum numbers $m_I = 1/2$ or $m_I = -1/2$. For deuterium atoms, where m_I can have the value 1, 0, or -1, each substate is split into three nuclear magnetic substates. Note that the order of the m_I substate energies is inverted when the electron spin m_J value is negative. The hyperfine energy level diagram for the $2S_{1/2}$ states is described by the Breit-Rabi formula:

$$W = \frac{\Delta W}{2(2I+1)} \pm \frac{\Delta W}{2} \left(1 + \frac{2m_F}{I+1/2} X + X^2 \right)^{1/2} + \epsilon \Delta W X m_F,$$

where

$$X = B/B_1,$$

$$B_1 = \Delta W(1 + \epsilon)/(g_J \mu_0),$$

$$\epsilon = 1 / \left(\frac{1836.1 g_J}{g_I} - 1 \right),$$

g_J = Lande g factor,

μ_0 = Bohr magneton,

B = magnetic field,

ΔW = zero field hyperfine splitting,

$g_I = \mu_I/I$ = nuclear g factor, and

$$m_F = m_J + m_I.$$

The last term arises from the interaction of the nuclear magnetic moment with the applied magnetic field and is, for ordinary magnetic fields, very small.

The Breit-Rabi formula is only approximate for the $2P_{1/2}$ levels since, for the field strengths of interest here, J is only an approximately good quantum number. An exact calculation requires the diagonalization of the Hamiltonian including both fine structure and hyperfine structure terms; in the numerical results presented below we have only applied a first order correction to the Breit-Rabi formula by shifting the e and f lines downward by an amount calculated from the solution to the fine structure Zeeman splitting problem. Referred to the mean value of the multiplet, the correction⁵ is $\Delta W = -\frac{h}{9} W \left(\frac{B}{5214 \text{ G}} \right)$. The values for the constants associated with the cases of interest are tabulated in Table I.

Table I
Parameters Characterizing the Hyperfine Structure of the $n = 2$ States
of Hydrogen, Deuterium, and Tritium Atoms

Nucleus	State	g_J	g_I	$\Delta W(\text{MHz})$	ϵ	B_1 (in G)
Proton	$2S_{1/2}$	2.00229	5.585486	177.551	1.522×10^{-3}	63.448
Proton	$2P_{1/2}$	0.66589	5.585486	59.190	4.589×10^{-3}	63.796
Deuteron	$2S_{1/2}$	2.00229	0.857407	40.924	0.233×10^{-3}	14.605
Deuteron	$2P_{1/2}$	0.66589	0.857407	13.640	0.702×10^{-3}	14.644
Triton	$2S_{1/2}$	2.00229	5.957680	189.588	1.623×10^{-3}	67.755
Triton	$2P_{1/2}$	0.66589	5.957680	63.200	4.897×10^{-3}	68.138

In the numerical tabulations of the energy levels (Tables II-VII), all energies are expressed in equivalent frequency units (MHz) and are referred to the centroid of the $2S_{1/2}$ zero field multiplet. The latest published values of the Lamb shift^{6,7} have been used in this calculation (1058.05 MHz for H atoms and 1059.34 MHz for D atoms). A value of 1058.05 MHz has been used for T atoms.

The states are labeled by their strong field quantum numbers. Note that, for sufficiently high fields, the frequency separation for states whose m_I values differ by 1 unit is $\Delta W/2$ for spin 1/2 particles and $\Delta W/3$ for spin 1 particles. Note also that the magnitude of the field B_1 , which is customarily thought of as the field value which defines the weak and strong field regions, is much smaller here than is the case for ground-state atoms.

3. SELECTION RULES

The angular momenta involved in the complete description of a one-electron atomic state are the orbital angular momentum \vec{l} ; the spin angular momentum \vec{s} ; and the nuclear spin angular momentum \vec{I} . In a very strong magnetic field (i.e. in the Paschen-Back region, which is $\sim 10^5$ G or greater for $n = 2$ hydrogen atoms) the quantities \vec{l} , \vec{s} , and \vec{I} are completely decoupled. Thus, transitions may be induced which involve only one of the pairs of quantum numbers l, m_l ; s, m_s ; or I, m_I . In weaker

fields where \vec{l} and \vec{s} couple to form \vec{J} (usually known as the strong field region, which is in the range $\sim 10^2$ - 10^4 G for $n = 2$ hydrogen atoms), transitions can be induced which involve either J, m_J or I, m_I . Finally, for very weak fields, \vec{J} and \vec{I} couple to form \vec{F} , and transitions will involve changes in F, m_F . For a one-electron atom, s is a constant; I is always constant in atomic physics.

We are concerned here only with the lowest order transitions; i.e., with electric and magnetic dipole transitions.

a. Electric Dipole Selection Rules

The electric dipole operator is $e(\vec{E} \cdot \vec{r})$, where e is the electronic charge, \vec{E} is an applied (possibly oscillating) electric field, and \vec{r} is the electron-nucleus radius vector. Since this operator is odd, it can have nonzero matrix elements only between states of opposite parity; i.e., Δl must be odd. Further, if one expands the operator into spherical components, it can be shown (Section 6) that $\Delta l = \pm 1$ is required.

For very strong fields, then, the selection rule is $\Delta l = \pm 1$; $\Delta m_l = 0, \pm 1$ and $\Delta m_I = \Delta m_s = 0$, since this operator does not affect the spin functions. For strong fields we have $\Delta J = 0, \pm 1$; $\Delta m_J = 0, \pm 1$ and $\Delta m_I = 0$. For weak fields, we have $\Delta F = 0, \pm 1$; $\Delta m_F = 0, \pm 1$. If $\Delta m = 0$, where m represents whichever quantity is appropriate among m_I, m_l, m_s, m_J , or

TABLE II
HYDROGEN ATOM 2S STATES

GAUSS	X	ALPHA STATES		BETA STATES	
		$M_l=0.5$	$M_l=-0.5$	$M_l=0.5$	$M_l=-0.5$
0.0	0.000	44.39	44.39	44.39	-133.16
20.0	.315	72.46	48.69	16.32	-137.47
40.0	.630	100.53	60.56	-11.75	-149.33
60.0	.946	128.60	77.80	-39.82	-166.57
80.0	1.261	156.66	98.48	-67.89	-187.25
100.0	1.576	184.73	121.32	-95.96	-210.09
120.0	1.891	212.80	145.54	-124.03	-234.32
140.0	2.207	240.87	170.68	-152.10	-259.45
160.0	2.522	268.94	196.44	-180.17	-285.22
180.0	2.837	297.01	222.66	-208.24	-311.43
200.0	3.152	325.08	249.20	-236.30	-337.97
220.0	3.467	353.15	275.98	-264.37	-364.76
240.0	3.783	381.22	302.96	-292.44	-391.73
260.0	4.098	409.29	330.08	-320.51	-418.86
280.0	4.413	437.36	357.32	-348.58	-446.10
300.0	4.728	465.43	384.66	-376.65	-473.43
320.0	5.044	493.49	412.07	-404.72	-500.85
340.0	5.359	521.56	439.55	-432.79	-528.33
360.0	5.674	549.63	467.09	-460.86	-555.86
380.0	5.989	577.70	494.67	-488.93	-583.44
400.0	6.304	605.77	522.29	-517.00	-611.07
420.0	6.620	633.84	549.94	-545.07	-638.72
440.0	6.935	661.91	577.63	-573.13	-666.40
460.0	7.250	689.98	605.34	-601.20	-694.11
480.0	7.565	718.05	633.07	-629.27	-721.85
500.0	7.881	746.12	660.82	-657.34	-749.60
520.0	8.196	774.19	688.59	-685.41	-777.37
540.0	8.511	802.26	716.38	-713.48	-805.15
560.0	8.826	830.33	744.18	-741.55	-832.95
580.0	9.141	858.39	771.99	-769.62	-860.77
600.0	9.457	886.46	799.81	-797.69	-888.59
620.0	9.772	914.53	827.65	-825.76	-916.42
640.0	10.087	942.60	855.49	-853.83	-944.27
660.0	10.402	970.67	883.34	-881.90	-972.12
680.0	10.718	998.74	911.20	-909.97	-999.98
700.0	11.033	1026.81	939.07	-938.03	-1027.84
720.0	11.348	1054.88	966.94	-966.10	-1055.72
740.0	11.663	1082.95	994.82	-994.17	-1083.60
760.0	11.978	1111.02	1022.70	-1022.24	-1111.48
780.0	12.294	1139.09	1050.59	-1050.31	-1139.37
800.0	12.609	1167.16	1078.49	-1078.38	-1167.26
820.0	12.924	1195.22	1106.39	-1106.45	-1195.16
840.0	13.239	1223.29	1134.29	-1134.52	-1223.07
860.0	13.555	1251.36	1162.20	-1162.59	-1250.97
880.0	13.870	1279.43	1190.11	-1190.66	-1278.88
900.0	14.185	1307.50	1218.02	-1218.73	-1306.79
920.0	14.500	1335.57	1245.94	-1246.80	-1334.71
940.0	14.815	1363.64	1273.85	-1274.86	-1362.63
960.0	15.131	1391.71	1301.78	-1302.93	-1390.55
980.0	15.446	1419.78	1329.70	-1331.00	-1418.48
1000.0	15.761	1447.85	1357.63	-1359.07	-1446.40

TABLE III

HYDROGEN ATOM 2P STATES

GAUSS	X	ALPHA STATES		BETA STATES	
		$M_l = 0.5$	$M_l = -0.5$	$M_l = 0.5$	$M_l = -0.5$
0.0	0.000	-1043.25	-1043.25	-1043.25	-1102.44
20.0	.314	-1033.93	-1041.86	-1052.63	-1103.94
40.0	.627	-1024.64	-1037.98	-1061.99	-1107.95
60.0	.941	-1015.38	-1032.35	-1071.41	-1113.76
80.0	1.254	-1006.16	-1025.60	-1080.86	-1120.74
100.0	1.568	-996.96	-1018.16	-1090.34	-1128.47
120.0	1.881	-987.80	-1010.29	-1099.86	-1136.69
140.0	2.195	-978.67	-1002.15	-1109.40	-1145.25
160.0	2.508	-969.57	-993.83	-1118.98	-1154.05
180.0	2.822	-960.50	-985.39	-1128.59	-1163.03
200.0	3.135	-951.47	-976.87	-1138.23	-1172.15
220.0	3.449	-942.46	-968.30	-1147.90	-1181.38
240.0	3.762	-933.49	-959.70	-1157.61	-1190.71
260.0	4.076	-924.55	-951.08	-1167.35	-1200.12
280.0	4.389	-915.65	-942.45	-1177.12	-1209.60
300.0	4.703	-906.77	-933.82	-1186.92	-1219.15
320.0	5.016	-897.93	-925.20	-1196.75	-1228.75
340.0	5.330	-889.12	-916.59	-1206.62	-1238.41
360.0	5.643	-880.34	-907.99	-1216.51	-1248.12
380.0	5.957	-871.59	-899.40	-1226.44	-1257.87
400.0	6.270	-862.87	-890.84	-1236.40	-1267.67
420.0	6.584	-854.19	-882.30	-1246.39	-1277.51
440.0	6.897	-845.54	-873.77	-1256.42	-1287.39
460.0	7.211	-836.92	-865.27	-1266.48	-1297.32
480.0	7.524	-828.33	-856.80	-1276.56	-1307.28
500.0	7.838	-819.77	-848.35	-1286.68	-1317.28
520.0	8.151	-811.25	-839.92	-1296.84	-1327.32
540.0	8.465	-802.76	-831.52	-1307.02	-1337.40
560.0	8.778	-794.30	-823.15	-1317.24	-1347.51
580.0	9.092	-785.87	-814.81	-1327.48	-1357.65
600.0	9.405	-777.47	-806.49	-1337.76	-1367.84
620.0	9.719	-769.11	-798.20	-1348.08	-1378.06
640.0	10.032	-760.78	-789.94	-1358.42	-1388.31
660.0	10.346	-752.48	-781.71	-1368.80	-1398.60
680.0	10.659	-744.21	-773.51	-1379.20	-1408.92
700.0	10.973	-735.97	-765.34	-1389.64	-1419.27
720.0	11.286	-727.77	-757.19	-1400.12	-1429.66
740.0	11.600	-719.59	-749.08	-1410.62	-1440.08
760.0	11.913	-711.45	-741.00	-1421.15	-1450.54
780.0	12.227	-703.34	-732.94	-1431.72	-1461.03
800.0	12.540	-695.27	-724.92	-1442.32	-1471.55
820.0	12.854	-687.22	-716.92	-1452.95	-1482.11
840.0	13.167	-679.21	-708.96	-1463.62	-1492.70
860.0	13.481	-671.23	-701.03	-1474.31	-1503.32
880.0	13.794	-663.28	-693.13	-1485.04	-1513.98
900.0	14.108	-655.36	-685.25	-1495.80	-1524.66
920.0	14.421	-647.47	-677.41	-1506.59	-1535.38
940.0	14.735	-639.62	-669.60	-1517.41	-1546.14
960.0	15.048	-631.80	-661.82	-1528.26	-1556.92
980.0	15.362	-624.01	-654.07	-1539.15	-1567.74
1000.0	15.675	-616.25	-646.35	-1550.07	-1578.59

TABLE IV

DEUTERIUM ATOM 2S STATES

		ALPHA STATES				BETA STATES			
GAUSS	X	M _I =1	M _I =0	M _I =-1	M _I =-1	M _I =0	M _I =1		
0.0	0.000	13.64	13.64	13.64	13.64	-27.28	-27.28		
20.0	1.369	41.68	33.01	21.84	-14.40	-35.49	-46.64		
40.0	2.739	69.72	58.95	46.03	-42.44	-59.70	-72.56		
60.0	4.108	97.76	86.10	72.77	-70.48	-86.45	-99.71		
80.0	5.477	125.80	113.66	100.17	-98.52	-113.86	-127.25		
100.0	6.847	153.84	141.39	127.82	-126.56	-141.52	-154.97		
120.0	8.216	181.88	169.22	155.59	-154.60	-169.31	-182.78		
140.0	9.586	209.92	197.10	183.43	-182.64	-197.17	-210.65		
160.0	10.955	237.96	225.02	211.32	-210.68	-225.07	-238.55		
180.0	12.324	266.00	252.96	239.24	-238.72	-253.00	-266.48		
200.0	13.694	294.04	280.91	267.17	-266.76	-280.95	-294.42		
220.0	15.063	322.08	308.88	295.12	-294.80	-308.91	-322.38		
240.0	16.432	350.12	336.86	323.09	-322.83	-336.88	-350.35		
260.0	17.802	378.16	364.85	351.06	-350.87	-364.87	-378.32		
280.0	19.171	406.20	392.84	379.03	-378.91	-392.86	-406.30		
300.0	20.541	434.24	420.83	407.01	-406.95	-420.85	-434.28		
320.0	21.910	462.28	448.83	435.00	-434.99	-448.85	-462.27		
340.0	23.279	490.32	476.84	462.99	-463.03	-476.85	-490.26		
360.0	24.649	518.36	504.84	490.98	-491.07	-504.85	-518.25		
380.0	26.018	546.40	532.85	518.97	-519.11	-532.86	-546.24		
400.0	27.387	574.44	560.86	546.97	-547.15	-560.87	-574.24		
420.0	28.757	602.47	588.87	574.96	-575.19	-588.88	-602.24		
440.0	30.126	630.51	616.88	602.96	-603.23	-616.89	-630.24		
460.0	31.496	658.55	644.90	630.96	-631.27	-644.90	-658.24		
480.0	32.865	686.59	672.91	658.96	-659.31	-672.92	-686.24		
500.0	34.234	714.63	700.93	686.97	-687.35	-700.93	-714.24		
520.0	35.604	742.67	728.95	714.97	-715.39	-728.95	-742.25		
540.0	36.973	770.71	756.96	742.97	-743.43	-756.97	-770.25		
560.0	38.342	798.75	784.98	770.98	-771.47	-784.98	-798.26		
580.0	39.712	826.79	813.00	798.98	-799.51	-813.00	-826.26		
600.0	41.081	854.83	841.02	826.99	-827.55	-841.02	-854.27		
620.0	42.451	882.87	869.04	854.99	-855.59	-869.04	-882.27		
640.0	43.820	910.91	897.06	883.00	-883.63	-897.06	-910.28		
660.0	45.189	938.95	925.08	911.01	-911.67	-925.08	-938.29		
680.0	46.559	966.99	953.10	939.02	-939.71	-953.10	-966.30		
700.0	47.928	995.03	981.12	967.02	-967.75	-981.12	-994.30		
720.0	49.297	1023.07	1009.14	995.03	-995.79	-1009.14	-1022.31		
740.0	50.667	1051.11	1037.16	1023.04	-1023.83	-1037.17	-1050.32		
760.0	52.036	1079.15	1065.19	1051.05	-1051.87	-1065.19	-1078.33		
780.0	53.405	1107.19	1093.21	1079.06	-1079.91	-1093.21	-1106.34		
800.0	54.775	1135.23	1121.23	1107.07	-1107.95	-1121.23	-1134.35		
820.0	56.144	1163.27	1149.25	1135.08	-1135.99	-1149.25	-1162.36		
840.0	57.514	1191.31	1177.28	1163.09	-1164.03	-1177.28	-1190.37		
860.0	58.883	1219.35	1205.30	1191.10	-1192.07	-1205.30	-1218.38		
880.0	60.252	1247.39	1233.32	1219.11	-1220.11	-1233.32	-1246.39		
900.0	61.622	1275.43	1261.34	1247.12	-1248.14	-1261.35	-1274.40		
920.0	62.991	1303.47	1289.37	1275.13	-1276.18	-1289.37	-1302.41		
940.0	64.360	1331.51	1317.39	1303.14	-1304.22	-1317.39	-1330.42		
960.0	65.730	1359.55	1345.42	1331.15	-1332.26	-1345.42	-1358.43		
980.0	67.099	1387.59	1373.44	1359.16	-1360.30	-1373.44	-1386.44		
1000.0	68.469	1415.63	1401.46	1387.17	-1388.34	-1401.46	-1414.45		

TABLE V

DEUTERIUM ATOM 2P STATES

ALPHA STATES				BETA STATES			
GAUSS	X	M _I =1	M _I =0	M _I =-1	M _I =-1	M _I =0	M _I =1
0.0	0.000	-1054.79	-1054.79	-1054.79	-1054.79	-1068.43	-1068.43
20.0	1.366	-1045.48	-1048.37	-1052.10	-1064.14	-1071.18	-1074.89
40.0	2.731	-1036.20	-1039.80	-1044.10	-1073.51	-1079.27	-1083.55
60.0	4.097	-1026.96	-1030.85	-1035.29	-1082.92	-1088.24	-1092.66
80.0	5.463	-1017.74	-1021.79	-1026.30	-1092.35	-1097.47	-1101.93
100.0	6.829	-1008.56	-1012.72	-1017.25	-1101.82	-1106.81	-1111.29
120.0	8.194	-999.41	-1003.64	-1008.18	-1111.32	-1116.23	-1120.71
140.0	9.560	-990.29	-994.57	-999.13	-1120.86	-1125.70	-1130.18
160.0	10.926	-981.20	-985.53	-990.10	-1130.42	-1135.21	-1139.70
180.0	12.292	-972.15	-976.50	-981.08	-1140.02	-1144.77	-1149.26
200.0	13.657	-963.12	-967.51	-972.09	-1149.65	-1154.37	-1158.85
220.0	15.023	-954.13	-958.54	-963.13	-1159.31	-1164.00	-1168.48
240.0	16.389	-945.17	-949.60	-954.20	-1169.00	-1173.67	-1178.14
260.0	17.755	-936.24	-940.69	-945.30	-1178.72	-1183.37	-1187.84
280.0	19.120	-927.35	-931.81	-936.42	-1188.48	-1193.11	-1197.57
300.0	20.486	-918.48	-922.96	-927.58	-1198.27	-1202.88	-1207.34
320.0	21.852	-909.65	-914.14	-918.76	-1208.09	-1212.69	-1217.14
340.0	23.217	-900.85	-905.35	-909.98	-1217.94	-1222.52	-1226.97
360.0	24.583	-892.08	-896.60	-901.23	-1227.82	-1232.39	-1236.83
380.0	25.949	-883.34	-887.87	-892.51	-1237.73	-1242.29	-1246.73
400.0	27.315	-874.64	-879.17	-883.81	-1247.68	-1252.23	-1256.66
420.0	28.680	-865.96	-870.51	-875.16	-1257.66	-1262.20	-1266.62
440.0	30.046	-857.32	-861.88	-866.53	-1267.67	-1272.20	-1276.61
460.0	31.412	-848.71	-853.27	-857.93	-1277.71	-1282.23	-1286.64
480.0	32.778	-840.13	-844.70	-849.36	-1287.79	-1292.29	-1296.69
500.0	34.143	-831.58	-836.17	-840.83	-1297.89	-1302.39	-1306.78
520.0	35.509	-823.07	-827.66	-832.33	-1308.03	-1312.51	-1316.91
540.0	36.875	-814.59	-819.18	-823.86	-1318.20	-1322.67	-1327.06
560.0	38.241	-806.14	-810.74	-815.42	-1328.40	-1332.87	-1337.24
580.0	39.606	-797.72	-802.33	-807.01	-1338.63	-1343.09	-1347.46
600.0	40.972	-789.33	-793.95	-798.63	-1348.90	-1353.34	-1357.71
620.0	42.338	-780.97	-785.60	-790.29	-1359.20	-1363.63	-1367.99
640.0	43.703	-772.65	-777.28	-781.97	-1369.53	-1373.95	-1378.30
660.0	45.069	-764.36	-768.99	-773.69	-1379.89	-1384.30	-1388.65
680.0	46.435	-756.10	-760.74	-765.44	-1390.28	-1394.69	-1399.03
700.0	47.801	-747.87	-752.52	-757.22	-1400.70	-1405.10	-1409.43
720.0	49.166	-739.67	-744.33	-749.03	-1411.16	-1415.55	-1419.88
740.0	50.532	-731.51	-736.17	-740.88	-1421.65	-1426.03	-1430.35
760.0	51.898	-723.38	-728.04	-732.76	-1432.17	-1436.54	-1440.85
780.0	53.264	-715.28	-719.94	-724.66	-1442.72	-1447.08	-1451.39
800.0	54.629	-707.21	-711.88	-716.60	-1453.30	-1457.66	-1461.96
820.0	55.995	-699.17	-703.85	-708.57	-1463.92	-1468.26	-1472.55
840.0	57.361	-691.16	-695.85	-700.58	-1474.56	-1478.90	-1483.19
860.0	58.727	-683.19	-687.88	-692.61	-1485.24	-1489.57	-1493.85
880.0	60.092	-675.25	-679.94	-684.68	-1495.95	-1500.28	-1504.54
900.0	61.458	-667.34	-672.03	-676.78	-1506.69	-1511.01	-1515.27
920.0	62.824	-659.46	-664.16	-668.90	-1517.47	-1521.77	-1526.03
940.0	64.189	-651.61	-656.32	-661.07	-1528.27	-1532.57	-1536.82
960.0	65.555	-643.80	-648.51	-653.26	-1539.11	-1543.40	-1547.64
980.0	66.921	-636.02	-640.73	-645.48	-1549.98	-1554.26	-1558.50
1000.0	68.287	-628.27	-632.98	-637.74	-1560.88	-1565.16	-1569.38

TABLE VI
TRITIUM ATOM 2S STATES

		ALPHA STATES		BETA STATES	
GAUSS	X	MI=0.5	MI=-0.5	MI=-0.5	MI=0.5
0.0	0.000	47.40	47.40	47.40	-142.19
20.0	.295	75.47	51.44	19.32	-146.23
40.0	.590	103.54	62.68	-8.75	-157.48
60.0	.886	131.61	79.22	-36.82	-174.02
80.0	1.181	159.69	99.28	-64.89	-194.07
100.0	1.476	187.76	121.60	-92.96	-216.39
120.0	1.771	215.83	145.40	-121.04	-240.20
140.0	2.066	243.90	170.20	-149.11	-265.00
160.0	2.361	271.97	195.70	-177.18	-290.49
180.0	2.657	300.05	221.68	-205.25	-316.48
200.0	2.952	328.12	248.04	-233.32	-342.83
220.0	3.247	356.19	274.66	-261.40	-369.46
240.0	3.542	384.26	301.50	-289.47	-396.30
260.0	3.837	412.33	328.51	-317.54	-423.30
280.0	4.133	440.41	355.65	-345.61	-450.44
300.0	4.428	468.48	382.89	-373.68	-477.69
320.0	4.723	496.55	410.23	-401.76	-505.02
340.0	5.018	524.62	437.64	-429.83	-532.43
360.0	5.313	552.69	465.11	-457.90	-559.90
380.0	5.608	580.77	492.63	-485.97	-587.42
400.0	5.904	608.84	520.20	-514.04	-614.99
420.0	6.199	636.91	547.81	-542.12	-642.60
440.0	6.494	664.98	575.45	-570.19	-670.24
460.0	6.789	693.05	603.11	-598.26	-697.91
480.0	7.084	721.13	630.81	-626.33	-725.60
500.0	7.379	749.20	658.53	-654.40	-753.32
520.0	7.675	777.27	686.26	-682.48	-781.06
540.0	7.970	805.34	714.02	-710.55	-808.81
560.0	8.265	833.41	741.79	-738.62	-836.58
580.0	8.560	861.49	769.58	-766.69	-864.37
600.0	8.855	889.56	797.37	-794.76	-892.17
620.0	9.151	917.63	825.18	-822.84	-919.98
640.0	9.446	945.70	853.01	-850.91	-947.80
660.0	9.741	973.77	880.84	-878.98	-975.63
680.0	10.036	1001.85	908.67	-907.05	-1003.47
700.0	10.331	1029.92	936.52	-935.12	-1031.32
720.0	10.626	1057.99	964.38	-963.20	-1059.17
740.0	10.922	1086.06	992.24	-991.27	-1087.03
760.0	11.217	1114.13	1020.11	-1019.34	-1114.90
780.0	11.512	1142.21	1047.98	-1047.41	-1142.77
800.0	11.807	1170.28	1075.86	-1075.48	-1170.65
820.0	12.102	1198.35	1103.74	-1103.56	-1198.54
840.0	12.398	1226.42	1131.63	-1131.63	-1226.42
860.0	12.693	1254.49	1159.52	-1159.70	-1254.32
880.0	12.988	1282.57	1187.42	-1187.77	-1282.21
900.0	13.283	1310.64	1215.32	-1215.84	-1310.11
920.0	13.578	1338.71	1243.22	-1243.92	-1338.02
940.0	13.873	1366.78	1271.13	-1271.99	-1365.93
960.0	14.169	1394.85	1299.04	-1300.06	-1393.84
980.0	14.464	1422.93	1326.95	-1328.13	-1421.75
1000.0	14.759	1451.00	1354.87	-1356.20	-1449.66

TABLE VII

TRITIUM ATOM 2P STATES

		ALPHA STATES		BETA STATES	
GAUSS	X	MI=0.5	MI=-0.5	MI=0.5	MI=-0.5
0.0	0.000	-1042.25	-1042.25	-1042.25	-1105.45
20.0	.294	-1032.93	-1040.95	-1051.63	-1106.87
40.0	.587	-1023.64	-1037.28	-1060.99	-1110.67
60.0	.881	-1014.38	-1031.88	-1070.41	-1116.25
80.0	1.174	-1005.15	-1025.34	-1079.86	-1123.03
100.0	1.468	-995.95	-1018.07	-1089.35	-1130.58
120.0	1.761	-986.79	-1010.34	-1098.86	-1138.66
140.0	2.055	-977.66	-1002.31	-1108.41	-1147.11
160.0	2.348	-968.56	-994.08	-1117.99	-1155.82
180.0	2.642	-959.49	-985.72	-1127.60	-1164.72
200.0	2.935	-950.45	-977.26	-1137.24	-1173.78
220.0	3.229	-941.45	-968.75	-1146.91	-1182.96
240.0	3.522	-932.48	-960.19	-1156.62	-1192.24
260.0	3.816	-923.54	-951.61	-1166.36	-1201.62
280.0	4.109	-914.63	-943.02	-1176.13	-1211.06
300.0	4.403	-905.75	-934.42	-1185.93	-1220.58
320.0	4.696	-896.91	-925.82	-1195.77	-1230.15
340.0	4.990	-888.10	-917.24	-1205.63	-1239.79
360.0	5.283	-879.32	-908.66	-1215.53	-1249.47
380.0	5.577	-870.57	-900.09	-1225.46	-1259.20
400.0	5.871	-861.85	-891.55	-1235.42	-1268.99
420.0	6.164	-853.17	-883.02	-1245.42	-1278.81
440.0	6.458	-844.51	-874.51	-1255.44	-1288.68
460.0	6.751	-835.89	-866.02	-1265.50	-1298.59
480.0	7.045	-827.30	-857.56	-1275.59	-1308.54
500.0	7.338	-818.75	-849.12	-1285.71	-1318.53
520.0	7.632	-810.22	-840.71	-1295.87	-1328.55
540.0	7.925	-801.73	-832.32	-1306.05	-1338.62
560.0	8.219	-793.27	-823.96	-1316.27	-1348.72
580.0	8.512	-784.84	-815.62	-1326.52	-1358.86
600.0	8.806	-776.44	-807.31	-1336.80	-1369.03
620.0	9.099	-768.08	-799.03	-1347.11	-1379.24
640.0	9.393	-759.74	-790.78	-1357.46	-1389.49
660.0	9.686	-751.44	-782.56	-1367.84	-1399.77
680.0	9.980	-743.17	-774.36	-1378.25	-1410.08
700.0	10.273	-734.93	-766.20	-1388.69	-1420.43
720.0	10.567	-726.73	-758.06	-1399.16	-1430.81
740.0	10.860	-718.55	-749.95	-1409.66	-1441.23
760.0	11.154	-710.41	-741.87	-1420.20	-1451.68
780.0	11.448	-702.30	-733.82	-1430.77	-1462.16
800.0	11.741	-694.23	-725.80	-1441.37	-1472.68
820.0	12.035	-686.18	-717.82	-1452.00	-1483.23
840.0	12.328	-678.17	-709.86	-1462.67	-1493.81
860.0	12.622	-670.18	-701.93	-1473.37	-1504.43
880.0	12.915	-662.23	-694.03	-1484.09	-1515.08
900.0	13.209	-654.32	-686.16	-1494.85	-1525.76
920.0	13.502	-646.43	-678.32	-1505.65	-1536.48
940.0	13.796	-638.57	-670.52	-1516.47	-1547.23
960.0	14.089	-630.75	-662.74	-1527.33	-1558.01
980.0	14.383	-622.96	-655.00	-1538.22	-1568.82
1000.0	14.676	-615.20	-647.28	-1549.14	-1579.67

m_F , the field required to induce the transition is parallel to the quantization axis, while if $\Delta m = \pm 1$, it is perpendicular to the quantization axis.

b. Magnetic Dipole Selection Rules

The magnetic dipole operator is of the form $-\vec{\mu} \cdot \vec{B}$, where \vec{B} is usually an oscillating or rotating magnetic field, and where $\vec{\mu}$ may be an electronic or nuclear magnetic moment. This operator can have nonzero matrix elements only between states of the same parity. This means, at least for the present case, $\Delta l = 0$.

For very strong fields we have $\Delta m_L = 0, \pm 1$ and $\Delta l = \Delta m_L = \Delta m_S = 0$; or $\Delta m_S = 0, \pm 1$ and $\Delta l = \Delta m_L = \Delta m_I = 0$. For intermediate fields we have $\Delta J = 0, \pm 1$; $\Delta m_J = 0, \pm 1$ and $\Delta m_I = 0$; or $\Delta m_I = 0, \pm 1$ and $\Delta J = \Delta m_J = 0$. For weak fields we have $\Delta F = 0, \pm 1$, $\Delta m_F = 0, \pm 1$. Again the magnitude of Δm determines, in the same way as above, the parallel or perpendicular nature of the field required to induce the transition.

Finally, we note that $F = 0 \rightarrow F = 0$ is absolutely forbidden for one-quantum transitions.

4. DISCUSSION OF THE GENERAL SPIN STATE SELECTION PROBLEM

A wide assortment of methods exists which might be used to polarize a metastable hydrogen atomic beam. This is in contrast to the problem of spin state selection in an ordinary (ground state) hydrogen atomic beam where only magnetic dipole transitions between the various hyperfine components, or adiabatic reduction of the magnetic field, may be considered.

It is believed that a "three-level interaction," in which the applied fields may simultaneously cause transitions among three levels, offers the best solution to the selection problem. This technique, which was first demonstrated and explained by Lamb and Retherford,⁵ and Lamb,⁸ is the method used in the LASL ion source. However, we first consider some of the various other possibilities by which a polarized metastable atomic beam may be produced.

In a magnetic field of about 575 G the β and e states become degenerate. If a small (a few V/cm) transverse electric field is applied, the β -states are coupled to the short-lived e -states (the half-life of the e -states is ~ 1.6 nsec) and decay rapidly.

Thus one can obtain a beam of α metastables. Such a beam is analogous to the beam obtained in conventional polarized ion sources after separation in a quadrupole or sextupole field. That is, there is 100% electronic polarization but no nuclear polarization. Such a beam could then be converted to a partially polarized negative ion beam by adiabatically reducing the magnetic field to near zero before the $H^{2S} + A \rightarrow H^- + A^+$ reaction is allowed to occur. However, these particles have a relatively high velocity ($\sim 3 \times 10^7$ cm/sec) and thus a long and carefully designed decreasing B field region is probably needed. Drake and Krotkov,⁹ who first used this method, attributed the fact that they obtained only $\sim 2/3$ of the theoretical polarization to an inadequate length in their B field transition region.

To obtain increased polarization, one must turn to a selective transition scheme of some sort. We first consider the use of a magnetic dipole transition between a particular α state and a particular β state in exactly the fashion often used in conventional polarized ion sources. One finds, however (see Section 6), that the electric dipole matrix elements are of the order of $1/\alpha$ (≈ 137) times larger than the magnetic dipole matrix elements. Even though a line through an rf cavity can be found where B is maximum and E is zero, for practical beam sizes the average E field will be sufficiently large to make the electric dipole transition rate far exceed the magnetic dipole transition rate.

We ask if these electric dipole transitions might be directly employed for our purposes. For hydrogen or tritium atoms the α -f frequency separation for the two m_I values is approximately 120 MHz; this is to be compared with the natural width of 100 MHz for the f (and e) levels. Thus one could possibly obtain a reasonable polarization with such a transverse electric field transition. However, both the beam intensity and polarization depend critically on the rf power level. For deuterium atoms the corresponding frequency separation is only about 18 MHz, so for this case the method is infeasible. The corresponding α -e (longitudinal electric field) transitions are separated by one-half the corresponding α -f separation; thus these

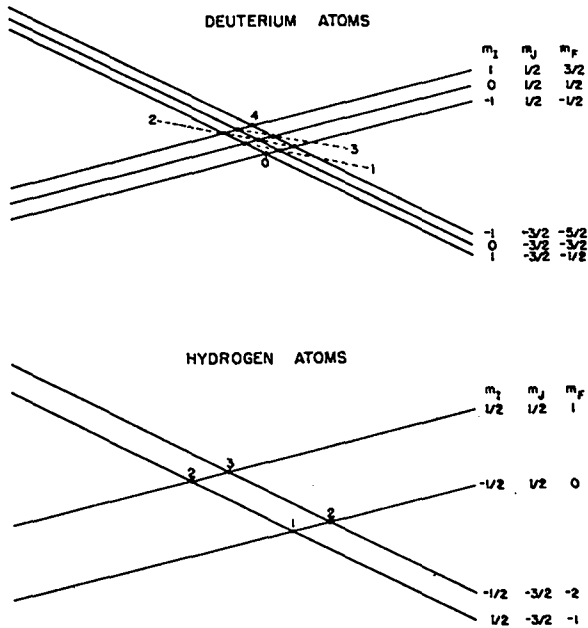


Fig. 4. Schematic diagram of the α -d crossing; the numbers correspond to the Δm_F required for a transition between the two crossing states.

transitions would be even less favorable.

It has been demonstrated¹⁰ that at the α -d crossing (~ 2360 G) a static electric field may be used to preferentially quench a single nuclear spin state. For protons or tritons, only $\alpha(m_I = -1/2)$ and $d(m_I = 1/2)$ can be coupled by electric dipole radiation. Since this transition violates the strong field selection rules $\Delta m_I = 0$, $\Delta m_J = 0, \pm 1$, it is "first-order forbidden." However, the remaining transitions involve $\Delta m_F > 1$ and, because they are incompatible with dipole radiation, are more highly forbidden. Figure 4 illustrates this situation for both spin 1/2 and spin 1 nuclei. It is seen that, in the deuteron case, two transitions are compatible with $\Delta m_F = 1$ (transverse electric field) and one with $\Delta m_F = 0$ (longitudinal electric field). Thus one could selectively quench one magnetic substate for spin 1/2 systems and either one or two magnetic substates for spin 1 systems. Since the transitions here are first-order forbidden, relatively large electric fields are needed and serious loss will occur through the α -f or α -e transitions. It has been estimated¹⁰ that, for protons, one might obtain 50% polarization with 25% α state survival.

Another proposal¹¹ involves the use of a radio-

frequency transition at zero magnetic field. The $2S_{1/2}(F = 1)$ level may be coupled to the $2P_{1/2}(F = 0)$ level by longitudinal or transverse radiation of the appropriate frequency. A small magnetic field is permissible if both transverse and longitudinal radiations are present. The $2S_{1/2}(F = 0)$ state is not appreciably quenched by coupling to the $2P_{1/2}(F = 1)$ state because the frequency difference is ~ 236 MHz; the $2S_{1/2}(F = 0)$ to $2P_{1/2}(F = 0)$ transition is strictly forbidden. Thus, one might obtain a pure $2S_{1/2}(F = 0)$ metastable beam. If the field were then adiabatically increased to a high value, the metastable beam would have 100% nuclear and 100% electronic longitudinal polarization. This scheme, however, is applicable only to protons or tritons.

5. QUANTUM MECHANICAL FORMULATION OF THE FOUR-LEVEL PROBLEM

We consider only the four-level system $\alpha, \beta, e,$ and f since the $2P_{3/2}$ levels are sufficiently distant to have no significant effect on our problem. In addition, since we are working in a strong magnetic field, the nuclear magnetic quantum number m_I is conserved and we may therefore consider separately each group of four atomic levels associated with a particular nuclear spin orientation.

For the amplitudes of the $\alpha, \beta, e,$ and f states, we use the notation $a, b, c,$ and d . We use ω (with or without subscripts) to denote an angular frequency.

The Schrodinger equation may be written:

$$(H_0 + H')\psi = i\hbar \frac{\partial \psi}{\partial t},$$

where H_0 is a time-independent Hamiltonian whose eigenfunctions satisfy the equation $H_0 u_n = E_n u_n$. If the exact wave function is written in the form

$$\psi = \sum a_n(t) u_n e^{-iE_n t/\hbar},$$

it is easy to show that the coefficients $a_n(t)$ must satisfy the differential equations

$$i\hbar \dot{a}_k = \sum H'_{kn} a_n e^{i\omega_{kn} t},$$

where

$$\omega_{kn} = (E_k - E_n)/\hbar,$$

and

$$H'_{kn} = \int u_k^* H' u_n d\tau.$$

For the four-level case, these equations may be written out explicitly as:

$$\begin{bmatrix} i\hbar\dot{a} \\ i\hbar\dot{b} \\ i\hbar\dot{c} \\ i\hbar\dot{d} \end{bmatrix} = \begin{bmatrix} 0 & H'_{\alpha\beta} e^{i\omega_{\alpha\beta}t} \\ H'_{\beta\alpha} e^{i\omega_{\beta\alpha}t} & 0 \\ H'_{e\alpha} e^{i\omega_{e\alpha}t} & H'_{e\beta} e^{i\omega_{e\beta}t} \\ H'_{f\alpha} e^{i\omega_{f\alpha}t} & H'_{f\beta} e^{i\omega_{f\beta}t} \end{bmatrix} \begin{bmatrix} H'_{ae} e^{i\omega_{ae}t} & H'_{af} e^{i\omega_{af}t} \\ H'_{\beta e} e^{i\omega_{\beta e}t} & H'_{\beta f} e^{i\omega_{\beta f}t} \\ -i\gamma/2 & H'_{ef} e^{i\omega_{ef}t} \\ H'_{fe} e^{i\omega_{fe}t} & -i\gamma/2 \end{bmatrix} \begin{bmatrix} a \\ b \\ c \\ d \end{bmatrix}$$

where the damping terms $-i\gamma/2$ and $-i\gamma_d/2$ have been added to account for the decay of the e and f states. Except for the damping terms, the above matrix is Hermitian. The α - β and e-f transitions may be induced only by a transverse magnetic field; the α -f and β -e transitions may be induced only by a transverse electric field; and the α -e and β -f transitions may be induced only by a longitudinal electric field.

We assume a longitudinal oscillating electric field (angular frequency ω), with an associated transverse oscillating magnetic field, and a transverse static electric field. The matrix elements may then be written in the form

$$\begin{aligned} H'_{\beta\alpha} &= \hbar M \cos \omega t \\ H'_{fe} &= \hbar M' \cos \omega t \end{aligned}$$

$$\begin{aligned} H'_{e\alpha} &= \hbar R \cos \omega t \\ H'_{f\beta} &= \hbar R' \cos \omega t \\ H'_{e\beta} &= \hbar V \\ H'_{f\alpha} &= \hbar V' \end{aligned}$$

where M and M' represent magnetic dipole matrix elements, R and R' represent longitudinal electric dipole matrix elements, and V and V' represent transverse electric dipole matrix elements. (The notation R and V is selected since R and R' will be associated with a radio-frequency electric field, and V and V' will be associated with a static electric field.) These matrix elements are discussed in Section 6; for the present we merely observe that the magnitude of dipole matrix elements is directly proportional to the relevant applied field. Note that the unprimed matrix elements relate to the e level, and the primed matrix elements relate to the f level.

In this notation our equations become:

$$\begin{bmatrix} i\dot{a} \\ i\dot{b} \\ i\dot{c} \\ i\dot{d} \end{bmatrix} = \begin{bmatrix} 0 & M^* e^{i\omega_{\alpha\beta}t} \cos \omega t \\ M e^{-i\omega_{\alpha\beta}t} \cos \omega t & 0 \\ R e^{-i\omega_{e\alpha}t} \cos \omega t & V e^{-i\omega_{\beta e}t} \\ V' e^{-i\omega_{\alpha f}t} & R' e^{-i\omega_{\beta f}t} \cos \omega t \end{bmatrix} \begin{bmatrix} R^* e^{i\omega_{ae}t} \cos \omega t & V'^* e^{i\omega_{af}t} \\ V^* e^{i\omega_{\beta e}t} & R'^* e^{i\omega_{\beta f}t} \cos \omega t \\ -i\gamma/2 & M'^* e^{i\omega_{ef}t} \cos \omega t \\ M' e^{-i\omega_{ef}t} \cos \omega t & -i\gamma/2 \end{bmatrix} \begin{bmatrix} a \\ b \\ c \\ d \end{bmatrix}$$

The equations are used in this form for the numerical integration studies discussed in Sections 8 and 9. However, the effect of the f state on the system is not large--it merely causes a slow overall decay of the metastable beam. For our first discussion of the system, we neglect the f level effects.

Also, except in the numerical integration studies, we follow the standard practice¹² and drop the term in $\cos \omega t = \frac{1}{2} (e^{i\omega t} + e^{-i\omega t})$ which is incapable of resonance. (We note that this approximation cannot be made for both frequencies if one uses an oscillating transverse electric field as well as an oscillating longitudinal electric field, since then at least two frequency terms can always resonate. In fact, one then obtains interference between the two contributions.) With these approximations the equations become:

$$\begin{bmatrix} i\dot{a} \\ i\dot{b} \\ i\dot{c} \end{bmatrix} = \begin{bmatrix} 0 & M^* e^{i(\omega_{\alpha\beta} - \omega)t} \\ M e^{-i(\omega_{\alpha\beta} - \omega)t} & 0 \\ R e^{-i(\omega_{\alpha e} - \omega)t} & V e^{-i\omega_{\beta e} t} \end{bmatrix} \begin{bmatrix} a \\ b \\ c \end{bmatrix}$$

These are the equations given by Lamb.⁸ In Section 7 we follow the method indicated by Lamb to obtain an analytic solution to these equations for the special case of constant field magnitudes during the interaction time.

6. MATRIX ELEMENTS

Neglecting the nuclear hyperfine interaction, the wave functions which describe the $n = 2$ states of the hydrogen atom may be written in the form given in Table VIII.* The coefficients $\epsilon_1 - \epsilon_4$ can be expressed as follows. Define the dimensionless parameter $\xi = \mu_B B / \Delta E$, where ΔE is the fine structure splitting (10,968 MHz). (ξ becomes unity at a field of about 7800 G; thus, as far as fine structure is concerned, we are interested primarily in the weak field region. Accordingly, Table VIII is subdivided into the weak field groups (where J and m_J are good quantum numbers) although the wave functions are exact for all fields.) We may write

$$\epsilon_1 = \sqrt{\frac{3}{4}(1 + \delta_+)}$$

$$\epsilon_2 = \sqrt{\frac{3}{2}(1 - \delta_+)}$$

$$\epsilon_3 = \sqrt{\frac{3}{2}(1 + \delta_-)}$$

$$\epsilon_4 = \sqrt{\frac{3}{4}(1 - \delta_-)}$$

where

$$\delta_+ = (\xi + 1/3) / \sqrt{1 + 2\xi/3 + \xi^2}$$

and

$$\delta_- = (\xi - 1/3) / \sqrt{1 - 2\xi/3 + \xi^2}$$

The quantities ξ , δ_+ , δ_- , and $\epsilon_1 - \epsilon_4$ are tabulated,

$$\begin{bmatrix} R^* e^{i(\omega_{\alpha e} - \omega)t} \\ V^* e^{i\omega_{\beta e} t} \\ -i\gamma/2 \end{bmatrix} \begin{bmatrix} a \\ b \\ c \end{bmatrix}$$

for various magnetic fields, in Table IX. We note that, for zero field, $\xi_+ \rightarrow 1/3$, $\xi_- \rightarrow -1/3$ and $\epsilon_1 - \epsilon_4$ become unity. In that case, the coefficients in Table IX become the usual Clebsch-Gordan coefficients which couple angular momenta 1 and 1/2. For large fields, $\xi_+ \rightarrow 1$ and $\xi_- \rightarrow 1$; thus ϵ_2 and ϵ_4 become zero while $\epsilon_1 \rightarrow \sqrt{3}/2$ and $\epsilon_3 \rightarrow \sqrt{3}$. In this case, we obtain the wave functions for which l , m_l , s , and m_s are the appropriate quantum numbers.

We now consider the effect of the nuclear hyperfine

* The values of $\epsilon_1 - \epsilon_4$ were obtained from Bethe and Salpeter,¹³ Section 46. The Clebsch-Gordan coefficients and angular functions used throughout this section are, however, those of Condon and Shortley.¹⁴ The tables of matrix elements given in Ref. 13 may be used if account is taken of the $(-1)^m$ difference in phase conventions for the spherical harmonics.

TABLE VIII

n = 2 Hydrogen Atom Wave Functions in a Magnetic Field

Multiplet	State	m_J	Function
$2P_{3/2}$	a	3/2	$R_{21}\psi_{11} \quad (\uparrow)$
	b	1/2	$\sqrt{\frac{2}{3}}\epsilon_1 R_{21}\psi_{10} \quad (\uparrow) + \sqrt{\frac{1}{3}}\epsilon_2 R_{21}\psi_{11} \quad (\uparrow)$
	c	-1/2	$\sqrt{\frac{1}{3}}\epsilon_3 R_{21}\psi_{1-1} \quad (\uparrow) + \sqrt{\frac{2}{3}}\epsilon_4 R_{21}\psi_{10} \quad (\uparrow)$
	d	-3/2	$R_{21}\psi_{1-1} \quad (\uparrow)$
$2P_{1/2}$	e	1/2	$-\sqrt{\frac{1}{3}}\epsilon_2 R_{21}\psi_{10} \quad (\uparrow) \quad \sqrt{\frac{2}{3}}\epsilon_1 R_{21}\psi_{11} \quad (\uparrow)$
	f	-1/2	$-\sqrt{\frac{2}{3}}\epsilon_4 R_{21}\psi_{1-1} \quad (\uparrow) + \sqrt{\frac{1}{3}}\epsilon_3 R_{21}\psi_{10} \quad (\uparrow)$
$2S_{1/2}$	α	1/2	$R_{20}\psi_{00} \quad (\uparrow)$
	β	-1/2	$R_{20}\psi_{00} \quad (\uparrow)$

NOTATION

 (\uparrow) and (\downarrow) are electron spinors

$$R_{20} = \frac{1}{\sqrt{2}} e^{-\frac{1}{2}r} (1 - \frac{1}{2}r)$$

$$R_{21} = \frac{1}{2\sqrt{6}} r e^{-\frac{1}{2}r}$$

$$\psi_{11} = -\sqrt{\frac{3}{8\pi}} \sin\theta e^{i\phi}$$

$$\psi_{10} = \sqrt{\frac{3}{4\pi}} \cos\theta$$

$$\psi_{1-1} = \sqrt{\frac{3}{8\pi}} \sin\theta e^{-i\phi}$$

$$\psi_{00} = \sqrt{\frac{1}{4\pi}}$$

TABLE IX
Factors Required for the Computation of the Hydrogen Atom Wave Functions
in an Arbitrary Magnetic Field

Field (G)	ξ	δ_+	δ_-	ϵ_1	ϵ_2	ϵ_3	ϵ_4
0	0	.3333	-.3333	1	1	1	1
390	.05	.3833	-.2833	1.016	.983	1.034	.967
780	.1	.4333	-.2333	1.031	.965	1.068	.935
3,900	.5	.8333	-.1666	1.117	.872	1.113	.712
7,800	1.0	1.3333	+.6666	1.167	.563	1.538	.525
39,000	5.0	5.3333	4.6666	1.220	.122	1.724	.152
78,000	10.0	10.3333	9.6666	1.224	.084	1.730	.111

interaction. The magnetic fields of interest are in the region of 500-600 G. The parameter which defines the strong and weak field regions (with respect to the hyperfine interaction) is $X \cong \mu_0 B / \Delta W$, where ΔW corresponds to the zero field hyperfine splitting. The magnetic field at which X is unity varies from ~ 15 to ~ 65 G for the cases of present interest (see Table I) and we are thus interested in the strong field region as far as the hyperfine interaction is concerned. This means that the appropriate wave functions which include the nuclear spin are of the form given in Table VIII multiplied by a nuclear spin wave function which corresponds to a particular m_I . (These are only approximately correct wave functions; in fact, a small amount of nuclear spin component of other than the predominant m_I value will be present. The situation is analogous to the situation discussed above for the fine structure wave functions, if \vec{F} , \vec{J} , and \vec{I} replace \vec{J} , \vec{L} , and \vec{S} . The α -d crossing technique¹⁰ discussed in Section 4 makes use of this fact.)

Turning to the evaluation of the matrix elements which connect the various states, we assume that m_I is a good quantum number; i.e., that we may use electron wave functions of the form given in Table VIII multiplied by a nuclear spinor. The selection rule $\Delta m_I = 0$ holds for the transitions of interest so the nuclear spin wave function is omitted in the following discussion. Further, we assume that the direction of the static magnetic field defines the +z axis of the system.

We first consider the magnetic dipole matrix elements

which connect the β to the α and the f to the e states. The perturbing interaction is

$$H' = -\vec{\mu} \cdot \vec{B}' = -g_L \mu_0 \vec{L} \cdot \vec{B}' - g_S \mu_0 \vec{S} \cdot \vec{B}'$$

where, neglecting radiative corrections, $g_L = 1$ and $g_S = 2$, and where μ_0 is the Bohr magneton. We may write:

$$\vec{L} \cdot \vec{B}' = \frac{1}{2}(B'_x + iB'_y)(L_x - iL_y) + \frac{1}{2}(B'_x - iB'_y)(L_x + iL_y) + B'_z L_z \cong \frac{1}{2}B'_+ L_- + \frac{1}{2}B'_- L_+ + B'_z L_z.$$

Using this expression together with the similar expression for $\vec{S} \cdot \vec{B}'$, the $\beta \rightarrow \alpha$ matrix element may be written:

$$H'_{\alpha\beta} = -\mu_0 \int R_{20} \psi_{00}^*(+) [\frac{1}{2}B'_+ (g_L L_- + g_S s_-) + \frac{1}{2}B'_- (g_L L_+ + g_S s_+) + B'_z (g_L L_z + g_S s_z)] R_{20} \psi_{00}(+) d\tau.$$

The operators L_+ , L_- , and L_z obey the equations¹³

$$L_+ \psi_{l m_l} = \sqrt{(l - m_l)(l + m_l + 1)} \psi_{l m_l + 1},$$

$$L_- \psi_{l m_l} = \sqrt{(l + m_l)(l - m_l + 1)} \psi_{l m_l - 1}, \text{ and}$$

$$L_z \psi_{l m_l} = m_l \psi_{l m_l}.$$

The operators s_+ , s_- , and s_z obey identical equa-

TABLE X

n = 2 Electric Dipole Matrix Elements

Units: ea.

Transition	Δm	Matrix Element of $e\vec{E} \cdot \vec{r}$	Matrix Element of		
			$x E_x$	$y E_y$	$z E_z$
$\alpha \rightarrow a$	+1	$-3E_-/\sqrt{2}$	$-3E_x/\sqrt{2}$	$3iE_y/\sqrt{2}$	0
$\beta \rightarrow d$	-1	$3E_+/\sqrt{2}$	$3E_x/\sqrt{2}$	$3iE_y/\sqrt{2}$	0
$\alpha \rightarrow b$	0	$\sqrt{6}\epsilon_1 E_z$	0	0	$\sqrt{6}\epsilon_1 E_z$
$\beta \rightarrow c$	0	$\sqrt{6}\epsilon_4 E_z$	0	0	$\sqrt{6}\epsilon_4 E_z$
$\alpha \rightarrow c$	-1	$\sqrt{3/2}\epsilon_3 E_+$	$\sqrt{3/2}\epsilon_3 E_x$	$\sqrt{3/2}\epsilon_3 iE_y$	0
$\beta \rightarrow b$	+1	$-\sqrt{3/2}\epsilon_2 E_-$	$-\sqrt{3/2}\epsilon_2 E_x$	$\sqrt{3/2}\epsilon_2 iE_y$	0
$\alpha \rightarrow d$	-2	0	0	0	0
$\beta \rightarrow a$	+2	0	0	0	0
$\alpha \rightarrow e$	0	$-\sqrt{3}\epsilon_2 E_z$	0	0	$-\sqrt{3}\epsilon_2 E_z$
$\beta \rightarrow f$	0	$+\sqrt{3}\epsilon_3 E_z$	0	0	$+\sqrt{3}\epsilon_3 E_z$
$\alpha \rightarrow f$	-1	$-\sqrt{3}\epsilon_4 E_+$	$-\sqrt{3}\epsilon_4 E_x$	$-\sqrt{3}\epsilon_4 iE_y$	0
$\beta \rightarrow e$	+1	$-\sqrt{3}\epsilon_1 E_-$	$-\sqrt{3}\epsilon_1 E_x$	$\sqrt{3}\epsilon_1 iE_y$	0

tions (where $s = 1/2$, $m_s = \pm 1/2$). In spinor notation, only the following operations yield non-zero results:

$$\begin{aligned} s_+(+) &= (+) \\ s_-(+) &= (+) \\ s_z(+) &= \frac{1}{2}(+) \\ s_z(-) &= -\frac{1}{2}(-) \end{aligned}$$

For the present example, the l_+ , l_- , and l_z operators yield zero and the only contribution to the integral is from the $\frac{1}{2}g_s B'_+ S_+$ term. We thus obtain $H'_{\alpha\beta} = -\frac{1}{2}g_s \mu_0 B'_+ = -\mu_0 B'_+$. In the notation of Section 5 this corresponds to $M = -\mu_0 B'_+/h$ or $M = -i\mu_0 B'_y/h$ for oscillating fields in the x and y directions, respectively.

The matrix element connecting f to e can be similarly evaluated; the result is:

$$H'_{ef} = [-g_l(\epsilon_2\epsilon_4 + \epsilon_1\epsilon_3)/3 + g_s\epsilon_2\epsilon_3/6]\mu_0 B'_-$$

For the magnetic fields of interest here, ϵ_1 , ϵ_2 , ϵ_3 , and ϵ_4 are very near unity. If it is assumed that they are exactly unity, we have

$$H'_{ef} = -\mu_0 B'_-/3$$

(This limiting result could have been readily obtained by considering the effective interaction to be $-g_l \mu_0 \vec{J} \cdot \vec{B}'$ together with the Jm_J representation of the state.) In the notation of Section 5, this result corresponds to $M' = -\epsilon_l \mu_0 B'_x/3h$ or $M' = -i\epsilon_l \mu_0 B'_y/3h$ for oscillating fields in the x and y directions, respectively, where ϵ is given by:

$$\epsilon = g_l(\epsilon_2\epsilon_4 + \epsilon_1\epsilon_3) - g_s\epsilon_2\epsilon_3/2$$

We note that $\epsilon \approx 1$ for field strengths of present interest. Numerically the quantity μ_0/h is 2π times (1.401) MHz/G. Note that M and M' have units of angular frequency.

We now turn to the electric dipole matrix elements. In this case the perturbing part of the Hamiltonian is of the form $H' = e\vec{E} \cdot \vec{r}$ where e is the electronic charge, \vec{E} an electric field strength, and \vec{r} is the electron position vector.

For example, the matrix element which causes the

transition $\alpha \rightarrow e$ may be written

$$H'_{\alpha e} = \int [\epsilon_2 R_{21} \psi_{10}^*(t) + \epsilon_1 R_{21} \psi_{11}^*(t)] [e\vec{E} \cdot \vec{r}] R_{20} \psi_{00}(t) dt .$$

Noting the orthonormality of the electron spinors and expanding $e\vec{E} \cdot \vec{r}$, this becomes

$$H'_{\alpha e} = \epsilon_2 e \int R_{21} \psi_{10}^* [\frac{1}{2} E_+ x_- + \frac{1}{2} E_- x_+ + E_z z] R_{10} \psi_{00} dt .$$

If we use the following facts

$$\begin{aligned} z &= r \cos \theta \\ x_+ &= r \sin \theta e^{i\phi} \\ x_- &= r \sin \theta e^{-i\phi} \\ d\tau &= r^2 \sin \theta d\theta d\phi , \end{aligned}$$

we obtain

$$H'_{\alpha e} = \epsilon_2 e \int_0^\pi R_{21}(r) R_{10}(r) r^3 dr \int_0^{2\pi} \int_0^\pi \psi_{10}^* (E_z \cos \theta + \frac{1}{2} E_+ \sin \theta e^{-i\phi} + \frac{1}{2} E_- \sin \theta e^{i\phi}) \psi_{00} \sin \theta d\theta d\phi .$$

The radial integral¹³ has the value $3\sqrt{3}a_0$, where a_0 is the Bohr radius. The angular integrals can be evaluated either directly or by reference to tables.¹³ In this case, only $E_z \cos \theta$ survives the ϕ integration, and we obtain

$$H'_{\alpha e} = -\sqrt{3} \epsilon_2 e a_0 E_z .$$

In Table X the matrix elements are given with the assumption of the Condon-Shortley¹⁴ conventions for the vector coupling coefficients and wave functions. Any modification of sign in which ϵ_1 and ϵ_3 , or ϵ_2 and ϵ_4 are changed simultaneously, or in which the overall phase of a wave function is changed, preserves the orthogonality and eigenvalues of the functions and is therefore acceptable. Thus, for the $2S_{1/2} - 2P_{1/2}$ transitions, many possible consistent sets of signs for the matrix elements are possible.

In the notation of Section 5, the electric dipole matrix elements may be written

$$\begin{aligned} R &= -\sqrt{3} \epsilon_2 e a_0 E_z \\ R' &= \sqrt{3} \epsilon_3 e a_0 E_z , \end{aligned}$$

and

$$V = -\sqrt{3} \epsilon_1 e a_0 E_x \quad \text{or} \quad -\sqrt{3} \epsilon_1 e a_0 i E_y$$

$$V' = -\sqrt{3} \epsilon_4 e a_0 E_x \quad \text{or} \quad \sqrt{3} \epsilon_4 e a_0 i E_y ,$$

depending on whether the transverse field is along the x or y axis. For the magnetic fields of interest, $\epsilon_1 - \epsilon_4$ differ from unity by only a few percent. Neglecting these small differences, we may write

$$R' = -R^* \quad \text{and} \quad V' = V^* .$$

This form is used in some of the later discussion. In fact, any relative signs between the matrix elements such that $\arg(R/V) = -\arg(R^*/V^*)$ will result in identical answers for any calculation which involves only these matrix elements.

Numerically, the quantity $\sqrt{3} e a_0 / \hbar$ is given by $\sqrt{3} \times (1.60206 \times 10^{-19} \text{ C}) \times (5.29172 \times 10^{-9} \text{ cm}) \times 10^7 / (1.05443 \times 10^{-27} \text{ erg-sec}) = 13.9257 \text{ (cm/V) MHz}$.

Note that the quantity $\sqrt{3} e a_0 E / \hbar$, where E is an electric field strength (V/cm), has the units of angular frequency.

7. ANALYTIC SOLUTION OF THE THREE-LEVEL PROBLEM

For the case of interest, where the magnetic field is such that the β and e levels are nearly degenerate, the f level has little effect on the system. Thus, to good approximation, we may neglect its presence. (The quality of this approximation will be examined in Section 8.)

The equations which characterize the three-level system are then

$$\begin{aligned} i\dot{a} &= \frac{1}{2} M^* b e^{i\delta t} + \frac{1}{2} R^* c e^{i(\delta + \omega_{\beta e})t} \\ i\dot{b} &= \frac{1}{2} M a e^{-i\delta t} + V^* c e^{i\omega_{\beta e} t} \\ i\dot{c} &= \frac{1}{2} R a e^{-i(\delta + \omega_{\beta e})t} + V b e^{-i\omega_{\beta e} t} - \frac{1}{2} (i\gamma c) , \end{aligned}$$

where we have defined the angular frequency difference $\delta = \omega_{\alpha\beta} - \omega$.

Let us first consider the easily-solved special case which corresponds to $\delta = 0$ and $\omega_{\beta e} = 0$. In other words, we assume a magnetic field strength such that the β and e levels are degenerate (crossing) and an rf frequency such that $\omega/2\pi = \omega_{\alpha\beta}/2\pi$ (resonance). Note that we are speaking of a particular nuclear spin magnetic quantum number, since

simultaneous resonance and crossing occur at a different magnetic field (and corresponding frequency) for the various m_{\perp} values. We also neglect M (for the reasons given in Section 6).

With these assumptions the equations become

$$\begin{aligned} i\dot{a} &= \frac{1}{2}R^*c \\ i\dot{b} &= V^*c \\ i\dot{c} &= \frac{1}{2}Ra + Vb - \frac{1}{2}(i\gamma c) \end{aligned}$$

If one differentiates the third of these equations and substitutes the first two equations into the third, the result is

$$\ddot{c} + \frac{1}{2}\gamma\dot{c} + P^2c = 0,$$

where $P^2 = \frac{1}{2}R^*R + V^*V$. The general solution of this equation is

$$c = C_1 e^{-\mu_1 t} + C_2 e^{-\mu_2 t},$$

where μ_1 and μ_2 are the two roots of $\mu^2 - \frac{1}{2}\gamma\mu + P^2 = 0$:

$$\mu_{1,2} = \gamma/4 \pm \sqrt{(\gamma/4)^2 - P^2}.$$

To evaluate the constants, we assume some initial conditions. For a particle initially in its α -state, $a = 1$ and $b = c = 0$ at $t = 0$; this implies that $\dot{c} = \frac{1}{2}iR$ at $t = 0$. Applying these conditions, we obtain:

$$c = \frac{iR}{4\eta} \left(e^{-\mu_1 t} - e^{-\mu_2 t} \right),$$

where $\eta = \sqrt{(\gamma/2)^2 - P^2}$. This solution is valid for all values of P^2 except the critically damped case $P^2 = (\gamma/2)^2$; for this case $c = \frac{-iR}{2} t e^{-(\gamma/4)t}$. The solutions for c may be put back into the equations for \dot{a} and \dot{b} to obtain

$$\begin{aligned} a &= A_3 + \frac{1}{2}iR^* \int c dt \\ b &= B_3 + \int V^* c dt, \end{aligned}$$

where A_3 and B_3 are integration constants. We obtain:

$$a = 1 - \frac{R^*R}{4P^2} + \frac{R^*R}{8\eta} \left(\frac{e^{-\mu_2 t}}{\mu_2} - \frac{e^{-\mu_1 t}}{\mu_1} \right)$$

$$b = -\frac{V^*R}{2P^2} + \frac{V^*R}{4\eta} \left(\frac{e^{-\mu_2 t}}{\mu_2} - \frac{e^{-\mu_1 t}}{\mu_1} \right).$$

After a sufficiently long time the exponential terms decay to zero, since the real parts of μ_1 and μ_2 are positive for all values of P^2 .

Thus, our asymptotic solutions are

$$a \rightarrow \frac{V^*V}{\frac{1}{2}R^*R + V^*V}$$

$$b \rightarrow \frac{-\frac{1}{2}V^*R}{\frac{1}{2}R^*R + V^*V}$$

$$c \rightarrow 0.$$

That is, an equilibrium population of the α and β states is established. Since we are dealing with amplitudes, a definite phase relation exists between a and b ; i.e., we have a coherent mixture of the α and β states, while the amplitude for the c state has decayed to zero.

We note that our asymptotic solutions satisfy the condition $\frac{1}{2}Ra + Vb = 0$. From inspection of the equations, it is clear that we have a solution if $c = \dot{c} = 0$. The physical nature of the phenomenon is one of interference; the relative phase of the transition matrix elements is such that contributions from a and b to the c state population destructively interfere; i.e., $\frac{1}{2}Ra + Vb = 0$.

We now turn to the solution of the general three-level equations following the method indicated by Lamb.⁸ First, let us generalize the equations slightly to allow for an arbitrary phase for the rf field at $t = 0$. That is, we assume

$$H'_{ea} = H'_{ae} = \hbar R \cos(\omega t + \delta_0),$$

where δ_0 is the phase at $t = 0$. This may be written as

$$\frac{1}{2} [\hbar(\text{Re } e^{i\delta_0}) e^{i\omega t} + \hbar(\text{Re } e^{-i\delta_0}) e^{-i\omega t}].$$

We may perform a similar decomposition of M . Dropping the negative frequency term, as before, and defining $\text{Re } e^{i\delta_0} = R_0$ and $\text{Re } e^{-i\delta_0} = M_0$, the equations remain the same except $R \rightarrow R_0$ and $M \rightarrow M_0$:

$$i\dot{a} = R_0^* c e^{i(\delta + \omega_{\beta e})t} + \frac{1}{2} M_0^* b e^{i\delta t}$$

$$i\dot{b} = V^* c e^{i\omega_{\beta e}t} + \frac{1}{2} M_0 a e^{-i\delta t}$$

$$i\dot{c} = R_0 a e^{-i(\delta + \omega_{\beta e})t} + V b e^{-i\omega_{\beta e}t} - \frac{1}{2}(i\gamma c)$$

Following Lamb,⁸ we assume a solution of the form

$$a = A_1 e^{-\mu_1 t} + A_2 e^{-\mu_2 t} + A_3 e^{-\mu_3 t}$$

$$b = (B_1 e^{-\mu_1 t} + B_2 e^{-\mu_2 t} + B_3 e^{-\mu_3 t}) e^{-i\delta t}$$

$$c = (C_1 e^{-\mu_1 t} + C_2 e^{-\mu_2 t} + C_3 e^{-\mu_3 t}) e^{-i\delta t - i\omega_{\beta e}t}$$

Substituting this form into the equations and equating coefficients of $e^{-\mu_1 t}$, for example, we obtain

$$\begin{bmatrix} i\mu_1 & M_0^* & R_0^* \\ M_0 & i\mu_1 - \delta & V^* \\ R_0 & V & i\mu_1 - \delta - \omega_{\beta e} - \frac{1}{2}i\gamma \end{bmatrix} \begin{bmatrix} A_1 \\ B_1 \\ C_1 \end{bmatrix} = 0,$$

with identical equations holding for μ_2 and μ_3 . We use the general subscript k from here on since the following discussion applies to μ_1 , μ_2 , and μ_3 . For any but the trivial solution $A_k = B_k = C_k = 0$, the determinant of the coefficients must vanish; thus, the three values of μ are the roots of the complex cubic equation:

$$i\mu_k(i\mu_k - \delta)(i\mu_k - \delta - \omega_{\beta e} - \frac{1}{2}i\gamma) + (M_0^* V R_0 + M_0 V R_0^*) - R_0 R_0^* (i\mu_k - \delta) - V V^* (i\mu_k) - M_0 M_0^* (i\mu_k - \delta - \omega_{\beta e} - \frac{1}{2}i\gamma) = 0.$$

This may be written in the form

$$\mu_k^3 + P\mu_k^2 + Q\mu_k + R = 0,$$

where

$$P = -i(\Delta_{\alpha\beta} + \Delta_{\alpha e})$$

$$Q = V^* V + \frac{1}{2}(R_0^* R_0 + M_0^* M_0) - \Delta_{\alpha\beta} \Delta_{\alpha e}$$

$$R = i(M_0^* V R_0 + M_0 V R_0^* - \frac{1}{2}(R_0^* R_0 \Delta_{\alpha\beta} + M_0^* M_0 \Delta_{\alpha e})),$$

and where $\Delta_{\alpha\beta} = -\delta$ and $\Delta_{\alpha e} = -\delta - \omega_{\beta e} - \frac{1}{2}i\gamma$.

Such a complex cubic equation may be solved algebraically as follows. Define $\mu_k = z + P/3$. The equation for z is then $z^3 + az + b$ where $a = Q - P^2/3$ and $b = 2P^3/27 - PQ/3 + R$. Then a solution for z is of the form $z = u - a/3u$, where u satisfies the equation $u^3 = -b/2 \pm \sqrt{(b/2)^2 + (a/3)^2}$. All the operations defined are valid for complex numbers; however, we find six values for u of which three lead to redundant solutions. To improve computation precision, we select the + or - sign in the equation for u^3 according to which gives the larger absolute value. It was found necessary to use double-precision arithmetic to achieve satisfactory accuracy for the values of the coefficients of interest to the present problem. The FORTRAN IV code for this procedure is included in Appendix A.

Returning to the matrix equation, once we know that the determinant of the coefficients is zero, we may use any two equations to relate the quantities B_k and C_k to A_k , which we will assume to be arbitrary. (That is, A_1 , A_2 , and A_3 will be taken to be the three independent constants characteristic of the solution of a system of three first-order differential equations.) One finds

$$B_k = -\frac{1}{2} A_k [M_0 (i\mu_k - \delta - \omega_{\beta e} - \frac{1}{2}i\gamma) - R_0 V^*] / D_k$$

$$C_k = -\frac{1}{2} A_k [R_0 (i\mu_k - \delta) - M_0 V] / D_k,$$

where

$$D_k = (i\mu_k - \delta - \omega_{\beta e} - \frac{1}{2}i\gamma)(i\mu_k - \delta) - V^* V.$$

Thus, defining $B_k = \epsilon_k A_k$ and $C_k = \delta_k A_k$, our general solution of the equations is of the form

$$\begin{bmatrix} a \\ b \\ c \end{bmatrix} = \begin{bmatrix} 1 & 1 & 1 \\ \epsilon_1 & \epsilon_2 & \epsilon_3 \\ \delta_1 & \delta_2 & \delta_3 \end{bmatrix} \begin{bmatrix} A_1 e^{-\mu_1 t} \\ A_2 e^{-\mu_2 t} \\ A_3 e^{-\mu_3 t} \end{bmatrix}.$$

To evaluate the coefficients A_1 , A_2 , and A_3 , it is necessary to assume some initial conditions. If there is no e -state component in the initial beam, we may achieve sufficient generality by assuming each of the initial conditions $a = 1, b = 0, c = 0$ and $a = 0, b = 1, c = 0$. The solution to the problem corresponding to a beam which contains an incoherent mixture of α -state atoms and β -state atoms can then be written by combining these solutions appropriately (i.e., by an average over initial states). We could use some other set of spinors as a basis system; a natural basis system for this problem will be discussed later. For $a = 1, b = 0$, and $c = 0$ at $t = 0$, the solution of the linear equations yields

$$A_1 = (\epsilon_2 \delta_3 - \epsilon_3 \delta_2)/D$$

$$A_2 = (\epsilon_3 \delta_1 - \epsilon_1 \delta_3)/D$$

$$A_3 = (\epsilon_1 \delta_2 - \epsilon_2 \delta_1)/D,$$

where

$$D = (\epsilon_2 \delta_3 - \epsilon_3 \delta_2) + (\epsilon_3 \delta_1 - \epsilon_1 \delta_3) + (\epsilon_1 \delta_2 - \epsilon_2 \delta_1).$$

For $a = 0, b = 1$, and $c = 0$ at $t = 0$ we obtain

$$A_1 = (\delta_2 - \delta_3)/D$$

$$A_2 = (\delta_3 - \delta_1)/D$$

$$A_3 = (\delta_1 - \delta_2)/D.$$

The present solutions have been evaluated numerically by computer methods (Appendix A). In summary, the assumptions made in obtaining these solutions are:

- the three-level approximation equations are adequate,
- R_0 , V , and M_0 are constant during the interaction time,
- the effect of the $e^{-i\omega t}$ term (the Bloch-Siegert term) is small.

These restrictions will be relaxed in the numerical integration results to be described later.

We note that the initial phase of the rf field plays no role in the solutions. Accordingly, we will refer to R and M , not R_0 and M_0 , in most of the fol-

lowing discussion. The coefficients A_k , B_k , and C_k are slowly varying functions of the angular frequency difference $\delta = \omega_{\alpha\beta} - \omega$. The character of the variation of A_3 and B_3 , the coefficients of the most slowly decaying term, depends on the sign and magnitude of $\omega_{\beta e}$ at the magnetic field for which $\delta = 0$; i.e., to the difference between the resonance and crossing frequencies. Figure 5 shows the modulus and argument of A_3 for $m_I = 0$ deuterium atoms, as a function of $B - B_0$ (where $B_0 = B(\delta = 0)$), or $\delta/2\pi$, for the following 3 cases:

Case	$\omega/2\pi$ (MHz)	B_0 (G)	$\omega_{\beta e}/2\pi$	$ R_0 $ (MHz)	$ V $ (MHz)
1	1471.90	525	89.95	250	250
2	1611.99	575	-1.57	250	250
3	1752.09	625	-92.53	250	250

The numerical values of the matrix elements ($|R_0| = 250$ MHz and $|V| = 250$ MHz) correspond to a longitudinal rf field of $250/(13.93 \times .975) = 18.41$ V/cm and to a transverse static field of $250/(13.93 \times 1.021) = 17.58$ V/cm. The particular frequencies chosen correspond to a resonance ~ 50 G below crossing, approximately at crossing, and ~ 50 G above crossing. (The exact field for which $\omega_{\beta e} = 0$ for $m_I = 0$ deuterium atoms is 574.14 G, for which $\omega_{\alpha\beta}/2\pi = 1609.57$ MHz.) Since the line shape depends only on $\omega_{\beta e}/2\pi$, the curves in Figures 5-8 apply to any of the hydrogen, deuterium, or tritium

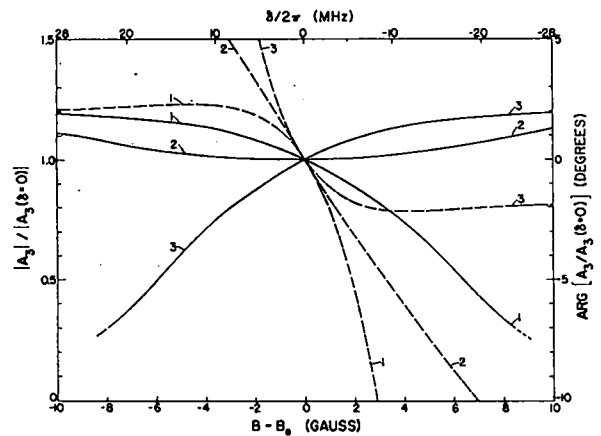


Fig. 5. The variation of $|A_3|$ (solid curves) and $\arg A_3$ (dashed curves) for cases 1, 2, and 3. One of the $|A_3|$ curves is terminated at -8 G where $\text{Re}(\mu_2)$ becomes smaller than $\text{Re}(\mu_3)$.

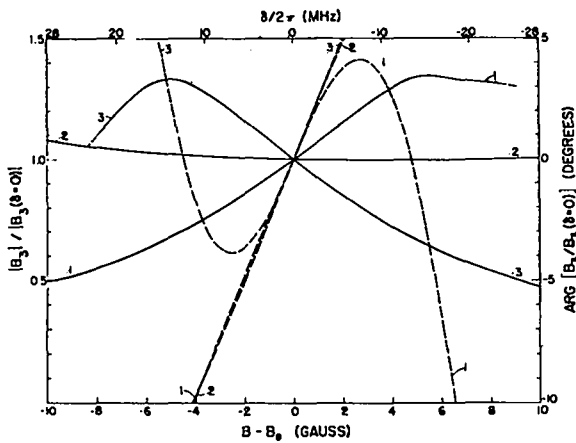


Fig. 6. The variation of $|B_3|$ (solid curves) and $\arg B_3$ (dashed curves) for cases 1, 2, and 3. One of the $|B_3|$ curves is terminated at 8.5 G, and a second curve at -8 G, where $\text{Re}(\mu_2)$ becomes smaller than $\text{Re}(\mu_3)$.

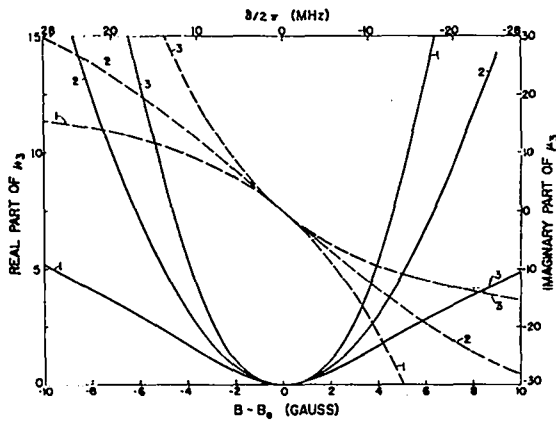


Fig. 7. The variation of the real part (solid curves) and imaginary part (dashed curves) of μ_3 (in MHz angular frequency) for cases 1, 2, and 3.

substates. However, the values of $\omega/2\pi$ and B_0 given above are specifically for $m_I = 0$ deuterium atoms. Since, for a given fixed frequency, $\omega_{\beta e}$ will be different for the different substates of the species being polarized, the line shape corresponding to each will be slightly different. The cases 1 and 3 chosen for illustration are probably a little too far from crossing for reasonable separation of deuterium magnetic substates; a range of ± 35 G from the crossing field would appear to be

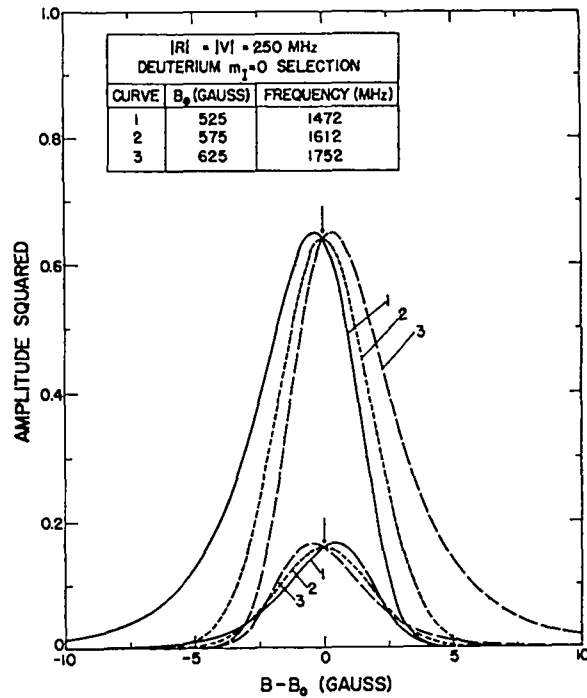


Fig. 8. The "transmission" $|a|^2$ (upper three curves) and $|b|^2$ (lower three curves) evaluated at $t = 0.4$ usec, for cases 1, 2, and 3.

acceptable. For hydrogen or tritium atoms, where the line shape is of little consequence, a much larger difference is acceptable.

Figure 6 shows the modulus and argument of B_3 as a function of $B - B_0$ or $\delta/2\pi$, for the same three cases. Note that the slopes of the $|A_3|$ and $|B_3|$ curves are opposite in sign for a given $\omega_{\beta e}$.

Figure 7 shows the real and imaginary parts of the small decay constant μ_3 , as a function of $B - B_0$ or $\delta/2\pi$, for the same cases. Figure 8 shows the transmission $|a|^2$ and $|b|^2$ after a time $t = 0.4$ usec (12 cm). At a time as large as this, only the μ_3 terms survive, so

$$|a|^2 = |A_3 e^{-\mu_3 t}|^2$$

and

$$|b|^2 = |B_3 e^{-\mu_3 t}|^2.$$

The opposite shift in the apparent resonant field for $|a|^2$ and $|b|^2$ transmission is because of the opposite slopes of the $|A_3|$ and $|B_3|$ curves noted above.

It is relevant to inquire about the transmission of

TABLE XI

1. Transmission of Unselected Substates

$ R / V $	$\frac{1}{2} R ^2 + V ^2$ Units: (125 MHz) ² Angular Frequency	$ A_3 $	Re. (μ_3) (μsec^{-1})
0.5	2	1.03	5.3
1.0	2	1.15	20.1
1.5	2	1.39	43.2
0.5	5	.98	5.5
1.0	5	.90	17.4
1.5	5	.75	26.5
0.5	10	.95	3.3
1.0	10	.81	9.3
1.5	10	.68	13.2

2. Transmission of the Selected Substate

$ R / V $	$ A_3 $
0.5	0.9412
1.0	0.8000
1.5	0.6400

atoms with other than the desired m_I quantum number. For hydrogen or tritium atoms, this may easily be made zero. For deuterium atoms, some care must be taken in the choice of parameters. If the optimum driving frequency of 1609.57 MHz is chosen, the transmission curves for $m_I = 1, 0,$ and -1 are highly symmetric and therefore almost identical. The relevant quantity is the transmission of a given state when the magnetic field is tuned to an adjacent state. For example, for $\omega/2\pi = 1609.57$ MHz, the resonant fields for $m_I = 1, 0,$ and -1 deuterium atoms are 564.48, 574.14, and 583.96 G. In the case of $m_I = 0$ deuterium atom selection, we are interested in the transmission of $m_I = 1$ and $m_I = 3$ atoms at 574.14 G; i.e., at 9.56 G above and at 9.82 G below their respective resonant fields. The relative contributions from either of these may be determined from Table XI. Thus, for $|R| = |V| = 250$ MHz, the fractional contamination of $m_I = 0$ states with $m_I = 1$ states would be $|0.90e^{-17.4t}/.80|^2$ which, for $t = 0.4$ μsec , is about 10^{-6} . For other driving frequencies the selection is less favorable; however, as mentioned above, the selection would appear to be reasonably satisfactory for a frequency range of $\sim \pm 100$ MHz (corresponding to $\sim \pm 35$ G). The quality of the selection in these cases can be estimated

from Figures 5-7.

We now write simpler expressions for the special case of resonance ($\delta = 0$). As noted above, the coefficients do not vary rapidly, so some statements about the general nature of the solutions at resonance will apply approximately to the off-resonance solutions. We neglect the small matrix element M . For this case, the cubic equation becomes

$$\mu^3 - (\gamma/2 - i\omega_{\beta e})\mu^2 + P^2\mu = 0,$$

where $P^2 = \frac{1}{2}RR^* + VV^*$ as before. The roots are

$$\mu_{1,2} = (\gamma/4 - i\omega_{\beta e}/2) \pm \sqrt{(\gamma/4 - i\omega_{\beta e}/2)^2 - P^2}$$

$$\mu_3 = 0,$$

which are seen to be consistent with the solutions obtained above for $\omega_{\beta e} = 0$.

Inserting these values for the μ_k in the general relations, we obtain

$$\epsilon_k = +\frac{1}{2}RV^*/D_k$$

and

$$\delta_k = -\frac{1}{2}iR\mu_k/D_k,$$

where

$$\begin{aligned} D_k &= i\mu_k(1\mu_k - \omega_{\beta e} - i\gamma/2) - V^*V \\ &= -\mu_k^2 + 2\mu_k(\gamma/4 - i\omega_{\beta e}/2) - V^*V. \end{aligned}$$

If we define $\xi = (\gamma/4 - i\omega_{\beta e}/2)$ and $\eta =$

$\sqrt{(\gamma/4 - i\omega_{\beta e}/2)^2 - P^2}$ we can tabulate the $D_k, \epsilon_k,$ and δ_k as follows:

k	μ_k	D_k	ϵ_k	δ_k
1	$\xi + \eta$	$R^*R/4$	$2V^*/R$	$-2i(\xi + \eta)/R$
2	$\xi - \eta$	$R^*R/4$	$2V^*/R$	$-2i(\xi - \eta)/R$
3	0	$-V^*V$	$-R/2V$	0

The determinant D may be written

$$D = -\frac{8iV^*\eta}{R^*R^*} \left(1 + \frac{R^*R}{4V^*V}\right).$$

For the initial condition $a = 1, b = 0, c = 0$, we obtain the coefficients

k	A_k	B_k	C_k
1	$\frac{R^*R}{8P^2} (1 - \frac{\xi}{\eta})$	$\frac{RV^*}{4P^2} (1 - \frac{\xi}{\eta})$	$\frac{iR}{4\eta}$
2	$\frac{R^*R}{8P^2} (1 + \frac{\xi}{\eta})$	$\frac{RV^*}{4P^2} (1 + \frac{\xi}{\eta})$	$-\frac{iR}{4\eta}$
3	$\frac{V^*V}{P^2}$	$-\frac{RV^*}{2P^2}$	0

For large times, the solutions are therefore

$$a \rightarrow \frac{V^*V}{P^2} \quad b \rightarrow \frac{-RV^*}{2P^2}$$

Note that a and b have asymptotic values identical to those obtained if $\omega_{\beta e} = 0$; thus, only the transient terms are affected by $\omega_{\beta e} \neq 0$ for $\delta = 0$.

For frequencies slightly off resonance, neglecting the slight variation of the coefficients, we have

$$a \approx \frac{V^*V}{P^2} e^{-\mu_3 t} \quad b \approx \frac{-RV^*}{2P^2} e^{-(\mu_3 + i\delta)t}$$

where μ_3 is a rapidly varying function of δ (see Figure 7).

For the initial conditions $a = 0$, $b = 1$, $c = 0$, we obtain the solutions

k	A_k	B_k	C_k
1	$\frac{R^*V}{4P^2} (1 - \frac{\xi}{\eta})$	$\frac{V^*V}{4P^2} (1 - \frac{\xi}{\eta})$	$\frac{iV}{2\eta}$
2	$\frac{R^*V}{4P^2} (1 + \frac{\xi}{\eta})$	$\frac{V^*V}{2P^2} (1 + \frac{\xi}{\eta})$	$-\frac{iV}{2\eta}$
3	$-\frac{R^*V}{2P^2}$	$\frac{R^*R}{4P^2}$	

From the symmetry of the equations, one can see that the relation between the sets of coefficients for the two assumed initial conditions must involve only the simultaneous interchange of $R/2$ with V and the definition of A_k with that of B_k .

In general, the roots of the cubic equation are complex. The imaginary components correspond to (time dependent) energy shifts from the unperturbed eigenenergies characterizing the wave functions given in Table VIII. Consider, for illustrative purposes, the situation at crossing and resonance

where

$$\mu_{1,2} = \gamma/4 \pm \sqrt{(\gamma/4)^2 - P^2}, \quad \mu_3 = 0.$$

It is clear that if $P^2 < (\gamma/4)^2$, all the roots are real and the unperturbed energies remain correct. If, however, $P^2 > (\gamma/4)^2$, μ_1 and μ_2 will have an imaginary component and the level energies will be shifted. This is related to the phenomena of level repulsion in which, under certain circumstance, the energies of two states as a function of magnetic field do not cross, but rather repel, and thus interchange roles.⁸ This effect does not result in a shift of the position of the three-level resonance, however, since this is determined solely by the frequency at which $\text{Re}(\mu_3) = 0$, and this frequency will correspond* to $\delta = 0$ for any value of $\omega_{\beta e}$ or P^2 . For $\delta \neq 0$, μ_3 has an imaginary component (see Figure 7) and the slowly decaying states α and β may be regarded as slightly energy-shifted. The energy shift of the rapidly decaying components has no significance at large times.

Figures 9-11 illustrate the time dependence of $|a|^2$ and $|b|^2$ for the cases 1, 2, and 3 defined above (initial conditions $a = 1$, $b = 0$, and $c = 0$). Figure 9 corresponds to resonance ($\delta = 0$), Figure 10 corresponds to 1 G off resonance ($\delta/2\pi = 2.8$ MHz), and Figure 11 corresponds to 9.6 G off resonance ($\delta/2\pi = 26.9$ MHz). The last value is chosen for presentation since 9.6 G is approximately the difference in magnetic field values at which the various deuterium magnetic substates resonate.

Figure 12 illustrates the time dependence of $|a|^2$ and $|b|^2$ at resonance ($\delta = 0$) for the cases 1, 2, and 3 but for the initial conditions $a = 0$, $b = 1$, and $c = 0$.

Figures 13-15 show the transmission of hydrogen metastable atoms versus magnetic field for an rf field of fixed frequency and strength (here taken to be 1610 MHz and 18.41 V/cm, respectively) and for several values of the transverse field (8.79,

*As has been noted above, the apparent resonant frequency sometimes differs slightly from $\delta = 0$. This is due only to the slow variation of the coefficients $|A_3|$ and $|B_3|$ with frequency, and is unrelated to the energy shifts presently under discussion.

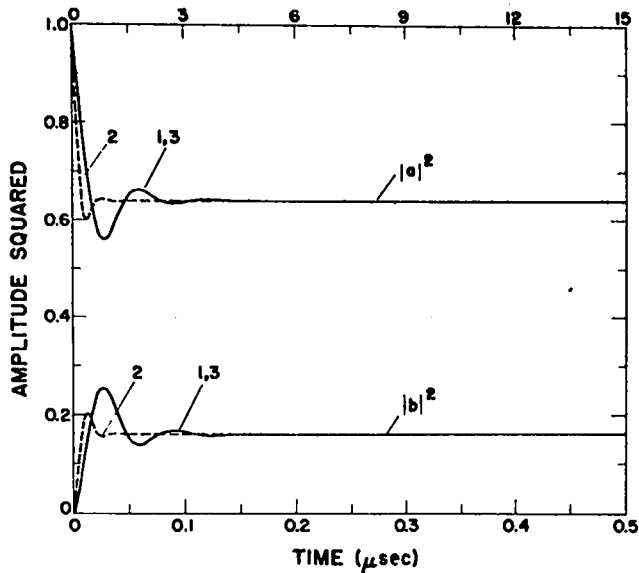


Fig. 9. The variation of $|a|^2$ and $|b|^2$ vs time for $B = B_0$ ($\delta = 0$) with initial conditions $a(0) = 1$, $b(0) = c(0) = 0$ for cases 1, 2, and 3.

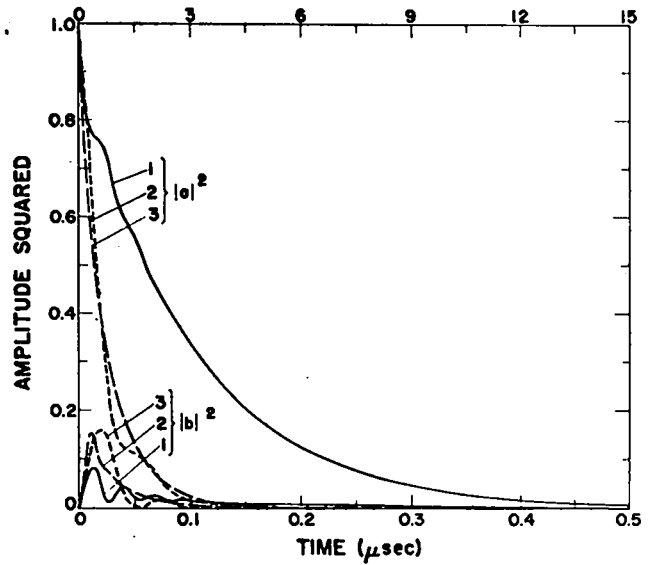


Fig. 11. The variation of $|a|^2$ and $|b|^2$ vs time for $B - B_0 = -9.6$ G ($\delta/2\pi \approx 26.9$ MHz) with initial conditions $a(0) = 1$, $b(0) = c(0) = 0$ for cases 1, 2, and 3.

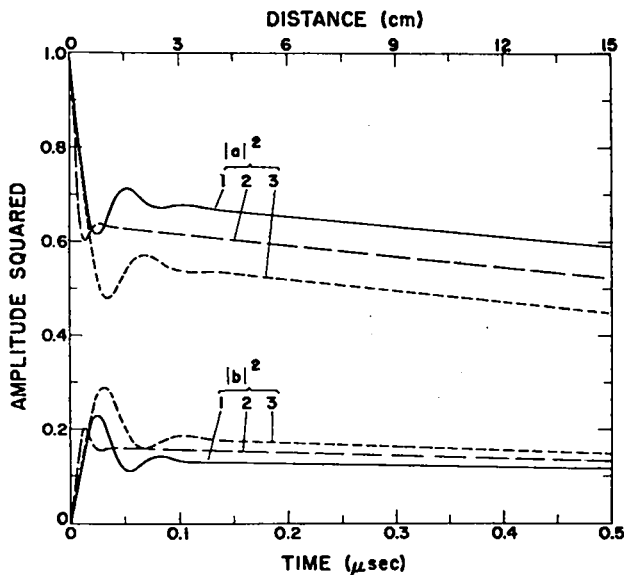


Fig. 10. The variation of $|a|^2$ and $|b|^2$ vs time for $B - B_0 = -1$ G ($\delta/2\pi \approx 2.8$ MHz) with initial conditions $a(0) = 1$, $b(0) = c(0) = 0$ for cases 1, 2, and 3.

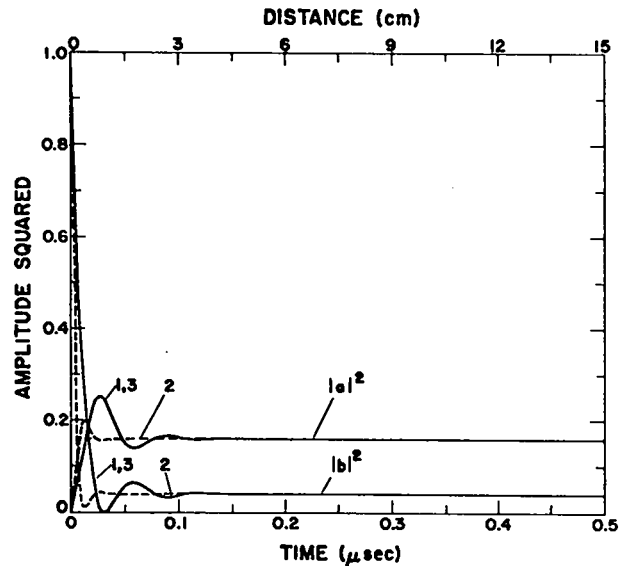


Fig. 12. The variation of $|a|^2$ and $|b|^2$ vs time for $B = B_0$ ($\delta = 0$) with initial conditions $b(0) = 1$, $a(0) = c(0) = 0$ for cases 1, 2, and 3.

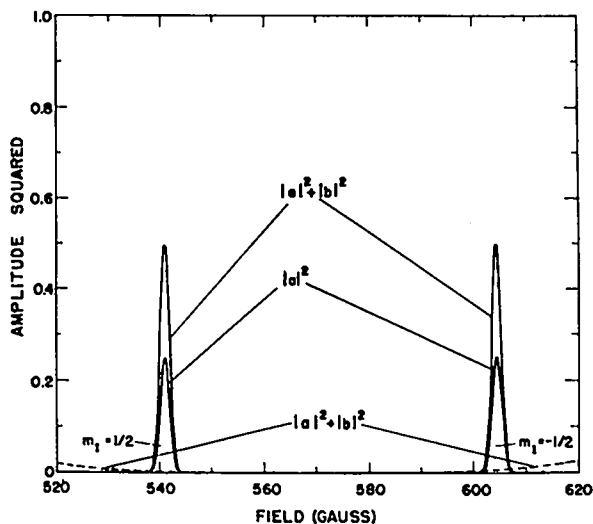


Fig. 13. The transmission of hydrogen metastable atoms ($|a|^2 + |b|^2$ and $|a|^2$) vs magnetic field for 1610 MHz; $|R| = 250$ MHz, and $|V| = 125$ MHz. The solid curves correspond to initial condition $a(0) = 1$ and the dashed curves correspond to $b(0) = 1$.

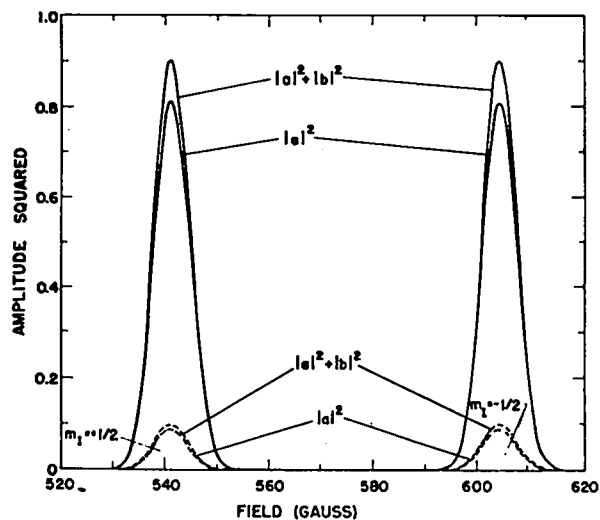


Fig. 15. The transmission of hydrogen metastable atoms ($|a|^2 + |b|^2$ and $|a|^2$) vs magnetic field for 1610 MHz; $|R| = 250$ MHz, and $|V| = 375$ MHz. The solid curves correspond to initial condition $a(0) = 1$ and the dashed curves correspond to $b(0) = 1$.

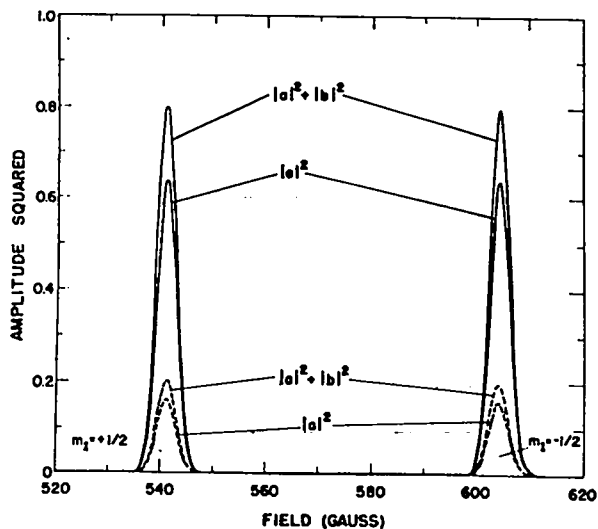


Fig. 14. The transmission of hydrogen metastable atoms ($|a|^2 + |b|^2$ and $|a|^2$) vs magnetic field for 1610 MHz; $|R| = 250$ MHz, and $|V| = 250$ MHz. The solid curves correspond to initial condition $a(0) = 1$ and the dashed curves correspond to $b(0) = 1$.

17.58, and 26.37 V/cm). The peaks at different magnetic field strengths correspond, of course, to different nuclear spin substates. An interaction time of 0.4 μ sec (corresponding to a cavity length 12 cm) is assumed. The solid curves correspond to an ini-

tial pure alpha-state beam ($a(0) = 1$) and the dashed curves correspond to a pure beta-state beam ($b(0) = 1$). For the highly symmetric case ($\frac{1}{2}|R| = |V|$) shown in Figure 13, the two initial conditions result, except in the "tail" region, in identical solutions. The quantities $|a|^2 + |b|^2$ and $|a|^2$ are plotted in each case.

Figures 16-18 show the transmission of deuterium metastable atoms for the same cases and conditions.

Several observations about the general nature of the solutions may be made from the graphs:

1. For fixed $|R|$, both the height and width of the lines which correspond to a $a(0) = 1$ increase with increasing $|V|$. (For fixed $|V|$, the height and width of the peaks which correspond to $b(0) = 1$ increase with increasing $|R|$, although this is not shown here.) The heights, of course, vary in the manner stated previously, and depend only on $|R|/|V|$. For the case $\frac{1}{2}|R| = |V|$, the $a(0) = 1$ and $b(0) = 1$ solutions become nearly identical. This result is apparent from the symmetry of the equations.
2. From Figures 9-11, one can see that the width of the resonance lines must decrease monotonically as the interaction time in-

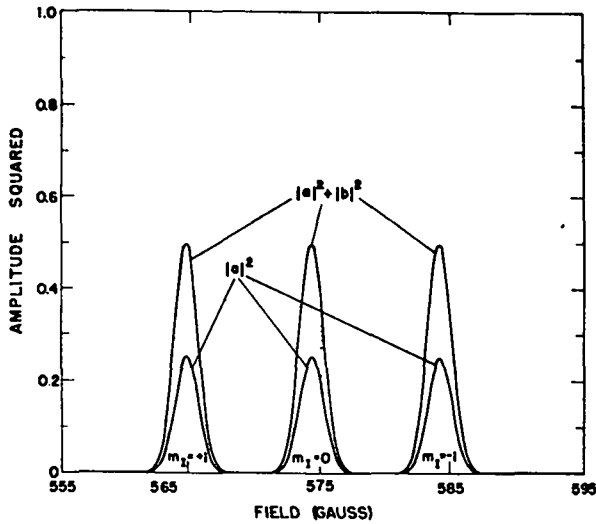


Fig. 16. The yield of deuterium metastable atoms ($|a|^2 + |b|^2$ and $|a|^2$) vs magnetic field for 1610 MHz; $|R| = 250$ MHz, and $|V| = 125$ MHz. For this case, curves corresponding to initial condition $a(0) = 1$ and to $b(0) = 1$ are identical.

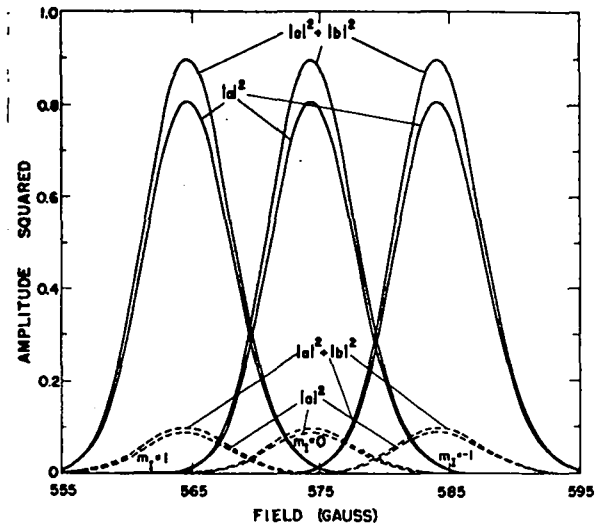


Fig. 18. The yield of deuterium metastable atoms ($|a|^2 + |b|^2$ and $|a|^2$) vs magnetic field for 1610 MHz; $|R| = 250$ MHz, and $|V| = 375$ MHz. The solid curves correspond to initial condition $a(0) = 1$ and the dashed curves to $b(0) = 1$.

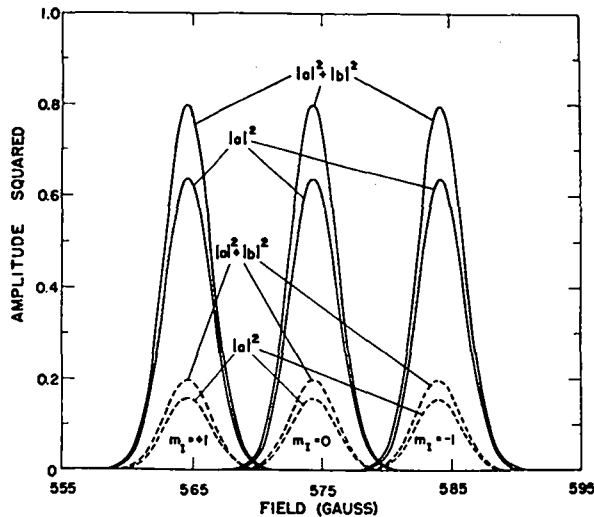


Fig. 17. The yield of deuterium metastable atoms ($|a|^2 + |b|^2$ and $|a|^2$) vs magnetic field for 1610 MHz; $|R| = 250$ MHz, and $|V| = 250$ MHz. The solid curves correspond to initial condition $a(0) = 1$ and the dashed curves to $b(0) = 1$.

creases. The curves shown in Figures 13-18 are for $t = 0.4$ μ sec, which corresponds to a cavity length of 12 cm for a beam with the velocity of interest (30 cm/ μ sec).

3. The separation of metastable hydrogen or

tritium atoms with different nuclear spin orientations appears to be very easy in the sense that the parameters may vary over a wide range. However, for metastable deuterium atoms, if one uses too large a field strength, the width of the lines will be too large. Thus, the minimum cavity length appears to be ~ 6 cm for deuterium atoms, but could be shorter for hydrogen or tritium atoms. (This is because $|R|/|V|$ must be held constant to achieve a given transmission at resonance. Since $|V| < |V|_{\max}$ is required, $|R| < |R|_{\max}$ is also required. But the decay constants corresponding to the unwanted nuclear spin states are approximately proportional to $|R|$; this implies $l > l_{\min}$ where l is the cavity length.)

For an incident unpolarized beam of metastables (i.e., 1/2 of beam in the α state, 1/2 in the β state) the transmission at resonance of the "spin filter" is exactly 50%, as may be verified from Figures 9 and 12 and from Figures 13-18. This follows from the expressions already derived which are repeated here in a matrix form:

$$\begin{pmatrix} a(t \rightarrow \infty) \\ b(t \rightarrow \infty) \end{pmatrix} = \frac{1}{P^2} \begin{pmatrix} V^*V & -\frac{R^*V}{2} \\ -RV^* & \frac{R^*R}{4} \end{pmatrix} \begin{pmatrix} a(0) \\ b(0) \end{pmatrix} .$$

The initial beam may be regarded as an incoherent mixture of α and β states although the final beam is a coherent mixture. If we average over initial and sum over final states, we find

$$|a(t \rightarrow \infty)|^2 + |b(t \rightarrow \infty)|^2 = \frac{1}{2}|a(0)|^2 + \frac{1}{2}|b(0)|^2 ;$$

i.e., 50% of an (electron) unpolarized beam is quenched.

We next consider the physical nature of the states which are transmitted through the spin filter.

As a first step we eliminate the explicit time dependence by defining the new variables

$$A = ae^{-i(\omega_\alpha - \omega)t}$$

$$B = be^{-i\omega_\beta t}$$

$$C = ce^{-i\omega_e t} .$$

The equations for these new variables are found to be

$$i\dot{A} = (\omega_\alpha - \omega)A + \frac{1}{2}R^*C$$

$$i\dot{B} = \omega_\beta B + V^*C$$

$$i\dot{C} = \frac{1}{2}RA + VB + (\omega_e - \frac{1}{2}i\gamma)C .$$

We choose $\omega_\beta = 0$ (which we may do since the energy scale is arbitrary) and define as usual $\delta = \omega_{\alpha\beta} - \omega$. The equations and definitions are then

$$i\dot{A} = \delta A + \frac{1}{2}R^*C$$

$$i\dot{B} = V^*C$$

$$i\dot{C} = \frac{1}{2}RA + VB - (\omega_{\beta e} + \frac{1}{2}i\gamma)C$$

$$A = ae^{-i\delta t}$$

$$B = b$$

$$C = ce^{+i\omega_{\beta e} t} .$$

Let us define the spinors r and s , with amplitudes p and q , as follows:

$$r = \frac{1}{P} (\frac{1}{2}R^*\alpha' + V^*\beta)$$

$$s = \frac{1}{P} (V\alpha' - \frac{1}{2}R\beta) ,$$

where the spinor $\alpha' = ae^{+i\delta t}$. The total wave function, neglecting the e state (i.e., for $t \rightarrow \infty$) is then of the form $\psi = a\alpha + b\beta = (ae^{-i\delta t})\alpha e^{i\delta t} + b\beta = A(\alpha e^{i\delta t}) + B\beta = A\alpha' + B\beta$. Notice that r and s are orthonormal. We can invert the definitions of r and s to find:

$$\alpha' = \frac{1}{P} (\frac{1}{2}Rr + V^*s)$$

$$\beta = \frac{1}{P} (Vr - \frac{1}{2}R^*s) .$$

Substituting these expressions into the definition of ψ :

$$\psi = pr + qs = A\alpha' + B\beta$$

we obtain:

$$p = \frac{1}{P} (\frac{1}{2}RA + VB) \quad A = \frac{1}{P} (\frac{1}{2}R^*p + Vq)$$

$$q = \frac{1}{P} (V^*A - \frac{1}{2}R^*B) \quad B = \frac{1}{P} (V^*p - \frac{1}{2}Rq) .$$

We now derive the differential equations for p and q :

$$i\dot{p} = Pc + \frac{R\delta A}{2P}$$

$$i\dot{q} = \frac{V^*\delta A}{P}$$

$$i\dot{C} = Pp - (\omega_{\beta e} + \frac{1}{2}i\gamma)C .$$

If we specialize to resonance ($\delta = 0$) these equations become

$$i\dot{p} = PC$$

$$i\dot{q} = 0$$

$$i\dot{C} = Pp - (\omega_{\beta e} + \frac{1}{2}i\gamma)C .$$

The variables may be further separated as follows:

$$-i\dot{p} = P(i\dot{C}) = P(Pp - i(\omega_{\beta e} + \frac{1}{2}i\gamma)C)$$

$$= P^2 p + (\frac{1}{2}\gamma - i\omega_{\beta e})\dot{p}$$

$$-\ddot{\vec{c}} = P(i\dot{\vec{p}}) - i(\omega_{\beta e} + \frac{1}{2}i\gamma)\dot{\vec{c}} = P^2\vec{c} + (\frac{1}{2}\gamma - i\omega_{\beta e})\dot{\vec{c}} .$$

Thus our three equations are

$$\ddot{\vec{p}} + (\frac{1}{2}\gamma - i\omega_{\beta e})\dot{\vec{p}} + P^2\vec{p} = 0$$

$$\dot{\vec{q}} = 0$$

$$\ddot{\vec{c}} + (\frac{1}{2}\gamma - i\omega_{\beta e})\dot{\vec{c}} + P^2\vec{c} = 0 .$$

These equations have the solutions

$$\vec{p} = p_1 e^{-\mu_1 t} + p_2 e^{-\mu_2 t}$$

$$\vec{q} = q_1$$

$$\vec{c} = c_1 e^{-\mu_1 t} + c_2 e^{-\mu_2 t} ,$$

where $\mu_{1,2} = (\gamma/4 - i\omega_{\beta e}/2) \pm \sqrt{(\gamma/4 - i\omega_{\beta e})^2 - P^2}$, i.e., μ_1 and μ_2 are the two large decay constants defined earlier. For times of interest to us, therefore:

$$p \rightarrow 0$$

$$q = q_1$$

$$c \rightarrow 0 .$$

Thus the amplitude of the spinor s is conserved while the amplitude of r decays exactly as does the amplitude of e .

Let us momentarily allow an arbitrary initial phase; i.e., we put, once again, $R = R_0$. In spinor notation, for $\delta = 0$, r and s may be written

$$r = \frac{R_{20}\psi_{00}}{P} \begin{pmatrix} \frac{1}{2}R_0^* e^{-i\omega_\alpha t} \\ V^* e^{-i\omega_\beta t} \end{pmatrix}$$

$$s = \frac{R_{20}\psi_{00}}{P} \begin{pmatrix} V e^{-i\omega_\alpha t} \\ -\frac{1}{2}R_0 e^{-i\omega_\beta t} \end{pmatrix} .$$

The expectation values of the Pauli operators for these states are tabulated below:

	r	s
$\langle \sigma_x \rangle$	$\epsilon_\perp \cos(\omega_{\alpha\beta} t + \Delta)$	$-\epsilon_\perp \cos(\omega_{\alpha\beta} t + \Delta)$
$\langle \sigma_y \rangle$	$\epsilon_\perp \sin(\omega_{\alpha\beta} t + \Delta)$	$-\epsilon_\perp \sin(\omega_{\alpha\beta} t + \Delta)$
$\langle \sigma_z \rangle$	ϵ_\parallel	$-\epsilon_\parallel$

In the above table, $e^{i\Delta} = R_0 V^* / |R_0 V^*|$, $\epsilon_\perp = |R_0 V^*| / P^2$, and $\epsilon_\parallel = (\frac{1}{2}R_0^* R_0 - V^* V) / P^2$. Thus the spinors r and s point opposite directions at all times, make an angle of $\theta = \tan^{-1} \frac{\epsilon_\perp}{\epsilon_\parallel}$ with respect to the z axis, and rotate with the Larmor frequency $\omega_{\alpha\beta}/2\pi$. The phase of the rotation is such that the direction of r is parallel and s antiparallel to the direction of the transverse field at the time the longitudinal rf field has its maximum positive value. (This can be most easily seen by considering the static transverse field to define the x axis, so that R_0 and V are both real.)

From this formulation we can again conclude that 50% of an (electron) unpolarized beam will survive the spin filter, since in that case a given particle has a 50% probability of being in either of any two orthonormal spin states, including the r and s states defined above.

We note that our resulting metastable beam has both 100% electron polarization (rotating) and 100% nuclear polarization, and that the relative direction of the electron spin can be varied. Further, the phase of the electron spin rotation is related to the cavity rf phase.

8. THE FOUR-LEVEL PROBLEM

We now consider the effect of the f -level on the solutions previously discussed. Qualitatively, it is clear that the transverse electric field will induce quenching through the $\alpha - f$ transition and the longitudinal rf electric field will induce quenching through the $\beta - f$ transition.

The four-level equations were stated in Section 5. The frequency dependent quantities which enter into these equations are

$$e^{i\omega_\alpha t} \cos \omega t = \frac{1}{2} e^{i(2\omega_{\alpha\beta} + \omega_{\beta f} - \delta)t} + \frac{1}{2} e^{i(\omega_{\beta e} + \delta)t}$$

and

$$e^{i\omega_\beta t} \cos \omega t = \frac{1}{2} e^{i(\omega_{\alpha f} - \delta)t} + \frac{1}{2} e^{i(\omega_{\beta f} - \omega_{\alpha\beta} + \delta)t} ,$$

where $\delta = \omega_{\alpha\beta} - \omega$ as before. The first of these expressions, as noted in the discussion of the three-level system, may be approximated (near $\delta = 0$) by the second term alone. For the second of these expressions, on the other hand, the two terms

are of roughly equal importance. Thus the simplest equations which reasonably describe the four level system are:

$$\begin{aligned} i\dot{a} &= \frac{1}{2}R^*ce^{i(\omega_{\beta e} + \delta)t} + Vde^{i\omega_{\alpha f}t} \\ i\dot{b} &= V^*ce^{i\omega_{\beta e}t} - \frac{1}{2}Rde^{-i\omega_{\alpha f}t} \cos(\omega_{\alpha\beta} - \delta)t \\ i\dot{c} &= \frac{1}{2}Rae^{-i(\omega_{\beta e} + \delta)t} + Vbe^{-i\omega_{\alpha f}t} \\ i\dot{d} &= V^*ae^{-i\omega_{\alpha f}t} - \frac{1}{2}R^*be^{-i\omega_{\beta e}t} \cos(\omega_{\alpha\beta} - \delta)t, \end{aligned}$$

where we have put $R' = -R^*$ and $V' = V^*$ in accordance with Table X and the discussion in Section 6. Note that these relations hold only in the zero field limit; i.e., if $\epsilon_1, \epsilon_2, \epsilon_3$, and $\epsilon_4 \rightarrow 1$. All four-level calculations presented here are based on this assumption. Note also that an arbitrary initial phase cannot be included in the four-level case by putting $R = R_0$ as was done in Section 7. The initial phase is, however, of no importance.

We first consider the quenching of α states by a transverse electric field with no rf longitudinal field present (i.e., $R = 0$). The equations above then separate into two independent pairs of which the $\alpha - f$ pair is

$$\begin{aligned} i\dot{a} &= Vde^{i\omega_{\alpha f}t} \\ i\dot{d} &= V^*ac^{-i\omega_{\alpha f}t} - \frac{1}{2}i\gamma d. \end{aligned}$$

These equations are easily solved if one assumes

$$\begin{aligned} a &= A_1 e^{-\mu_1 t} + A_2 e^{-\mu_2 t} \\ d &= (D_1 e^{-\mu_1 t} + D_2 e^{-\mu_2 t}) e^{-i\omega_{\alpha f}t}. \end{aligned}$$

One finds that μ_1 and μ_2 are the roots of

$$\mu^2 + 2\xi\mu + |V|^2 = 0,$$

where

$$\xi = \gamma/4 - i\omega_{\alpha f}/2.$$

Thus we may write $\mu_{1,2} = \xi \pm \eta$ where $\eta = \sqrt{\xi^2 - |V|^2}$. For the initial condition $a(0) = 1, d(0) = 0$, the general solution for a is found to be

$$a = \frac{1}{2}(1 - \frac{\xi}{\eta})e^{-(\xi + \eta)t} + \frac{1}{2}(1 + \frac{\xi}{\eta})e^{-(\xi - \eta)t}.$$

If $|\xi|^2 \gg |V|^2$, we may approximate η by

$$\eta = \xi - \frac{|V|^2}{2\xi}.$$

The expression for a becomes

$$a \approx \frac{|V|^2}{4\xi^2} e^{-2\xi t} + e^{-\left(\frac{|V|^2}{2\xi}\right)t}.$$

The first term has a small coefficient and rapid decay constant; for times of interest, we may write

$$|a|^2 \approx e^{-(\gamma^{\alpha f})t}, \quad \gamma^{\alpha f} = \frac{\gamma|V|^2}{\omega_{\alpha f}^2 + (\gamma/2)^2},$$

which is the Stark quenching formula given by Lamb and Retherford.⁵ Similar results are obtained for the $\beta - e$ quenching:

$$|b|^2 \approx e^{-(\gamma^{\beta e})t}, \quad \gamma^{\beta e} = \frac{\gamma|V|^2}{\omega_{\beta e}^2 + (\gamma/2)^2}$$

and for the $\alpha - e$ quenching:

$$|a|^2 \approx e^{-(\gamma^{\alpha e})t}, \quad \gamma^{\alpha e} = \frac{\gamma|R|^2/4}{(\omega_{\alpha e} - \omega)^2 + (\gamma/2)^2}.$$

This result is not applicable to the $\beta - f$ quenching, however. It should also be noted that for the field strength of present interest, the expansion of η used above will not be valid for the $\beta - e$ case if $\omega_{\beta e}$ is small or zero.

Thus, for α atoms in the presence of both rf and static electric fields, we would expect an effective decay constant of the order of, but greater than, $\gamma^{\alpha f}$. The situation is complicated, however, since the various contributions to the decay are coherent.

An analytic solution at $\delta = 0$ is possible if $e^{i\omega_{\beta f}t} \cos \omega_{\alpha\beta}t$ is approximated by $e^{i\omega_{\alpha f}t}$. As already noted, this is not a good approximation; however, it at least partially takes into account the $\beta - f$ interaction and is included here primarily for the physical insight that it may afford.

To obtain this solution, we first eliminate the oscillating time dependence with the substitution

$$A = ae^{-i\delta t}$$

$$B = b$$

$$C = ce^{i\omega_{\beta e} t}$$

$$D = de^{i(\omega_{\alpha f} - \delta)t}$$

The equations for these variables are

$$\begin{bmatrix} i\dot{A} \\ i\dot{B} \\ i\dot{C} \\ i\dot{D} \end{bmatrix} = \begin{bmatrix} \delta & 0 & \frac{1}{2}R^* & \gamma \\ 0 & 0 & V^* & -\frac{1}{2}R \\ \frac{1}{2}R & V & -(\omega_{\beta e} + \frac{1}{2}i\gamma) & 0 \\ V^* & -\frac{1}{2}R^* & 0 & -(\omega_{\alpha f} - \delta + \frac{1}{2}i\gamma) \end{bmatrix} \begin{bmatrix} A \\ B \\ C \\ D \end{bmatrix}$$

In terms of the previously defined amplitudes p and q , we can derive

$$i\dot{p} = R\delta A/2P + PC$$

$$i\dot{q} = V^*\delta A/P + PD$$

$$i\dot{C} = Pp - (\omega_{\beta e} + \frac{1}{2}i\gamma)C$$

$$i\dot{D} = Pq - (\omega_{\alpha f} - \delta + \frac{1}{2}i\gamma)D$$

$$P^2 = \frac{1}{2}R^*R + V^*V$$

At resonance ($\delta = 0$) the equations reduce to the two coupled pairs

$$i\dot{p} = PC$$

$$i\dot{C} = Pp - (\omega_{\beta e} + \frac{1}{2}i\gamma)C$$

and

$$i\dot{q} = PD$$

$$i\dot{D} = Pq - (\omega_{\alpha f} + \frac{1}{2}i\gamma)C$$

from which it follows that

$$\ddot{p} + 2\xi_{\beta e}\dot{p} + P^2p = 0$$

$$\ddot{C} + 2\xi_{\beta e}\dot{C} + P^2C = 0$$

$$\xi_{\beta e} = \gamma/4 - i\omega_{\beta e}/2$$

and

$$\ddot{q} + 2\xi_{\alpha f}\dot{q} + P^2q = 0$$

$$\ddot{D} + 2\xi_{\alpha f}\dot{D} + P^2D = 0$$

$$\xi_{\alpha f} = \gamma/4 - i\omega_{\alpha f}/2$$

Thus

$$p = p_1 e^{-\mu_1 t} + p_2 e^{-\mu_2 t}$$

$$\text{where } \mu_{1,2} = \xi_{\beta e} \pm \sqrt{\xi_{\beta e}^2 - P^2}$$

and

$$q = q_1 e^{-\mu'_1 t} + q_2 e^{-\mu'_2 t}$$

$$\text{where } \mu'_{1,2} = \xi_{\alpha f} \pm \sqrt{\xi_{\alpha f}^2 - P^2}$$

The quantities μ_1 and μ_2 are recognized as the two larger decay constants discussed in the three-level case; thus, for times of interest, $p \rightarrow 0$. However, $\xi_{\alpha f} \gg P^2$ for the present region of interest, so we may expand the square root (as before) to obtain

$$\mu'_1 \approx 2\xi = \gamma/2 - i\omega_{\alpha f}$$

$$\mu'_2 \approx P^2/2\xi = P^2/(\gamma/2 - i\omega_{\alpha f})$$

The μ'_1 term decays rapidly, so for times of interest

$$q \approx q_2 e^{-(P^2/2\xi)t}$$

Our initial conditions are $A(0) = 1$, $B(0) = C(0) = D(0) = 0$. Now

$$q(0) = \frac{1}{P} (V^*A(0) - \frac{1}{2}R^*B(0)) = \frac{V^*}{P}$$

and

$$\dot{q}(0) = \frac{1}{P} (V^*\dot{A}(0) - \frac{1}{2}R^*\dot{B}(0)) = 0$$

where the latter condition follows from the differential equations. These conditions yield

$$q_2 = \frac{\xi + \eta}{2\eta} \frac{V^*}{P} \approx \frac{V^*}{P}$$

Thus, for large times,

$$p \rightarrow 0; \quad q \rightarrow \frac{V^*}{P} e^{-(P^2/2\xi)t}$$

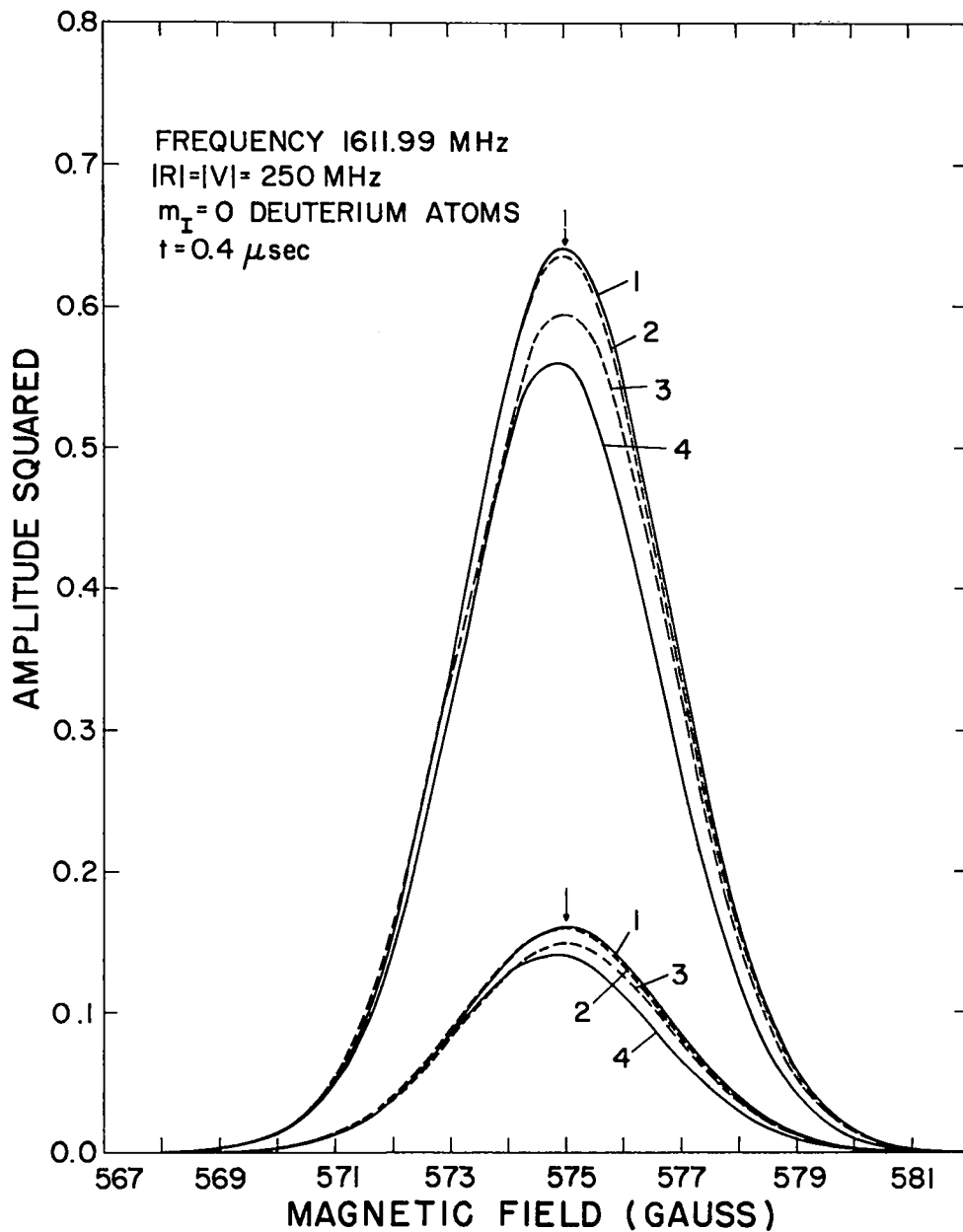


Fig. 19. The line shape as calculated with various approximations. The upper curves correspond to $|a|^2$ and the lower curves to $|b|^2$. The curves marked 1 correspond to the three-level theory. The curves marked 2 show the effect of inclusion of both terms of $\cos \omega t$ in the three-level theory. The curves marked 3 correspond to the approximate four-level theory in which $e^{i\omega_{\beta f} t} \cos \omega t$ is replaced by $e^{i(\omega_{\alpha f} - \delta)t}$ and $e^{i\omega_{\alpha e} t} \cos \omega t + e^{i(\omega_{\beta e} + \delta)t}$. The curves marked 4 correspond to the exact solutions of the four-level problem.

Inserting these into the definition of A and B, we obtain

$$A = \frac{1}{P} (\frac{1}{2}R^*P + Vq) \rightarrow \frac{|V|^2}{P^2} e^{-(P^2/2\xi)t}$$

$$B = \frac{1}{P} (V^*P - \frac{1}{2}Rq) \rightarrow \frac{-RV^*}{2P} e^{-(P^2/2\xi)t}$$

In the three-level case, for large time, we obtained

$$A \rightarrow \frac{|V|^2}{P^2} \quad B \rightarrow \frac{-RV^*}{2P}$$

Thus, both $|A|^2$ and $|B|^2$ are altered only by a multiplicative factor $e^{-\gamma^{af}t}$ where

$$\gamma^{af} = \frac{\gamma P^2}{\omega_{af}^2 + (\gamma/2)^2}, \quad P^2 = \frac{1}{2}|R|^2 + |V|^2$$

A point worth noticing with respect to these solutions is that only the state with amplitude q (the s state) is coupled directly to the f state. That is, if the e level were not present, the α - f - β interaction, in this approximation, would select the r state and quench the s state. This is exactly the opposite to the situation for the α - e - β interactions; thus this contribution from the f level is destructive.

In Figure 19 the line shape obtained by numerical integration, with various approximations, is shown. The calculation is for the case of $m_I = 0$ deuterium atoms at the (nearly) optimum frequency of 1611.99 MHz (which corresponds to $B_0 = 575$ G). The parameters are $|R| = |V| = 250$ MHz. We note that, as expected, the curve which corresponds to the ($\delta = 0$) analytic solution given above gives a result about midway between the three-level and the four-level results.

In Figure 20 the exact four-level results for the loss (at resonance) of $|a|^2$ are shown for various parameters and for the same frequency and magnetic field as above. These curves represent the ratio of $|a|^2$ (at 0.25 μ sec) to the three-level equilibrium value ($|a_0|^2$) which would obtain in the absence of the f level. The dashed curve represents the prediction of the approximate four-level analytic solution given above. Note that this predicted value depends only on $\frac{1}{2}|R|^2 + |V|^2$. The

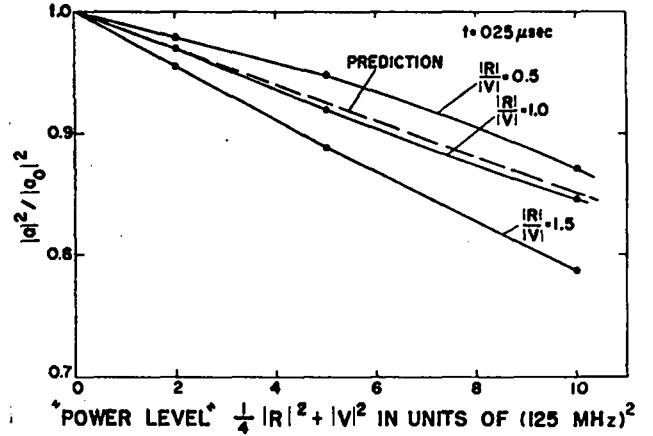


Fig. 20. The ratio of $|a|^2$ to $|a_0|^2$, where $|a_0|^2$ is the three-level equilibrium value of $|a|^2$, for $B_0 = 575$ G. The points are calculated from the exact four-level theory; the curves are visual fits to the points. The dashed curve represents the prediction obtained from the (approximate) four-level analytic solutions.

ratios vary approximately linearly with the interaction time t . The ratio of $|b|^2$ to $|b_0|^2$ is, for this case, indistinguishable from the ratio of $|a|^2$ to $|a_0|^2$.

Figure 21 shows the time dependence of the solutions, at $\delta = 0$, for the conditions used in Figure 19. Note that the inclusion of the antiresonant term in the three-level theory (the Bloch-Siegert correction term) results in a decay from the three-level equilibrium solution of about 2%/ μ sec.

Figure 22 shows the line shape for a frequency of 1508.326 MHz. Again the calculation is for $m_I = 0$ deuterons (for which this particular frequency corresponds to $B_0 = 538$ G) and for $|R| = |V| = 250$ MHz. Note the shift of the peaks from the resonant field.

Figure 23 shows the loss through the f state, for a frequency 1508.326 MHz and field 538 G ($m_I = 0$ deuterium atoms), for a variety of parameters $|R|$ and $|V|$. In this case, unlike that shown in Figure 20, the ratios $|a|^2/|a_0|^2$ and $|b|^2/|b_0|^2$ are not identical. Further, the loss through the f level appears to be somewhat greater. However, as may be seen by comparing Figures 19 and 22, the peak positions are shifted in the latter case, and therefore $\delta = 0$ does not, in general, correspond to maximum transmission. If both $|a|^2$ and $|b|^2$ transmission

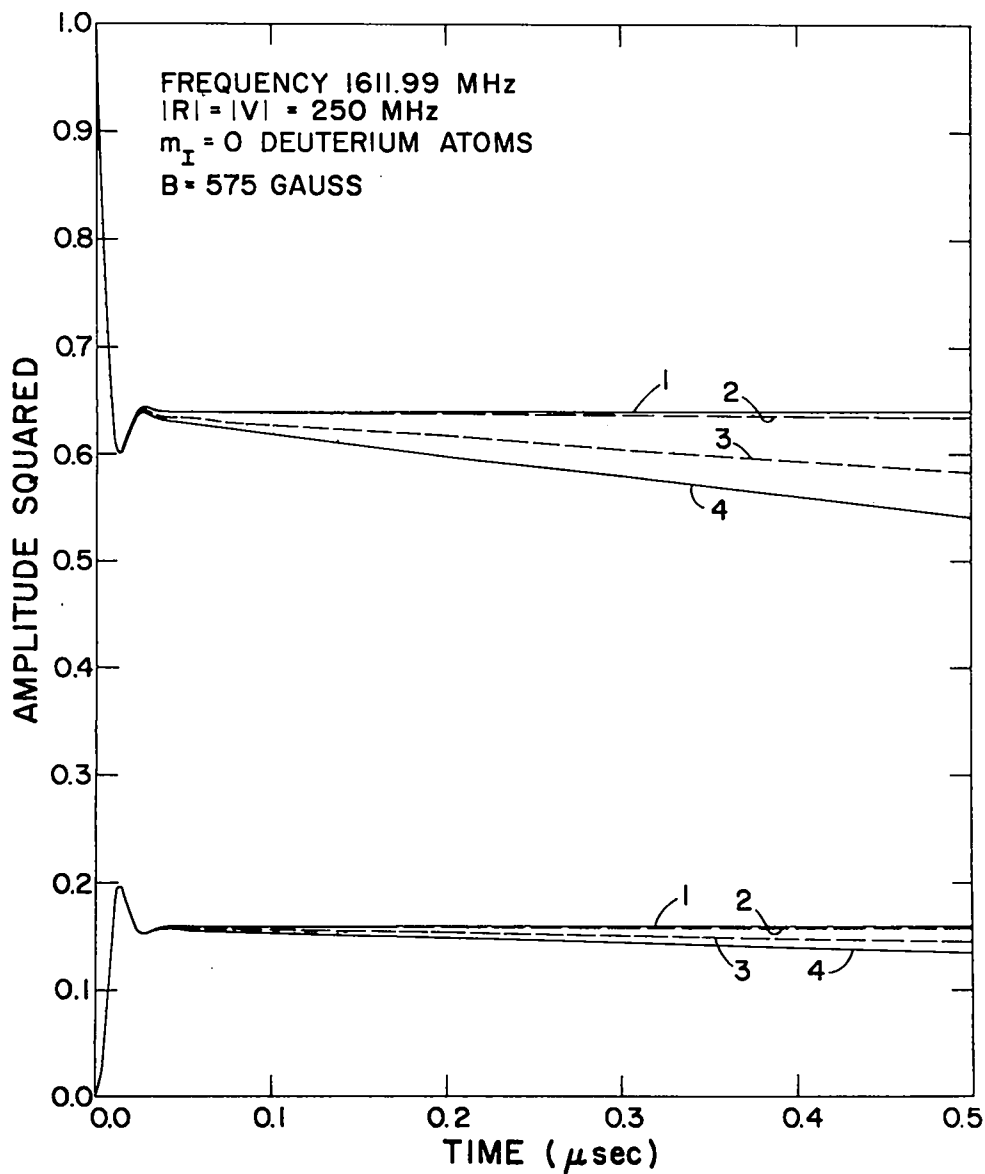


Fig. 21. The time dependence of the amplitudes $|a|^2$ and $|b|^2$, at $\delta = 0$, for various approximations. The curves are labeled as in Fig. 19.

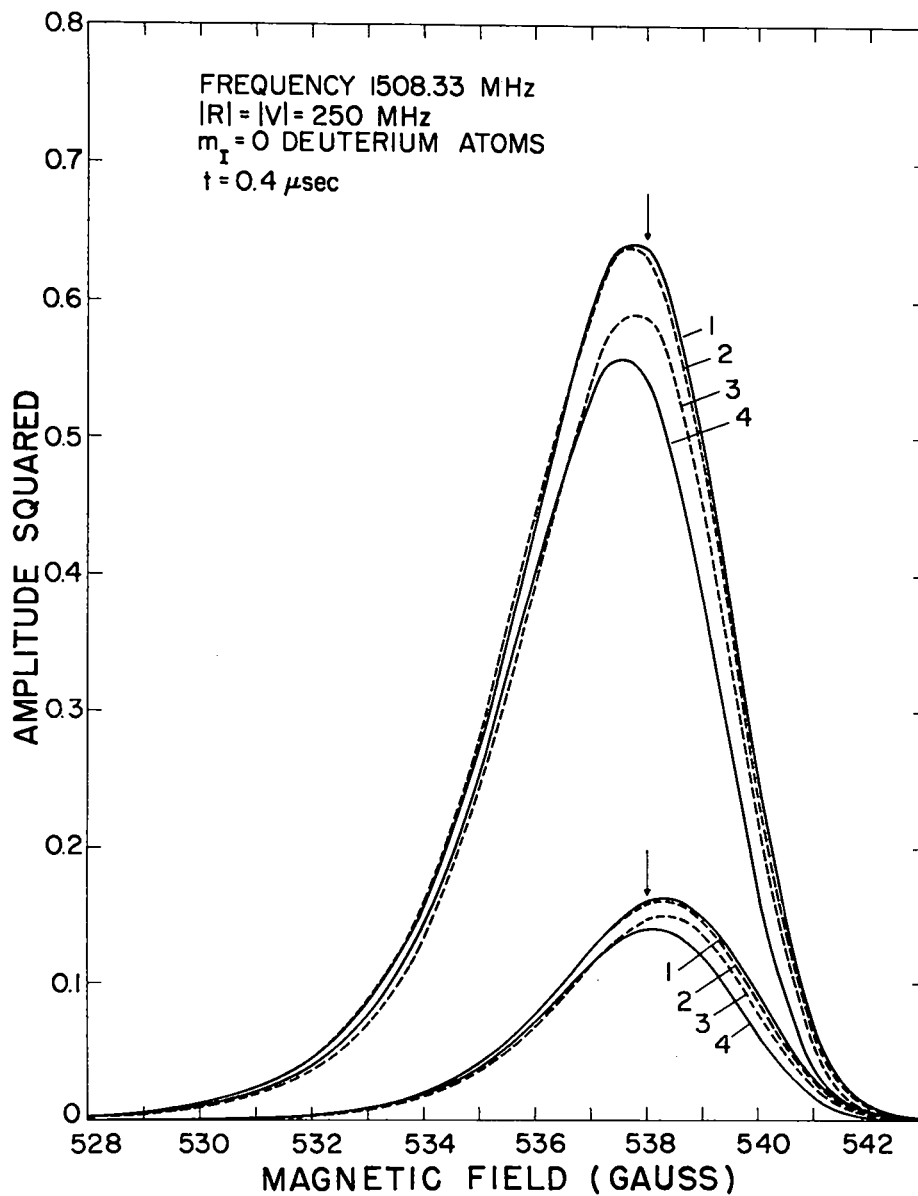


Fig. 22. The line shape as calculated with various approximations. The curves are labeled as in Fig. 19. Note the shift of the peaks from the resonant field (see arrows).

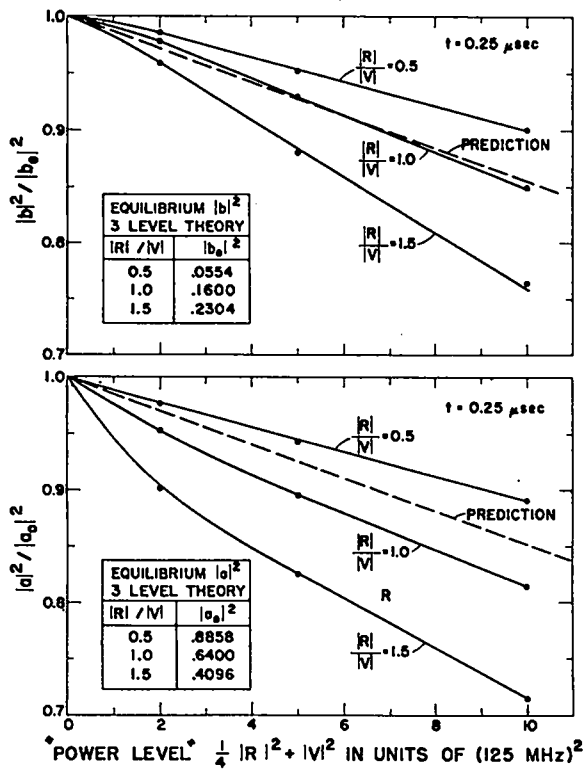


Fig. 23. The lower graph shows the ratio of $|a|^2$ to $|a_0|^2$, where $|a_0|^2$ is the three-level equilibrium value of $|a|^2$, for $B_0 = 538$ G. The upper graph shows the ratio of $|b|^2$ to $|b_0|^2$ for these conditions.

are of interest (see Section 9) the value of δ which results in maximum transmission of $|a|^2 + |b|^2$ will depend on the parameters. (This is true since the $|a|^2$ and $|b|^2$ curves are shifted in opposite directions for $\omega_{\beta\alpha} \neq 0$, and the relative contribution of $|a|^2$ and $|b|^2$ to the total transmitted beam depends on $|R|/|V|$.) Thus the curves given in Figure 23 predict greater loss, in general, than would be obtained by choosing an optimum value of δ .

Finally, calculations show that the three-level and four-level results agree to within $\sim 10\%$, for a wide range of parameters, in the tail region. Thus, the transmission of the unselected substates is adequately described by the results given in Table XI. The transmission of the selected substate can, however, be improved by the field shaping technique to be described in Section 9.

9. ADIABATIC VARIATION OF THE ELECTRIC FIELDS

In the preceding discussion, we have assumed that the various applied fields are constant throughout the spin filter. If this condition is not met, we must resort to numerical techniques to solve even the three-level equations, although some general features of the solutions may be deduced from the form of the equations.

For application to a practical polarized ion source, the optimum transmission of the desired nuclear spin substate can be achieved if (a) the static electric field is constant, and (b) the rf field increases slowly from zero at the entrance of the spin filter to a maximum near the center and then decreases to zero at the exit.

It was shown in Section 7 that, in three-level approximation, exactly 50% of an (electron) unpolarized H^{25} beam with the desired m_I value could be transmitted through a combination of static transverse and longitudinal rf electric fields. In a practical ion source, however, the β component of the atomic beam will almost certainly be quenched by the required "sweep" fields long before it reaches the spin filter. In addition, any β component which emerges from the filter will probably be quenched before reaching the argon exchange cell. For the parameters $|R| = |V| = 250$ MHz, for example, only 64% of an initially pure α beam would emerge from the spin filter in an α state, so that only about 1/3 of the initially produced unpolarized beam would be available at the argon exchange cell. (Note that we are referring always to the beam component with the desired m_I value; thus, in terms of the total atomic beam the 1/3 given above becomes 1/6 for hydrogen or tritium beams and 1/9 for deuterium beams.)

If the fields are shaped as indicated above, it is possible, in the three-level approximation, to achieve 100% transmission for a pure α beam. A spin filter with such field shaping will have 0% transmission for a β beam and thus will still have 50% transmission for an (electron) unpolarized beam. This is indicated in Figure 24 for a space variation of the rf field strength of the form $\sin(\frac{\pi z}{z_0})$ where z is the distance from the entrance to the rf region and z_0 is the total length of the rf region. For this example $|V|$ is assumed to have the constant

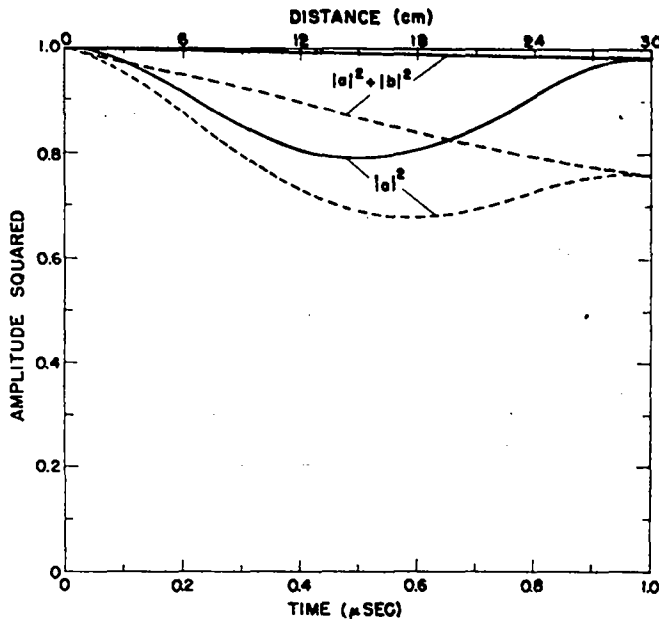


Fig. 24. The quantities $|a|^2 + |b|^2$ and $|a|^2$ vs time as a metastable beam ($a(0) = 1$) traverses a cavity whose rf strength varies as $\sin(\pi z/z_0)$, where $z_0 (= 30 \text{ cm})$ is the total length of the cavity. These curves correspond to $\delta/2\pi = 0$, $|R|_{\text{max}} = 250$ MHz, and to a constant static electric field such that $|V| = 250$ MHz.

value 250 MHz and $|R|_{\text{max}} = 250$ MHz. The results of both three-level and four-level theory are shown. (The deviation from 100% of the transmission which corresponds to three-level theory arises solely from the inclusion of both frequency terms in the expansion of $\cos(\omega t)$, while the discussion above is based on the assumption $\cos \omega t \cong \frac{1}{2}e^{i\omega t}$. All results presented in Figures 24 and 25 are based on calculations which include both terms of $\cos \omega t$.)

These results can be understood as follows. For simplicity, consider the special case of resonance ($\delta = 0$) and crossing ($\omega_{\beta e} = 0$). The three-level equations are then, as noted in Section 7:

$$i\dot{a} = \frac{1}{2}R^*c$$

$$i\dot{b} = V^*c$$

$$i\dot{c} = \frac{1}{2}Ra + Vb - \frac{1}{2}(i\gamma c)$$

Also as noted in Section 7, it is evident that one possible solution of these equations is

$$a = a_0, \quad b = b_0, \quad c = 0$$

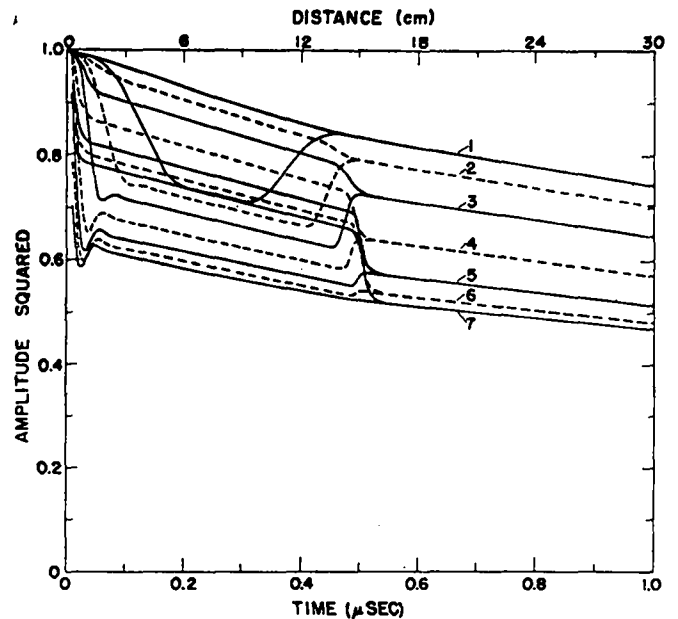


Fig. 25. The quantities $|a|^2 + |b|^2$ and $|a|^2$ vs time for various rates of increase and decrease of the rf field strength. The rising and falling portions of the rf field have the shape $\sin^2(\pi/2\tau)$. The curves numbered 1-7 correspond to $\tau = 0.2, 0.1, 0.05, 0.025, 0.00125, 0.000625$, and $0.0 \mu\text{sec}$, respectively. For all curves $\delta/2\pi = 0$ and $|R| = |V| = 250$ MHz. Note the decrease in the overall decay rate when the rf field is turned off.

where the constants a_0 and b_0 are related by

$$\frac{1}{2}Ra_0 + Vb_0 = 0$$

or, equivalently

$$a_0/b_0 = -2V/R.$$

(These are, in fact, the equilibrium solutions previously discussed.) If $|R| \rightarrow 0$, the equilibrium solution will correspond to a pure α state. If $|R| \rightarrow 0$ all nuclear substates are equivalent and no selection would occur. However, if $|R|$ is increased sufficiently gradually, so that the condition $\frac{1}{2}Ra + Vb = 0$ can be followed adiabatically, the nuclear spin selection can be made without loss. At this point, the amplitude which describes a particle in the beam will be a coherent mixture of α and β states. If $|R|$ is then slowly decreased to zero, the α and β mixture will be transformed back into a pure α state. Thus there are two important aspects to the field shaping: (a) a slow rise of $|R|$ prevents loss from occurring through the excitation of "transients" as the beam enters the cavity,

and (b) a slow fall of $|R|$ transforms the mixed α and β state back into the more stable pure α state. If no quenching between the rf region and the argon exchange region were likely to occur, the second part of the field shaping would be unnecessary. It is evident that the important parameter in these arguments is $|R|/|V|$, so that an exactly constant $|V|$ is not required.

The above can also be expressed in terms of the r and s spinors defined in Section 7. We recall that

$$s = \frac{1}{P} (V\alpha - \frac{1}{2}R\beta)$$

and has the constant amplitude q_1 . In terms of a and b , for $\delta = 0$,

$$q = q_1 = \frac{1}{P} (V^*a - \frac{1}{2}Rb) .$$

Thus, if $|R| \rightarrow 0$, $s \rightarrow \alpha$ and $q(t) = q_0 = a(0) = 1$. If $|R|$ is increased sufficiently gradually, the state s will be conserved and therefore a particular $\alpha + \beta$ mixture will be formed. If $|R|$ is then decreased sufficiently gradually, it will again be conserved and the mixture state will be transformed back into a pure α state.

It remains to determine what is meant by "sufficiently gradually." In Figure 25 the results for various assumed rise times for the rf field are presented. The exact four-level theory was used for these calculations. We assume a 30 cm overall path (velocity = 30 cm/ μ sec) and that only the static electric field acts over the last 15 cm. The rising and falling portions of the rf field is assumed to have the shape $\sin^2(t\pi/2\tau)$. The rf field is fully turned off at $t = 0$ and at $t = 0.5 \mu$ sec. The various curves are labeled with the parameter τ and in each case the upper curve represents $|a|^2 + |b|^2$, and the lower curve $|a|^2$. It is seen that no loss occurs for the case $\tau = 0.2 \mu$ sec. At the steepest part of the $\sin^2(t\pi/2\tau)$ curve, the fractional rate of change in $|R|$ is π/τ . For $\tau = 0.2 \mu$ sec, $\pi/\tau \approx$

$15.7 \times 10^6 \text{ sec}^{-1}$. Since the Larmor frequency is around $1600 \times 10^6 \text{ sec}^{-1}$, $|R|$ changes about 1% in a Larmor cycle. Thus, we have demonstrated that a satisfactory criterion for adiabaticity is that the strength of the rf field may change no more than about 1% per cycle. This is about the value that one would expect.

ACKNOWLEDGMENTS

It is a pleasure to acknowledge many helpful discussions with the following Los Alamos Scientific Laboratory colleagues: D. Dodder, B. Watt, R. Stevens, L. Heller, and J. Jackson. Professor C. Drake of Oregon State University also made some useful comments concerning this material. H. Butler kindly made available a very useful computer program for numerical integration.

REFERENCES

1. G. G. Ohlsen and J. L. McKibben, *Bull. Am. Phys. Soc.* 12, 463 (1967).
2. J. L. McKibben, G. G. Ohlsen, and R. R. Stevens, *Bull. Am. Phys. Soc.* 12, 463 (1967).
3. B. L. Donnally, T. Clapp, W. Sawyer, and M. Schulz, *Phys. Rev. Letters* 12, 502 (1964).
4. B. L. Donnally and W. Sawyer, *Phys. Rev. Letters* 15, 439 (1965).
5. Willis E. Lamb, Jr., and Robert C. Retherford, *Phys. Rev.* 81, 222 (1951).
6. R. T. Robiscoe and B. L. Cosens, *Phys. Rev. Letters* 17, 69 (1966).
7. R. T. Robiscoe and B. L. Cosens, *Bull. Am. Phys. Soc.* 11, 62 (1966).
8. Willis E. Lamb, Jr., *Phys. Rev.* 85, 259 (1952).
9. C. W. Drake and R. Krotkov, *Phys. Rev. Letters* 16, 848 (1966).
10. M. Leventhal, *Physics Letters* 20, 625 (1966).
11. B. Donnally, *Bull. Am. Phys. Soc.* 12, 509 (1967).
12. F. Bloch and A. Siegert, *Phys. Rev.* 57, 522 (1940).
13. H. A. Bethe and E. E. Salpeter, *Handbuch der Physik*, Vol. 35, p. 88 (Springer-Verlag, Berlin, 1957).
14. E. U. Condon and G. H. Shortley, *The Theory of Atomic Spectra* (Cambridge University Press, London, 1953).

APPENDIX A. A COMPUTER PROGRAM FOR EVALUATING THE ANALYTIC SOLUTION OF THE THREE-LEVEL EQUATIONS

A FORTRAN IV program which evaluates the solutions developed in Section 7 is given in this appendix. The version given computes the squared amplitudes $|a|^2$, $|b|^2$, $|c|^2$, and $|a|^2 + |b|^2$ as a function of time for a set of fixed driving frequencies and for fixed magnetic field. The modulus and phase of a, b, and c are also given. Other versions of the program exist in which time is held constant while the variation of the above quantities with magnetic field at fixed frequency, or with frequency at fixed magnetic field, is studied.

The input for the program is as follows:

Card 1 (FORMAT 6 F12.6)

XSPIN spin of nucleus (i.e., $\frac{1}{2}$ or 1)
 GJ g_J value for the $2S_{\frac{1}{2}}$ states ($\equiv 2$)
 XMU magnetic moment of the nucleus (in nuclear magnetons)
 DELW zero magnetic field hyperfine splitting for the $2S_{\frac{1}{2}}$ state (MHz)
 GJP g_J value for the $2P_{\frac{1}{2}}$ states ($\equiv 2/3$)
 DELWP zero magnetic field hyperfine splitting for the $2P_{\frac{1}{2}}$ states (MHz)

(The radiative correction to the g_J value is supplied by the subroutine BREIT and should not be included in GJ and GJP.)

Card 2 (FORMAT 6 F12.6)

FREQMN minimum applied frequency (MHz)
 FREQDL increment in applied frequency (MHz)
 FREQMX maximum applied frequency (MHz)
 TF maximum time at which solutions are to be evaluated (μsec)
 DELT increment in time at which solutions are to be evaluated (TF/DELT should not exceed 500)
 BGAUSS magnetic field (G)

Card 3 (FORMAT 6 F12.6)

XMM M in MHz (angular frequency)
 RR R in MHz (angular frequency)
 VV V in MHz (angular frequency)

where these quantities are complex and therefore appear as three pairs of numbers on the card. The real part of each quantity appears first. The relations between these units and practical units are given in the program listing.

Card 4 (FORMAT 6 I4)

IMODE If IMODE = 1, program returns to start.
 If IMODE = 2, program returns to read in new Card 3 and proceeds.
 ICSMN minimum case to be calculated
 ICSMX maximum case to be calculated

where $m_I = 1, 0, -1$ correspond to cases 1, 2, and 3 for deuterium atoms and $m_I = \frac{1}{2}, -\frac{1}{2}$, correspond to cases 1 and 2 for hydrogen and for tritium atoms.

The program consists of a main program together with several subroutines. The function of the various subroutines is as follows:

a) SUBROUTINE CUBIC (P, Q, R, RT1, RT2, RT3)

This subroutine evaluates the solutions of a cubic equation with complex coefficients of the form $x^3 + Px^2 + Qx + R = 0$. It uses double-precision arithmetic in order to obtain the required accuracy. The three complex roots, RT1, RT2, and RT3 are in order of decreasing real parts.

b) SUBROUTINE DPROD (XR, XI, YR, YI, ZR, ZI)

This subroutine multiplies the complex numbers X and Y together to give complex Z. Double-precision arithmetic is used; thus the real and imaginary parts are carried separately.

c) SUBROUTINE DARCTAN (Y, X, Z)

This subroutine finds $Z = \arctangent(Y/X)$ in the correct quadrant. Double-precision arithmetic is used.

d) SUBROUTINE BREIT (XI, FFF, XM, GJ, GI, DELW, BGAUSS, W, XGAUSS, EPS1)

This subroutine evaluates the energy of a given state according to the Breit-Rabi formula (see Section 2). The input variables are

XI spin of nucleus
 FFF F quantum number
 XM m_F quantum number
 GJ g_J value (atomic g factor) excluding radiative corrections
 GI g_I value (nuclear g factor)
 DELW zero magnetic field hyperfine splitting in MHz
 BGAUSS magnetic field in G

The output variables are

W energy of state in MHz
 XGAUSS value of the parameter X (defined in Section 2)

EPS1 nuclear moment correction term ϵ_1
(in MHz; already included in W)

The output from the program is fully labeled, and includes the values of the coefficients A_k , B_k , and C_k , the decay constants μ_k , and the relevant frequencies in MHz. In addition, the three quantities $F1$, $F2$, and $F3$, which are the values of $\mu_k^3 + \mu_k^2$

+ $Q\mu_k + R$ for $k = 1, 2, 3$, are given. The deviation of these quantities from zero gives some idea of the accuracy with which the roots have been determined.

Tape 10 is defined as input and Tape 9 as output for the particular system for which this program was written.

```

C TIME PLOT VERSION
C DIVIDE R AND V BY 13.94 TO OBTAIN VOLTS/CM PEAK TO ZERO
C DIVIDE M BY 8.80 TO OBTAIN GAUSS PFAK TO ZERO
C THAT IS, ENTER R,V, AND M IN MHZ ANGULAR FREQUENCY
  DIMENSION FFA(6),FFB(6),XMFA(6),XMFB(6)
  DIMENSION FARS(3),FACS(3),FBCS(3)
  DIMENSION ASQ(500),BSQ(500),CSQ(500),ABSQ(500),TIME(500)
  COMPLEX XMM,RR,VV,DELAC,P,Q,R,XMMSTR,RRSTAR,VVSTAR,XI,RT1,RT2,RT3,
  1XIMU(3),D,EPS(3),DEL(3),A(3),B(3),C(3),SUM
  COMPLEX X,F1,F2,F3,AA,BB,CC,PHASAH,PHASAC
  DOUBLE PRECISION PI
  COMMON PI
  1 FORMAT(6F12.6)
  2 FORMAT(6H A(K)= 6F9.4,7H MU(1)= 2F9.4,4H F1= 2F9.4)
  3 FORMAT(6H B(K)= 6F9.4,7H MU(2)= 2F9.4,4H F2= 2F9.4)
  4 FORMAT(6H C(K)= 6F9.4,7H MU(3)= 2F9.4,4H F3= 2F9.4)
  5 FORMAT(6H0FREQ= F10.3,5X,3HK=1,15X,3HK=2,15X,3HK=3 )
  6 FORMAT(122H0      TIME          A**2      B**2      C**2      A**2
  1+R**2      MOD A      PHASE A      MOD B      PHASE B      MOD C      PHASE C
  2
  )
  7 FORMAT(F12.3,4F12.6,6F10.3)
  8 FORMAT(1H1)
  9 FORMAT(4H MM= 2F12.6,4H RR= 2F12.6,4H VV= 2F12.6)
  10 FORMAT(6H FREQ= F12.3,7H GAMMA= F12.3,5H FAB= F12.3, 5H FAC= F12.
  13,5H FBC= F12.3 )
  12 FORMAT(40H DOUBLE PRECISION CUBIC SOLUTION METHOD )
  13 FORMAT(6I4)
  14 FORMAT(7H SPIN= 1F12.6,4H GJ= F12.6,5H MU= F12.6,6H DELW= F12.6,
  15H GJP= F12.6,7H DELWP= F12.6)
  15 FORMAT(14H STATE NUMBER 14,9H AT FIELD F7.1, 6H GAUSS )
  160 FORMAT(48H INITIAL CONDITIONS A=1, B=0, C=0 )
  161 FORMAT(48H INITIAL CONDITIONS A=0, B=1, C=0 )
  PI=4.0*DATAN(1.0D+0)
  GAMMA=200.*3.1415927
  XI=CMPLX(0.0,1.0)
  WRITE(9,8)
  19 READ(10,1)XSPIN,GJ,XMU,DELW,GJP,DELWP
  READ(10,1)FREQMN,FREQDL,FREQMX,F,DELT,BGAUSS
  GI=XMU/XSPIN
  ISPIN=XSPIN+1.0
  GO TO (100,101),ISPIN
100 NCASE=2
  FFA(1)=1.0
  XMFA(1)=1.0
  FFB(1)=0.0
  XMFB(1)=0.0
  FFA(2)=1.0
  XMFA(2)=0.0
  FFB(2)=1.0
  XMFB(2)=-1.0
  GO TO 20
101 NCASE=3
  FFA(1)=1.5
  XMFA(1)=1.5
  FFB(1)=0.5

```

```

XMF(1)=0.5
FFA(2)=1.5
XMFA(2)=0.5
FFB(2)=0.5
XMF(2)=-0.5
FFA(3)=1.5
XMFA(3)=-0.5
FFB(3)=1.5
XMF(3)=-1.5
20 READ(10,1)XMM,RR,VV
  READ(10,13)IMODE,ICSMN,ICSMX
C  IMODE 1 GO TO 19  2 GO TO 20
  WRITE(9,8)
  NFREQ=(FREQMX-FREQMN)/FREQDL
  NFREQ=NFREQ+1
  NTIME=TF/DELT
  NTIME=NTIME+1
  DO 132 INIT=1,2
  DO 110 ICASE=ICSMN,ICSMX
    CALL BREIT(XSPIN,FFA(ICASE),XMFA(ICASE),GJ,GI,DELW,BGAUSS,FA,XGAUS
1S,EPS1)
    CALL BREIT(XSPIN,FFB(ICASE),XMF(ICASE),GJ,GI,DELW,BGAUSS,FB,XGAUS
1S,EPS1)
    CALL BREIT(XSPIN,FFA(ICASE),XMFA(ICASE),GJP,GI,DELWP,HGAUSS,FC,BGA
1USS,EPS1)
    FC=FC-1058.070
    FAR=FA-FB
    FAC=FA-FC
    FABS(ICASE)=FAB
    FACS(ICASE)=FAC
    FBCS(ICASE)=FB-FC
    DO 110 I=1,NFREQ
      FI=I-1
      FREQ=FREQMN+FI*FREQDL
      DELAB=(FREQ-FAB)*2.0*3.1415927
      PHASAB=CMPLX(0.0,DELAB)
      ARL=(FREQ-FAC)*2.0*3.1415927
      PHASAC=CMPLX(0.0,ARL)
      AIM=-0.5*GAMMA
      DELAC=CMPLX(ARL,AIM)
      XMMSTR=CONJG(XMM)
      RRSTAR=CONJG(RR)
      VVSTAR=CONJG(VV)
      P=DELAB+DELAC
      Q=DELAB*DELAC-VV*VVSTAR-0.25*(RR*RRSTAR+XMM*XMMSTR)
      R=0.5*REAL(XMM*VV*RRSTAR)-0.25*(RR*RRSTAR*DELAB+XMM*XMMSTR*DELAC)
      P=-XI*P
      Q=-Q
      R=XI*R
      CALL CUBIC(P,0,R,RT1,RT2,RT3)
      X=RT1
      F1=X**3+P*X**2+Q*X+R
      X=RT2
      F2=X**3+P*X**2+Q*X+R
      X=RT3
      F3=X**3+P*X**2+Q*X+R
      XIMU(1)=RT1*XI
      XIMU(2)=RT2*XI
      XIMU(3)=RT3*XI
      DO 22 K=1,3
        D=(DELAC*XIMU(K))*(DELAB+XIMU(K))-VV*VVSTAR
        EPS(K)=-0.5*(XMM*(DELAC+XIMU(K))-RR*VVSTAR)/D
22  DEL(K)=-0.5*(RR*(DELAB+XIMU(K))-XMM*VV)/D
        A(1)=EPS(2)*DEL(3)-EPS(3)*DEL(2)
        A(2)=EPS(3)*DEL(1)-EPS(1)*DEL(3)
        A(3)=EPS(1)*DEL(2)-EPS(2)*DEL(1)
        SUM=A(1)+A(2)+A(3)
        GO TO (130,131),INIT
131 A(1)=DEL(2)-DEL(3)
        A(2)=DEL(3)-DEL(1)
        A(3)=DEL(1)-DEL(2)
130 DO 23 K=1,3

```

```

A(K)=A(K)/SUM
B(K)=EPS(K)*A(K)
23 C(K)=DFL(K)*A(K)
WRITE(9,8)
WRITE(9,14)XSPIN,GJ,XMU,DELOW,GJP,DELWP
WRITE(9,5)FREQ
WRITE(9,2)(A(K),K=1,3),RT1,F1
WRITE(9,3)(B(K),K=1,3),RT2,F2
WRITE(9,4)(C(K),K=1,3),RT3,F3
GO TO (150,151),IINIT
150 WRITE(9,160)
GO TO 152
151 WRITE(9,161)
152 WRITE(9,9)XMM,RR,VV
WRITE(9,10)FREQ,GAMMA,FABS(ICASE),FACS(ICASE),FBCS(ICASE)
WRITE(9,15)ICASE,HGAUSS
WRITE(9,6)
DO 114 ITIME=1,NTIME
FITIME=ITIME
T=(FITIME-1.0)*DEL T
TIME(ITIME)=T
X=RT1*T
F1=CEXP(X)
X=RT2*T
F2=CEXP(X)
X=RT3*T
F3=CEXP(X)
AA=A(1)/F1+A(2)/F2+A(3)/F3
BB=B(1)/F1+B(2)/F2+B(3)/F3
BB=BB*CEXP(PHASEB*T)
CC=C(1)/F1+C(2)/F2+C(3)/F3
CC=CC*CEXP(PHASEC*T)
ASQ(ITIME)=(CABS(AA))**2
BSQ(ITIME)=(CABS(BB))**2
CSQ(ITIME)=(CABS(CC))**2
ABSQ(ITIME)=ASQ(ITIME)+BSQ(ITIME)
XMODAA=CABS(AA)
XMODBB=CABS(BB)
XMODCC=CABS(CC)
PHASAA=ATAN2(AIMAG(AA),REAL(AA))
PHASAA=180.0*PHASAA/3.1415927
PHASBB=ATAN2(AIMAG(BB),REAL(BB))
PHASBB=180.0*PHASBB/3.1415927
PHASCC=ATAN2(AIMAG(CC),REAL(CC))
PHASCC=180.0*PHASCC/3.1415927
114 WRITE(9,7)TIME(ITIME),ASQ(ITIME),BSQ(ITIME),CSQ(ITIME),ABSQ(ITIME)
1,XMODAA,PHASAA,XMODBB,PHASBB,XMODCC,PHASCC
110 CONTINUE
132 CONTINUE
GO TO (19,20),IMODE
END

```

```

SUBROUTINE CUBIC(P,Q,R,RT1,RT2,RT3)
C DOUBLE PRECISION VERSION
C SOLVES CUBIC EQUATIONS OF THE FORM X**3+P*X**2+Q*X+R=0.0 WITH P, Q,
C AND R COMPLEX. THE THREE ROOTS RT1, RT2, AND RT3 ARE IN ORDER OF
C DECREASING REAL PART.
COMPLEX P,Q,R,RT1,RT2,RT3,RT(3),A,B,U,W120
DOUBLE PRECISION PR,PI,QR,QI,RR,RI,P2R,P2I,AR,AI,P3R,P3I,POR,PGI,
1BR,BI,B2R,B2I,A2R,A2I,A3R,A3I,R12R,RT2I,RTABS,RTARG,RTR,RTI,AR,
2AAI,DARG
W120=CMPLX(-0.5,0.8660254)
PR=REAL(P)
QR=REAL(Q)
RR=REAL(R)
PI=AIMAG(P)
QI=AIMAG(Q)
RI=AIMAG(R)
CALL DPRD(PR,PI,PR,PI,P2R,P2I)

```



```

AR=QR/3.0-P2R/9.0
AI=QI/3.0-P2I/9.0
ASNGLR=AR*3.0
ASNGLI=AI*3.0
A=CMPLX(ASNGLR,ASNGLI)
CALL DPROD(P2R,P2I,PR,P1,P3R,P3I)
CALL DPROD(PR,P1,QR,QI,POR,POI)
BR=P3R/27.0-POR/6.0+RR/2.0
BI=P3I/27.0-POI/6.0+RI/2.0
CALL DPROD(BR,BI,BR,BI,B2R,B2I)
CALL DPROD(AR,AI,AR,AI,A2R,A2I)
CALL DPROD(AR,AI,A2R,A2I,A3R,A3I)
RT2R=B2R+A3R
RT2I=B2I+A3I
RTABS=(RT2R**2+RT2I**2)**0.25
CALL DARCTN(RT2I,RT2R,RTARG)
RTARG=RTARG/2.0
RTR=RTABS*DCOS(RTARG)
RTI=RTABS*DSIN(RTARG)
ABSAA=DSQRT((RTR-BR)**2+(RTI-BI)**2)
ABSBB=DSQRT((RTR+BR)**2+(RTI+BI)**2)
IF(ABSAA.GE.ABSBB)GO TO 2
SGN=-1.0
GO TO 3
2 SGN=1.0
3 AAR=-BR+SGN*RTR
AAI=-BI+SGN*RTI
ABS=(AAR**2+AAI**2)**(1.0/6.0)
CALL DARCTN(AAI,AAR,DARG)
ARG=DARG/3.0
UR=ABS*DCOS(ARG)
UI=ABS*DSIN(ARG)
U=CMPLX(UR,UI)
DO 1 J=1,3
RT(J)=U-(P+A/U)/3.0
1 U=U*W120
R1=REAL(RT(1))
R2=REAL(RT(2))
R3=REAL(RT(3))
IF(R1.GE.R2)GO TO 10
IF(R3.GE.R2)GO TO 11
IF(R3.GE.R1)GO TO 12
J1=2
J2=1
J3=3
GO TO 15
12 J1=2
J2=3
J3=1
GO TO 15
11 J1=3
J2=2
J3=1
GO TO 15
10 IF(R3.GE.R1)GO TO 13
IF(R3.GE.R2)GO TO 14
J1=1
J2=2
J3=3
GO TO 15
14 J1=1
J2=3
J3=2
GO TO 15
13 J1=3
J2=1
J3=2
15 CONTINUE
RT1=RT(J1)
RT2=RT(J2)
RT3=RT(J3)
RETURN
END

```

```

SUBROUTINE DPROD(XR,XI,YR,YI,ZR,ZI)
DOUBLE PRECISION XR, XI, YR, YI, ZR, ZI
ZR=XR*YR-XI*YI
ZI=XI*YR+XR*YI
RETURN
END

```

```

SUBROUTINE DARCTN(Y,X,Z)
C FINDS DOUBLE PRECISION ARCTANGENT IN RADIAN IN CORRECT QUADRANT.
C DEFINES ZERO/ZERO=ZERO. USES RANGE PI TO - PI
DOUBLE PRECISION X,Y,Z,PI,YX
COMMON PI
YX=Y/X
IF(X)300,301,302
300 IF(Y)303,304,304
303 Z=DATAN(YX)-PI
GO TO 308
304 Z=DATAN(YX)+PI
GO TO 308
301 IF(Y)305,306,307
305 Z=-PI/2.0
GO TO 308
306 Z=0.0
GO TO 308
307 Z=PI/2.0
GO TO 308
302 Z=DATAN(YX)
308 RETURN
END

```

```

SUBROUTINE BREIT(XI,FFF,XM,GJ,GI,DELW,BGAUSS,W,XGAUSS,EPS1)
ISGN=FFF
F=ISGN
SGN=(F*2.0-1.0)*(DELW/2.0)
GJ1=GJ+0.00229*(GJ-1.0)
EPS=1.0/(GJ1*1836.1/GI-1.0)
XGAUSS=GJ1*9.2732*BGAUSS/(6.625*DELW*(1.0+EPS))
5 EPS1=EPS*DELW*XGAUSS
6 W=-DELW/(4.0*XI+2.0)+EPS1*XM
B=2.0*XM/(XI+0.5)
IF(B+1.0)1,1,2
1 IF(XGAUSS-1.0)2,3,3
3 SGN=-SGN
2 W=W+SGN*SQRT(1.0+B*XGAUSS+XGAUSS*XGAUSS)
IF(GJ.GE.1.0) RETURN
DELTA=ABS(W)*4.0*BGAUSS/(9.0*5214.0)
W=W-DELTA
RETURN
END

```

APPENDIX B. A COMPUTER PROGRAM FOR THE NUMERICAL INTEGRATION OF THE FOUR-LEVEL EQUATIONS

A FORTRAN IV program which numerically integrates the four-level equations is given in this appendix. The version given finds $|a|^2$, $|b|^2$, $|c|^2$, $|d|^2$, and $|a|^2 + |b|^2$ as a function of time for a set of fixed driving frequencies and fixed magnetic field. The real and imaginary parts of a, b, c, and d are also given. Other versions of the program exist in which time is held constant while the variation of the above quantities with magnetic field at fixed frequency, or with frequency at fixed magnetic field, is studied.

On a CDC 6600, the program requires (for the accuracy used here) about 1 minute of central processor time per microsecond of integration time. More precisely, the computation times and number of times the subroutine DERIV is called are as follows:

Case	DERIV Calls per usec	Computation Time per usec	Approximation
1	5,000	35 sec	3 level, $e^{i\omega t}$
2	80,000	66 sec	3 level, $\cos \omega t$
3	40,000	42 sec	4 level, $e^{i\omega t}$, $e^{-i\omega t}$
4	80,000	81 sec	4 level, $\cos \omega t$

where the case number is as given in Figure 20. The program is believed to maintain better than 1% accuracy for integration times at least up to 1 microsecond. The accuracy can be adjusted with the parameters RELTST and ABSTST in subroutine INTEG. Accuracy testing is done in subroutine ACCRY.

The program is set up to allow the transverse electric field to oscillate also. This case could be of interest if the metastable beam was mixed with a plasma, since rf fields could penetrate the plasma, under appropriate conditions, while static electric fields cannot.

The input for the program is as follows:

Card 1 (FORMAT F12.6)

Identical to Card 1 for program described in Appendix A.

Card 2 (FORMAT F12.6)

Identical to Card 2 for program described in Appendix A.

Card 3 (FORMAT F12.6)

FREQ2 driving transverse frequency in MHz (normally zero)

Card 4 (FORMAT 6 F12.6)

Identical to Card 3 for program described in Appendix A.

Card 5 (FORMAT 6 F12.6)

XMMP M' in MHz (angular frequency)
RRP R' in MHz (angular frequency)
VVP V' in MHz (angular frequency)

where these quantities are complex and again require two numbers each for their specification.

Cards 6, 7 (FORMAT 6 F12.6)

XO(1) initial real part of a
XO(2) initial imaginary part of a

XO(3) initial real part of b
XO(4) initial imaginary part of b
XO(5) initial real part of c
XO(6) initial imaginary part of c
XO(7) initial real part of d
XO(8) initial imaginary part of d

Card 8 (FORMAT 6 I4)

Identical to Card 4 of program described in Appendix A.

The program consists of a main program together with several subroutines. The function of the various subroutines is as follows:

a) SUBROUTINE INTEG (NN, TI, TTF, HH, HHP, MM, VVM, IP, XO, TT, XXP)

This subroutine integrates an arbitrary system of real linear differential equations. The arguments of this subroutine are defined by comments in the main program listing. The monitoring feature (a periodic test of a specified variable against some

limit) is not used. INTEG calls a number of sub-routines of which only those which are specific to the problem under discussion will be further described.

b) SUBROUTIN DERIV (T, V, FD)

This subroutine computes the value of the first derivatives FD(I) (for I = 1 to 8) given the value of the functions V(I) (for I = 1 to 8) and the time T. I = 1 and 2 correspond to the real and imaginary parts of a, 3 and 4 to the real and imaginary parts of b, and so on. (The four complex first-order differential equations have been rewritten as eight real first-order differential equations.)

c) SUBROUTINE PRINT (T, V)

This subroutine sets up the common variable arrays at the specified print-step intervals for later printout.

d) SUBROUTINE BREIT (XI, FFF, XM, GJ, GI, DELW,

BGAUSS, W, XGAUSS, EPS1)

This subroutine was described in Appendix A.

The output from the program is fully labeled. Tape 10 is defined as input and Tape 9 as output for the system for which this program was written.

The inclusion of fields whose strength varies as time (or displacement in a cavity) can be easily incorporated in the subroutine DERIV. It is required to give RR, RRP, MM, MMP, VV, and VVP the required time dependence, as indicated on comment cards.

It is important to simplify DERIV as much as possible, from the point of view of computation time, since it is in the innermost loop. The form listed here is more general than required for many problems, and, if computer time is important, it should be simplified in those cases.

```

PROGRAM LAMBV(INPUT,TAPE 10=INPUT,OUTPUT,TAPE 9= OUTPUT,FILM, TAPE
1 12=FILM)
C AMPLITUDES AS FUNCTION OF TIME VERSION. LONGITUDINAL AND TRANSVERSE
C DRIVING FREQUENCIES ALLOWED (TRANSVERSE FREQUENCY NORMALLY ZERO).
C DIMENSIONS ALLOW UP TO 5 FREQUENCY POINTS, 100 TIME POINTS
C (RESULTS STORED AS DIMENSIONED VARIABLES TO FACILITATE PLOTTING)
C DIVIDE R AND V BY 13.94 TO OBTAIN VOLTS/CM PEAK TO ZERO
C DIVIDE M BY 8.80 TO OBTAIN GAUSS PEAK TO ZERO
C THAT IS, ENTER P,V, AND M IN MHZ (ANGULAR FREQUENCY)
  COMMON XMM,XMMP,RR,RRP,VV,VVP
  COMMON ARL(3,100,5),BRL(3,100,5),CRL(3,100,5),DRL(3,100,5),
  LAIM(3,100,5),BIM(3,100,5),CIM(3,100,5),DIM(3,100,5),ICASE,IFREQ,
  ZITIME,TIME(100)
  COMMON/RLK3/XMM,XMMP,RR,RRP,VV,VVP,GAMMA2,WAB,WAE,WAF,WBE,WBF,WEF,
  WRFREQ1,WRFREQ2
  COMMON/RLK7/IDERIV
  DIMENSION ASQ(100),HSQ(100),CSQ(100),DSQ(100),ABSQ(100)
  DIMENSION FFA(3),XMFA(3),FFB(3),XMFB(3)
  DIMENSION XO(30),XXP(30),FREQ(5),FSP(3,6)
1 FORMAT(6F12.6)
6 FORMAT(132H          TIME          A**2          B**2          C**2          D**2 A**2
1+8**2      ARL      LAIM      BRL      BIM      CRL      CIM      DRL      DIM
2
7 FORMAT(F10.3,5F10.6,4F7.3)
8 FORMAT(1H1)
9 FORMAT(4H MM= 2F14.6,4H RR= 2F14.6, 4H VV= 2F14.6)
10 FORMAT(9H MGAUSS= F12.3, 8H GAMMA= F12.3,8H FREQ1= F12.3,
18H FREQ2= F12.3 )
11 FORMAT(5H MMP= F13.6,F14.6, 5H RRP= F13.6,F14.6, 5H VVP= F13.6,
1F14.6)
13 FORMAT(6I4)
14 FORMAT(7H SPIN= F12.6,4H GJ= F12.6,5H MU= F12.6,6H DELW= F12.6,
15H GJP= F12.6,7H DELWP= F12.6)
15 FORMAT(14H STATE NUMBER I4)
16 FORMAT(16H INITIAL VECTOR          4(F10.3,F7.3))
17 FORMAT(5H FAB= F10.3,5H FAE= F10.3,5H FAF= F10.3,5H FBE= F10.3,
15H FRF= F10.3,5H FEF= F10.3 )
  GAMMA=100.0*2.0*3.1415927
  GAMMA2=0.5*GAMMA
  WRITE(9,8)

```

```

19 READ(10,1)XSPIN,GJ,XMU,DELW,GJP,DELWP
   READ(10,1)FREQMN,FREQDL,FREQMX,TTF,HHP,BGAUSS
   READ(10,1)FREQ2
   GI=XMU/XSPIN
   ISPIN=XSPIN+1.0
   GO TO (100,101),ISPIN
100 NCASE=2
   FFA(1)=1.0
   XMFA(1)=1.0
   FFB(1)=0.0
   XMFB(1)=0.0
   FFA(2)=1.0
   XMFA(2)=0.0
   FFB(2)=1.0
   XMFB(2)=-1.0
   GO TO 20
101 NCASE=3
   FFA(1)=1.5
   XMFA(1)=1.5
   FFB(1)=0.5
   XMFB(1)=0.5
   FFA(2)=1.5
   XMFA(2)=0.5
   FFB(2)=0.5
   XMFB(2)=-0.5
   FFA(3)=1.5
   XMFA(3)=-0.5
   FFB(3)=1.5
   XMFB(3)=-1.5
20 READ(10,1)XMM,RR,VV
   READ(10,1)XMMP,RRP,VVP
   READ(10,1)(XO(I),I=1,8)
   READ(10,13)IMODE,ICSMN,ICSMX
   NFREQ=(FREQMX-FREQMN)/FREQDL
   NFREQ=NFREQ+1
   DO 110 ICASE=ICSMN,ICSMX
   IDERIV=0
   ITIME=0
   CALL BREIT(XSPIN,FFA(ICASE),XMFA(ICASE),GJ,GI,DELW,BGAUSS,FA,
1XGAUSS,EPS1)
   CALL BREIT(XSPIN,FFB(ICASE),XMFB(ICASE),GJ,GI,DELW,BGAUSS,FB,
1XGAUSS,EPS1)
   CALL BREIT(XSPIN,FFA(ICASE),XMFA(ICASE),GJP,GI,DELWP,BGAUSS,FE,
1XGAUSS,EPS1)
   CALL BREIT(XSPIN,FFB(ICASE),XMFB(ICASE),GJP,GI,DELWP,BGAUSS,FF,
1XGAUSS,EPS1)
   FE=FE-1058.070
   FF=FF-1058.070
   FAB=FA-FB
   FAE=FA-FE
   FAF=FA-FF
   FBE=FB-FE
   FBF=FB-FF
   FEF=FE-FF
   WAB=FAB*6.2831854
   WAE=FAE*6.2831854
   WAF=FAF*6.2831854
   WBE=FBE*6.2831854
   WBF=FBF*6.2831854
   WEF=FEF*6.2831854
   FSP(ICASE,1)=FAB
   FSP(ICASE,2)=FAE
   FSP(ICASE,3)=FAF
   FSP(ICASE,4)=FBE
   FSP(ICASE,5)=FBF
   FSP(ICASE,6)=FEF
   DO 112 IFREQ=1,NFREQ
   FIFREQ=IFREQ
   FREQ(IFREQ)=(FIFREQ-1.0)*FREQDL+ FREQMN
   FREQ1=FREQ(IFREQ)
   WFREQ1=6.2831854*FREQ1
   WFREQ2=6.2831854*FREQ2

```

```

WRITE(9,8)
NN=8
TI=0.0
HH=0.0001
MM=0
VVM=0.0
IP=0
CALL INTEG(NN, TI, TTF, HH, HHP, MM, VVM, IP, X0, TT, XXP)
C NN NUMBER OF FIRST ORDER DIFFERENTIAL EQUATIONS
C TI INITIAL VALUE OF INDEPENDENT VARIABLE
C TTF FINAL VALUE OF INDEPENDENT VARIABLE
C HH GUESS AT STEP SIZE
C HHP PRINT STEP SIZE
C MM VARIABLE TO BE MONITORED (0=NO, 1 TO NN YES )
C VVM VALUE TO MONITOR FOR
C IP NUMBER OF PARAMETERS
C X0 VECTOR OF STARTING VALUES
C TT VALUE OF TIME RETURNED AT END OF INTEGRATION
C XXP VARIABLE VALUES RETURNED AT END OF INTEGRATION
112 CONTINUE
110 CONTINUE
    NTIME=ITIME
    DO 26 IFREQ=1, NFREQ
    DO 25 ICASE=ICSMN, ICSMX
        WRITE(9,8)
        WRITE(9,14) XSPIN, GJ, XMU, DELW, GJP, DELWP
        WRITE(9,9) XMM, RR, VV
        WRITE(9,11) XMMP, RRP, VVP
        WRITE(9,10) BGAUSS, GAMMA, FREQ(IFREQ), FREQ2
        WRITE(9,15) ICASE
        WRITE(9,16) (X0(I), I=1,8)
        WRITE(9,17) (FSP(ICASE, IFS), IFS=1,6)
        WRITE(9,6)
        DO 24 ITIME=1, NTIME
            ASQ(ITIME)=AHL(ICASE, ITIME, IFREQ)**2, AIM(ICASE, ITIME, IFREQ)**2
            BSQ(ITIME)=BHL(ICASE, ITIME, IFREQ)**2, BIM(ICASE, ITIME, IFREQ)**2
            CSQ(ITIME)=CRL(ICASE, ITIME, IFREQ)**2, CIM(ICASE, ITIME, IFREQ)**2
            DSQ(ITIME)=DRL(ICASE, ITIME, IFREQ)**2, DIM(ICASE, ITIME, IFREQ)**2
            ABSQ(ITIME)=ASQ(ITIME)+BSQ(ITIME)
        24 WRITE(9,7) TIME(ITIME), ASQ(ITIME), BSQ(ITIME), CSQ(ITIME), DSQ(ITIME),
            1ABSQ(ITIME),
            2AHL(ICASE, ITIME, IFREQ), AIM(ICASE, ITIME, IFREQ),
            3BHL(ICASE, ITIME, IFREQ), BIM(ICASE, ITIME, IFREQ),
            4CRL(ICASE, ITIME, IFREQ), CIM(ICASE, ITIME, IFREQ),
            5DRL(ICASE, ITIME, IFREQ), DIM(ICASE, ITIME, IFREQ)
        25 CONTINUE
        26 CONTINUE
        GO TO (19,20), IMODE
    END

```

```

SUBROUTINE INTEG (NN, TI, TTF, HH, HHP, MM, VVM, P, X0, TT, XXP)
C INTEG() SOLVES A SYSTEM OF N FIRST ORDER DIFF EQNS BY A 4TH
C ORDER ADAMS P-C METHOD WITH AUTOMATIC ERROR CONTROL. STARTING
C IS BY RUNGA-KUTTA.
C
    INTEGER P, IJ
    REAL LB
    LOGICAL ACC
    COMMON/BLK1/N, T, TF, H, H0, HP, M, VM, J, ACC, LB, RELTST, ABSTST, FACTOR,
    1BND, X(30,5), F(30,5), E(30), XP(30)
    COMMON/BLK5/IDOU, I, NDOUBL
    DIMENSION X0(30), XXP(30)
C
C SET UP INITIAL VALUES
    N=NN
    TF=TTF
    H=HH
    HP=HHP
    M=MM

```

```

      VM=VVM
      DO 10 I=1,N
10  X(I,1)=X0(I)
      IF (P.EQ.0) GO TO 21
      L=N+1
      U=N+P
      DO 20 I=L,U
      XP(I)=X0(I)
      DO 20 J=1,5
20  X(I,J)=X0(I)
21  T=TI
      BND=TI+HP
      H0=H
      ABSB=1.0E-4
      RELB=ABSB
      ABSTST=ABSB*14.2
      RELTST=RELB*14.2
      FACTOR=RELB/ABSB
      LB=0.005*RELTST
      IDOUBL=0
      NDOUBL=3
      H=2.0*H
30  CALL START(IRETRN)
      GO TO (100,99),IRETRN
C  SHOULD ANY OF THE STARTING VALUES BE PRINTED OUT
100 T=T-3.0*H
      DO 35 J=2,4
      T=T+H
      CALL TEST(IRETRN)
      GO TO (35,60),IRETRN
35  CONTINUE
C  BEGIN ADAMS METHOD
40  CALL ADAMS
      CALL ACCRY
      IF (ACC) GO TO 50
      DO 45 I=1,N
45  X(I,1)=X(I,4)
      GO TO 30
50  CALL TEST(IRETRN)
      GO TO (101,60),IRETRN
101 CALL DOUBLE(IRETRN)
      GO TO (40,30),IRETRN
60  IF (J.EQ.5) GO TO 65
      DO 64 I=1,N
64  XP(I)=X(I,J)
65  CALL PRINT(T,XP)
      TI=T
      DO 70 I=1,N
70  XXP(I)=XP(I)
99  RETURN
      END

      SUBROUTINE START (IRETRN)
C  RUNGA-KUTTA STARTING METHOD
      LOGICAL ACC
      COMMON/BLK1/N,T,TF,H,H0,HP,M,VM,J,ACC,LB,RELTST,ABSTST,FACTOR,
1  BND,X(30,5),F(30,5),E(30),XP(30)
      COMMON/BLK2/G(30,4)
      J=2
      CALL RNGA
      DO 15 I=1,N
15  XP(I)=X(I,2)
C  XP(I)=DBL INTERVAL RESULT FOR ERROR ANALYSIS
      T=T-H
      H=0.5*H
      IF ((T+H).NE.T) GO TO 30
      WRITE (9,20)
20  FORMAT(50H EQUATIONS CANNOT BE SOLVED FURTHER WITHIN GIVEN ERROR )

```

```

TPLUS= T+H
WRITE(9,21) TPLUS, T
21 FORMAT(6H T+H= E15.10, 6H T= E15.10 )
IKFTRN=2
RETURN
30 DO 40 J=2,3
40 CALL RNGA
41 CALL ACCRY
IF (.NOT.ACC) GO TO 10
J=4
CALL RNGA
IKFTRN=1
RETURN
END

```

```

SUBROUTINE RNGA
C INTEGRATE N EQNS AHEAD ON THE J/TH STEP OF LENGTH H.
COMMON/BLK1/N,T,TF,H,H0,HP,M,VM,J,ACC,LB,RELTST,ABSTST,FACTOR,
1BND,X(30,5),F(30,5),E(30),XP(30)
COMMON/BLK2/G(30,4)
CALL DERIV(T,X(1,J-1),F(1,J-1))
DO 10 I=1,N
G(I,1)=H*F(I,J-1)
10 X(I,J)=X(I,J-1)+0.5*G(I,1)
TI=T+0.5*H
CALL DERIV(TT,X(1,J),F(1,J))
DO 20 I=1,N
G(I,2)=H*F(I,J)
20 X(I,J)=X(I,J-1)+0.5*G(I,2)
CALL DERIV(TT,X(1,J),F(1,J))
DO 30 I=1,N
G(I,3)=H*F(I,J)
30 X(I,J)=X(I,J-1)+G(I,3)
T=T+H
CALL DERIV(T,X(1,J),F(1,J))
DO 40 I=1,N
G(I,4)=H*F(I,J)
40 X(I,J)=X(I,J-1)+(G(I,1)+2.0*(G(I,2)+G(I,3))+G(I,4))/6.0
RETURN
END

```

```

SUBROUTINE ACCRY
C TESTS ABS AND REL ERROR AND SETS ACC .FALSE. IF NEITHER SATISFIED
LOGICAL ACC
COMMON/BLK1/N,T,TF,H,H0,HP,M,VM,J,ACC,LB,RELTST,ABSTST,FACTOR,
1BND,X(30,5),F(30,5),E(30),XP(30)
ACC=.TRUE.
DO 50 I=1,N
E(I)=ABS(XP(I)-X(I,J))
IF (E(I).GE.ABS(X(I,J))*RELTST) GO TO 10
E(I)=E(I)/ABS(X(I,J))
GO TO 50
10 IF (E(I).GE.ABSTST) GO TO 20
E(I)=E(I)*FACTOR
GO TO 50
20 T=T-H
H0=0.5*H
ACC=.FALSE.
75 FORMAT(1H , 16HSTEP SIZE CUT TO, F12.8, 6H AT T=, F12.8)
WRITE(9,75) H0,T
GO TO 99
50 CONTINUE
99 RETURN
END

```



```

SUBROUTINE TEST (IRETRN)
C MONITORS FOR VM, END OF INTEG N ON PRINT RANGE.
COMMON/RLK1/N,T,TF,H,H0,HP,M,VM,J,ACC,LB,RELTST,ABSTST,FACTOR,
1BND,X(30,5),F(30,5),E(30),XP(30)
DIMENSION X1(30),X2(30),F1(30),F2(30)
IF (M.EQ.0) GO TO 20
IF ((X(M,J).LE.VM).AND.(X(M,J-1).GT.VM)) GO TO 10
IF ((X(M,J).GT.VM).AND.(X(M,J-1).LE.VM)) GO TO 10
GO TO 20
10 CALL DIODE
IF(T-TF)70,70,30
70 IRETRN=2
RETURN
20 IF(ABS((T-TF)/TF)-1.0E-6) 80,81,81
80 IRETRN=2
RETURN
81 IF(T.LE.TF) GO TO 40
30 H=TF-T
DO 35 I=1,N
35 X(I,1)=X(I,J)
J=2
CALL RNGA
IRETRN=2
RETURN
40 IF(T.LT.BND) GO TO 50
C SAVE ALL VARIABLES WHICH MAY BE MODIFIED IN PRINT PROCEDURE
HSAVE=H
TSAVE=T
JSAVE=J
DO 45 I=1,N
X1(I)=X(I,1)
X2(I)=X(I,2)
F1(I)=F(I,1)
F2(I)=F(I,2)
45 X(I,1)=X(I,J)
J=2
H=BND-T
CALL RNGA
CALL PRINT(T,X(1,J))
BND=BND+HP
C RESTORE VARIABLES TO PROCEED
J=JSAVE
H=HSAVE
T=TSAVE
DO 46 I=1,N
X(I,1)=X1(I)
X(I,2)=X2(I)
F(I,1)=F1(I)
46 F(I,2)=F2(I)
50 IF (J.NE.5) GO TO 99
DO 60 I=1,N
X(I,4)=X(I,5)
DO 60 J=2,5
60 F(I,J-1)=F(I,J)
99 IRETRN=1
RETURN
END

```

```

SUBROUTINE DIODE
C FIND VALUE OF T WHERE THE M/T H VARIABLE REACHES THE VALUE VM
COMMON/RLK1/N,T,TF,H,H0,HP,M,VM,J,ACC,LB,RELTST,ABSTST,FACTOR,
1BND,X(30,5),F(30,5),E(30),XP(30)
DIMENSION D(30)
Y1=X(M,J)
Y0=X(M,J-1)
DELT=-ABS(H*Y1/(Y1-Y0))
10 H=DELT
DO 20 I=1,N
20 X(I,1)=X(I,J)

```

```

J=2
CALL RINGA
CALL DERIV(T,X(1,J),D)
DELT=(VM-X(M,J))/D(M)
IF (ABS(DELT).GE.1.0E-4) GO TO 10
X(M,J)=VM
RETURN
END

```

```

SUBROUTINE ADAMS
C INTEGRATE ONE STEP BY THE ADAMS PREDICTOR-CORRECTOR METHOD
COMMON/HLK1/N,T,TF,H,H0,HP,M,VM,J,ACC,LB,RELTST,ABSTST,FACTOR,
1BND,X(30,5),F(30,5),E(30),XP(30)
J=5
CALL DERIV(T,X(1,4),F(1,4))
DO 10 I=1,N
10 XP(I)=X(I,4)+0.041666667*H*(55.0*F(I,4)-59.0*F(I,3)
1+37.0*F(I,2)-9.0*F(I,1))
T=T+H
CALL DERIV(T,XP,F(1,5))
DO 20 I=1,N
20 X(I,5)=X(I,4)+0.041666667*H*(9.0*F(I,5)+19.0*F(I,4)
1-5.0*F(I,3)+F(I,2))
RETURN
END

```

```

SUBROUTINE DOUBLE (IRETRN)
C CAN INTERVAL BE DOUBLED
REAL LH
COMMON/HLK1/N,T,TF,H,H0,HP,M,VM,J,ACC,LB,RELTST,ABSTST,FACTOR,
1BND,X(30,5),F(30,5),E(30),XP(30)
COMMON/BLK5/IDOURL,NDOUBL
IDOUBL=IDOUBL+1
IF (IDOURL.LT.NDOUBL) GO TO 99
C ALLOWS DOUBLE ATTEMPT ONLY EVERY NDOUBL/TH CALL
IDOUBL=0
DO 10 I=1,N
IF (E(I).GT.LB) GO TO 99
10 CONTINUE
D1=HP/(2.0*H)
IF (D1.LE.2.0) GO TO 99
D2=(BND-T)/(2.0*H)
IF (D2.LE.2.0) GO TO 99
DO 20 I=1,N
20 X(I,1)=X(I,4)
HU=2.0*H
H=2.0*H0
30 FORMAT(18H STEP INCREASED TO F12.8, 6H AT T= F12.8)
WRITE(9,30)H0,T
IRETRN=2
RETURN
99 IRETRN=1
RETURN
END

```

```

SUBROUTINE DERIV(T,V,FD)
DIMENSION V(30),FD(30)
COMPLEX UBA,UFE,UFA,UFB,UFA,UFB
COMPLEX XMM,XMMP,RR,RRP,VV,VVP
COMMON/BLK3/XMM,XMMP,RR,RRP,VV,VVP,GAMMA2,WAB,WAE,WAF,WBE,WBF,WEF,
1WFREQ1,WFREQ2

```

```

COMMON/BLK7/IDERIV
IDERIV=IDERIV+1
FOFT1=COS(WFREQ1*T)
C REPLACE FOFT1 BY FOFT1*(DESIRED SLOW FUNCTION OF TIME) TO MODULATE
C RR,RRP,MM,MMP
FOFT2=COS(WFREQ2*T)
C IF FREQ2=0.0 IS ONLY CASE OF INTEREST SET FOFT2=1.0 TO SAVE COMPUTER
C TIME
C REPLACE FOFT2 BY FOFT2*(DESIRED SLOW FUNCTION OF TIME) TO MODULATE
C VV,VVP
UR=-SIN(WAE*T)
UI=-COS(WAE*T)
UEA=RR*FOFT1*CMLX(UR,UI)
UR=-SIN(WBE*T)
UI=-COS(WBE*T)
UEB=VV*FOFT2*CMLX(UR,UI)
UEAR=REAL(UEA)
UEBR=REAL(UEB)
UEAI=AIMAG(UEA)
UEBI=AIMAG(UEB)
FD(1)=-UEAR*V(5)-UEAI*V(6)
FD(2)=UEAI*V(5)-UEAR*V(6)
FD(3)=-UEBR*V(5)-UEBI*V(6)
FD(4)=UEBI*V(5)-UEBR*V(6)
FD(5)=UEAR*V(1)-UEAI*V(2)+UEBR*V(3)-UEBI*V(4)-GAMMA2*V(5)
FD(6)=UEAI*V(1)+UEAR*V(2)+UEBI*V(3)+UEBR*V(4)-GAMMA2*V(6)
FD(7)=-GAMMA2*V(7)
FD(8)=-GAMMA2*V(8)
IF(CABS(RRP).NE.0.0) GO TO 101
IF(CABS(VVP).NE.0.0) GO TO 101
GO TO 200
101 UR=-SIN(WBF*T)
UI=-COS(WBF*T)
UFB=RRP*FOFT1*CMLX(UR,UI)
UR=-SIN(WAF*T)
UI=-COS(WAF*T)
UFA=VVP*FOFT2*CMLX(UR,UI)
UFBR=REAL(UFB)
UFAR=REAL(UFA)
UFBI=AIMAG(UFB)
UFAI=AIMAG(UFA)
FD(1)=FD(1)-UFAR*V(7)-UFAI*V(8)
FD(2)=FD(2)+UFAI*V(7)-UFAR*V(8)
FD(3)=FD(3)-UFBR*V(7)-UFBI*V(8)
FD(4)=FD(4)+UFBI*V(7)-UFBR*V(8)
FD(7)=FD(7)+UFAR*V(1)-UFAI*V(2)+UFBR*V(3)-UFBI*V(4)
FD(8)=FD(8)+UFAI*V(1)+UFAR*V(2)+UFBI*V(3)+UFBR*V(4)
200 IF(CABS(XMM).NE.0.0) GO TO 201
IF(CABS(XMMP).NE.0.0) GO TO 201
GO TO 300
201 UR=-SIN(WAB*T)
UI=-COS(WAB*T)
UHA=XMM*FOFT1*CMLX(UR,UI)
UR=-SIN(WEF*T)
UI=-COS(WEF*T)
UFE=XMMP*FOFT1*CMLX(UR,UI)
UBAR=REAL(UHA)
UFER=REAL(UFE)
UBAI=AIMAG(UHA)
UFEI=AIMAG(UFE)
FD(1)=FD(1)-UBAR*V(3)-UBAI*V(4)
FD(2)=FD(2)+UBAI*V(3)-UBAR*V(4)
FD(3)=FD(3)+UBAR*V(1)-UBAI*V(2)
FD(4)=FD(4)+UBAI*V(1)+UBAR*V(2)
FD(5)=FD(5)-UFER*V(7)-UFEI*V(8)
FD(6)=FD(6)+UFEI*V(7)-UFER*V(8)
FD(7)=FD(7)+UFER*V(5)-UFEI*V(6)
FD(8)=FD(8)+UFEI*V(5)+UFER*V(6)
300 RETURN
END

```

```

SUBROUTINE PRINT(T,V)
DIMENSION V(30)
COMMON ARL(3,100,5),BRL(3,100,5),CRL(3,100,5),DRL(3,100,5),
1A1M(3,100,5),B1M(3,100,5),C1M(3,100,5),D1M(3,100,5),ICASE,IFREQ,
2ITIME,TIME(100)
COMMON/BLK1/N,T,TF,H,H0,HP,M,VM,J,ACC,LB,RELTST,ARSTST,FACTOR,
1BND,X(30,5),F(30,5),E(30),XP(30)
COMMON/BLK7/IDERIV
ITIME=ITIME+1
FITIME=ITIME
TIME(ITIME)=FITIME*HP
WRITE(9,10) ICASE,ITIME,IFREQ,IDERIV
10 FORMAT(6H ICASE I4,6H ITIME I4,6H IFREQ I4,13H DERIV CYCLES I10)
11 FORMAT(9F12.6)
WRITE(9,11) T,(V(I),I=1,8)
ARL(ICASE,ITIME,IFREQ)=V(1)
A1M(ICASE,ITIME,IFREQ)=V(2)
BRL(ICASE,ITIME,IFREQ)=V(3)
B1M(ICASE,ITIME,IFREQ)=V(4)
CRL(ICASE,ITIME,IFREQ)=V(5)
C1M(ICASE,ITIME,IFREQ)=V(6)
DRL(ICASE,ITIME,IFREQ)=V(7)
D1M(ICASE,ITIME,IFREQ)=V(8)
RETURN
END

```

```

SUBROUTINE BHEIT(XI,FFF,XM,GJ,GI,DELW,BGAUSS,W,XGAUSS,EPS1)
ISGN=FFF
F=ISGN
SGN=(F*2.0-1.0)*(DELW/2.0)
GJ1=GJ+0.00229*(GJ-1.0)
FPS=1.0/(GJ1*1836.1/GI-1.0)
XGAUSS=GJ1*9.2732*BGAUSS/(6.625*nELW*(1.0*EPS))
5 EPS1=EPS*DELW*XGAUSS
6 W=-DELW/(4.0*XI+2.0)+EPS1*XM
B=2.0*XM/(XI+0.5)
IF(B+1.0)1,1,2
1 IF(XGAUSS=1.0)2,3,3
3 SGN=-SGN
2 W=W+SGN*SQRT(1.0+B*XGAUSS+XGAUSS*XGAUSS)
IF(GJ.GE.1.0) RETURN
DELTA=ABS(W)*4.0*BGAUSS/(9.0*5214.0)
W=W-DELTA
RETURN
END

```